FACULTY OF SCIENCE AND TECHNOLOGY
BACHELOR THESIS

Study programme / specialisation:
Biological Chemistry

The autumn semester, 2022

Open

Author: Kaja Rimereit Houeland

Kaja Rimereit Houeland
(Signature author)

Supervisor: Sachin Maruti Chavan

Thesis title: Amine functionalized metal-organic framework for carbon capture

Credits (ECTS): 20

Keywords:
MOFs
MIP-202
Carbon capture
Characterization
Gas separation
Sorption

Pages: 54

+ appendix: 6

Stavanger, December 15th, 2022

Amine functionalized metal-organic framework for carbon capture

By
Kaja Rimereit Houeland

Bachelor of Science,
Biological Chemistry

University of Stavanger
2022

ABSTRACT

This thesis was all about synthesizing metal-organic frameworks, MOFs, with different compositions, and further on characterize and analyze the products using different analysis. The idea was to find out how we could make the most efficient MOF, with the main goal to capture carbon dioxide. The central emphasis was always using green, non-toxic chemicals, to keep the focus on sustainable energy and the environment. This was fulfilled by using only green solvents, and amino acids. In this work, there has mainly been used D-isomer, L-isomer, and a racemic mixture of these isomers.

MIP-202 samples were synthesized using both reflux with continually stirring below 120°C with different reaction times (1h vs 72h), dissimilar washing procedures and changing the heat parameter using autoclave for 120°C and 140°C. It showed huge differences in the analysis between the different reaction time, and it seems like 72 hours is the optimal time to produce a MOF which is stable and porous. There were surprisingly changes in nitrogen and carbon dioxide sorption for 72h synthesis products compared to the 1h synthesis and could also see a significant better uptake for those 72h samples washed with ethanol for three days. The DL-Aspartic acid with no treatment was calculated to have a specific surface area of 164 $m^2 g^{-1}$, with a total pore volume of 0,093 $cm^3 g^{-1}$. While the same product washed with ethanol for three days showed outstanding porosity with a surface area of 565 $m^2 g^{-1}$ and total pore volume of 0,268 $cm^3 g^{-1}$.

Many of the samples made, showed some good PXRD results, forming a MOF structure. However, the question along the way, was always how to improve the products to become even better. One of the issues was that chlorine got attached to some of the MOFs. Because of the harm to the environment chlorine can make when reacting with other chemicals, we tried to get rid of this. One of the experiments was to wash the MIP-202 with sodium acetate, but unfortunately the MOFs structure got destroyed. What could possibly be the reason for this, was that the chlorine attached to the MOFs containing zirconium and aspartic acid, are necessary for the MOF structure to stay stable.

24 different bulk samples were also made using high-throughput synthesis, where DL-Aspartic acid was used as linker, $ZrOCl_2 * 8H_2O$ or $Zr(SO_4)_2 * 4H_2O$ was the metal source, and different amounts of modulator, using either formic acid or acetic acid. Two of the samples containing sulfate and both zero and 30 equivalent formic acid were analyzed further. The idea was to try make a chlorine free product, switching from $ZrCl_4$ to $Zr(SO_4)_2$, but unfortunately the results were not satisfying.

ACKNOWLEDGMENT

Personally, I am very interested in the climate change, renewable energy and trying to achieve a safer future, and I have thought for several years that this is the path I want to take career-wise. I think that our knowledge must be in dialogue with oil and gas energy companies and figure out this together. Having the opportunity to learn and work more with MOFs is genuinely inspiring and exciting for me. This topic is relatively new, and all the information I am getting to know more about, will hopefully be useful in the future, and that is something I would love to take a part of. As we all know, CO_2 is one of the greenhouse gases, GHG, that contributes to the climate changes we are now facing, and carbon capture and storage (CCS), is crucial for achieving the goal expressed in the Paris Agreement. The fact that we can be able to capture and store this gas by using metal organic frameworks, is marvelous and essential for the future.

Three years at the University of Stavanger have been very educational and hopefully I will be able to show my understanding and knowledge through this Bachelor`s thesis. I would like to use this opportunity to show my gratitude for all the help I have received through my thesis and give an extra attention to my supervisor Professor Sachin Maruti Chavan for guiding me through it in a very helpful way. And not least I am very honored to get to know Simmy Rathod, John Senith Ravishan Fernando and Ananya Chari (including the rest of the team) more, and for all the help I have received by showing me how to handle the various instruments and the many questions I have had along the way. These last past months has been exciting, informative, and interesting.

ABBREVIATION

Asp: Aspartic Acid

CCS: Carbon Capture and Storage

EDS: Energy Dispersive X-Ray Spectroscopy

GHG: Greenhouse Gasses

MIP-202: Materials of the Institute of porous materials from Paris

MOF: Metal-Organic Framework

NMR: Nuclear Magnetic Resonance Spectroscopy

PXRD: Powder X-ray Diffraction

SEM: Scanning Electron Microscope

TGA: Thermogravimetric Analysis

ZrMOF: Zirconium based MOF

TABLE OF CONTENTS

1. Introduction

The global climate change is the defining issue nowadays and action to stop this is crucial for the future. The major, dramatic consequences of the man-made greenhouse gas emissions, among others are extreme weather, an increase in the temperature all over the world and sea, leading to higher sea levels and glacier melting and so on (D. Lv., et al. 2019). This all has big impacts on the ecosystem, humans, and some vulnerable species. In compliance with (P. Brewer, et al. 2018), the ocean takes up and stores a big amount of CO_2 emissions, and because of that, the water will become more acidic. As a result of both the glacier melting and pH under 7, several of animal species will become extinct.

Carbon dioxide, CO_2, is the primary greenhouse gas emitted through humans and the greenhouse gases, GHB, have been increasing a lot since pre-industrial times (L. Bernstein, et al. 2007). CO_2 enters the atmosphere through combustion energy from fossil fuels such as coal, oil, natural gas, trees, biological materials, solid waste, and some chemical reactions.

Measures must be taken early to try to reduce these climate emissions, and in December 2017, an international agreement called “Paris agreement”, was adopted to ensure that the world's countries were able to limit the climate change. The big goal was and still is to ensure that the temperature does not rise more than 2 degrees, ideally 1.5 degrees. In the present, all the countries have a responsibility to be able to achieve this goal.

Realising and admitting that we have a big problem right in front of us and still trying to figure out what and how we can do anything about it is necessary to contribute to the goal of reducing total emissions. For this reason, we must all think more renewable and make active choices in our everyday lives. One solution to work out these environmental issues, would be reducing the emissions with carbon capture and storage, CCS.

MOFs have shown big potentials for gas storage, purification, and separation, as well catalysis and sensing applications (Wang et al., 2018), and could possibly play a central role in the future. In this thesis, one must try to prove this theory, and by creating and analysing different variants, the modifications between them can be distinguished.

2. Literature Review

2.1 Carbon Capture

The world is currently runed mainly by fossil fuels, and it will continue in this direction for many years, despite the greenhouse effects of carbon dioxide (H. Demir., et al, 2022). Luckily one can see a significant change where renewable energies have received major focus these recent years. Nevertheless, it will not be sufficient to stop the climate crises since it will not help removing the CO_2. Because of that we need to use different techniques to capture carbon dioxide likewise.

Carbon capture has been a great challenge for the scientific world for many years, and this is the first step in carbon capturing and storage (CCS). CCS describes capturing CO_2 from flue gas and transport it and then for example store it many thousands of meters underground in a sandstone formation.

Carbon dioxide is captured by three main methods: post combustion CO_2 capture, pre combustion CO_2 capture and oxyfuel combustion. *Post combustion* process includes separating the CO_2 from combustion exhaust gases (R. Stanger., et al., 2015). The carbon dioxide can then be captured using different methods, and the most common post combustion process is amine purification (M. Ruud, 2019). This technique includes amines, and because of the properties for this chemical, it can both absorb and later release the carbon dioxide.

Pre combustion is the process where carbon is removed from the fuel consisting of carbon and hydrogen, so that the hydrogen can be burned alone. This is fulfilled by converting the fuel into a gaseous mix, where the two gases are being separated, and then CO_2 gets compressed for transport and storage.

Oxyfuel combustion is a process that is very similar to post combustion, but the main difference is that the fuel is burned with pure oxygen instead of air, meaning that nitrogen and oxygen are separated from each other. This leads to the flue gas only containing CO_2 and water vapor that can easily be separated, in comparison to if it contained nitrogen as well.

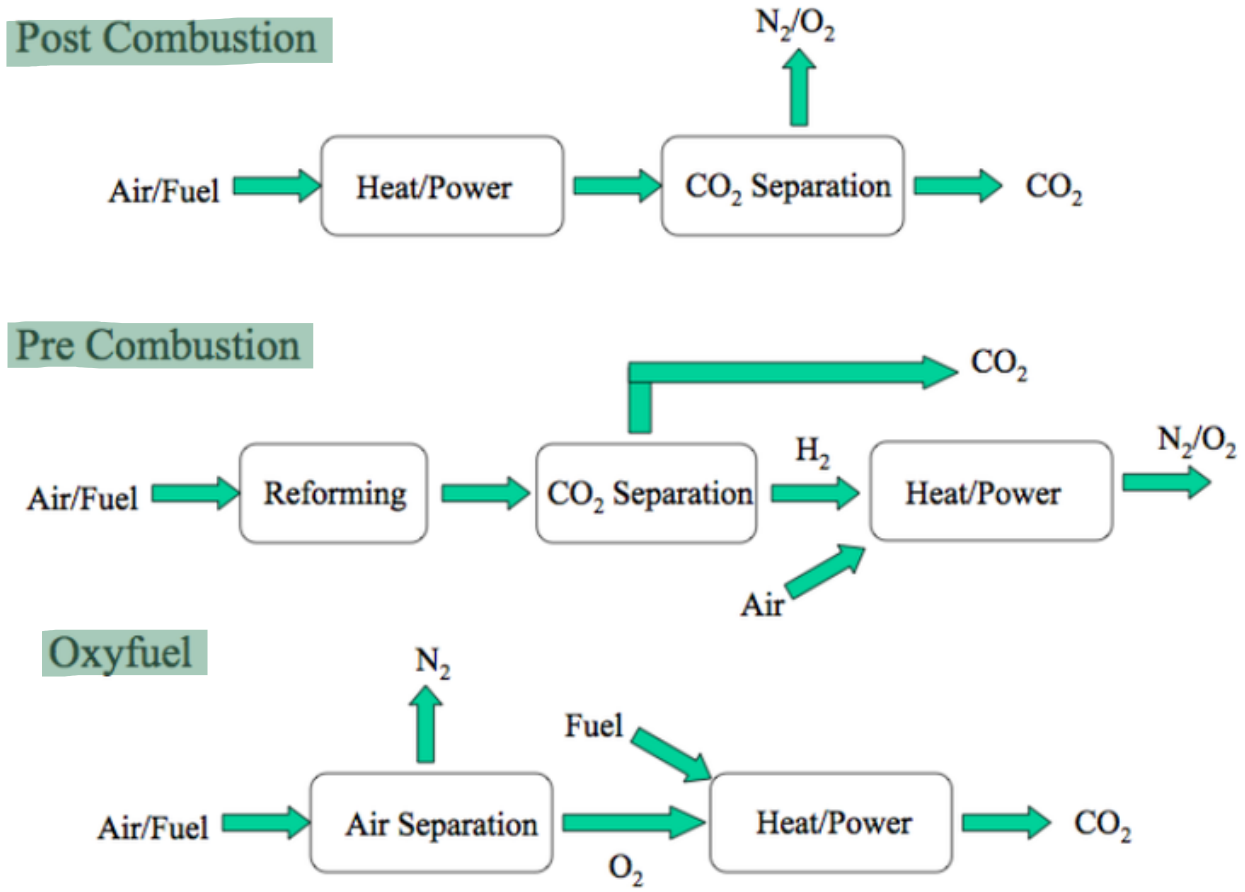

Figure 2.1. Various techniques for CO_2 capture. Collected from (F. Zeman, 2008).

2.2 Adsorption and Absorption

Adsorption is a process that occurs when an individual molecule, atom, or ion, such as gas or liquid binds to the surface of a solid. While *absorption* is when a liquid is soaked up completely into an absorbent material, like a visual sponge/cloth. In relation to (Yu et al., 2012), these two terms are believed to be very appropriate and important in CCS and when capturing CO_2 in MOFs.

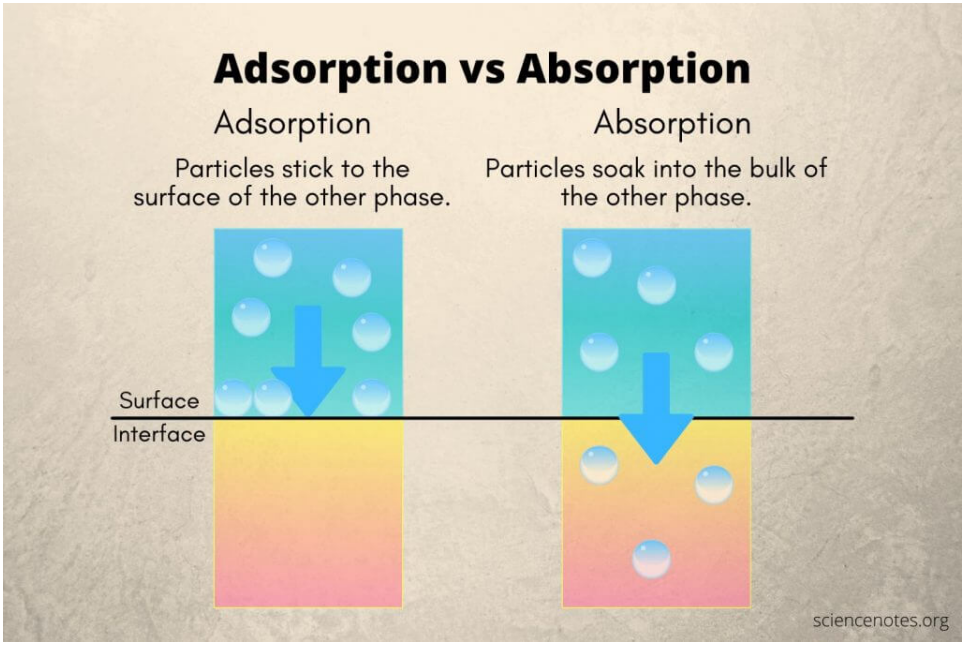

Figure 2.2.1 Adsorption vs Absorption. Collected from (Helmenstine, 2022).

As reported by (Samanidou, et al., 2019), Lewis's acid-base interactions are the most usual adsorptions mechanism for the metal ions in MOFs. The presence of oxygen, nitrogen and sulfur are some groups that works as Lewis-bases, are therefore important in interaction with aquatic solutions where metal ions work as Lewis-acids. Lewis's theory considered that Lewis's acids and bases are reactions of electron-pairs acceptor and donors, where Lewis bases can donate pair of electrons, and Lewis's acids can accept electrons to form covalent bonds between them.

The construction of a complex porous material consists of micro-, meso- and macro composite. These terms are important to understand absorption. In consonances by (Solano and Vega-Baudrit, 2015), micropores have a diameter less than 2 nm, while mesopores contain pores with a diameter between 2 nm and 50 nm and macropores a diameter bigger than 50 nm.

When measuring nitrogen or carbon dioxide levels in MOFs, pressure is being used to "push" the compounds into the "cages", accordingly micro-, meso- and macro pores, so that all empty place in the MOFs is taken advantage of. During physical adsorption, Van der Waals forces will bind the CO_2 inside the MOF without chemical reactions, according to (Y. Artioli., 2008), and iconic and covalent bonds could occur during chemical adsorption. Gas absorption is related to the re-distribution to when a gas phase is in contact with and dissolves in a liquid phase, and equilibrium is reached. The figure 2.2.2 below, will give an indication of how CO_2 sources could be captured both during absorption and adsorption.

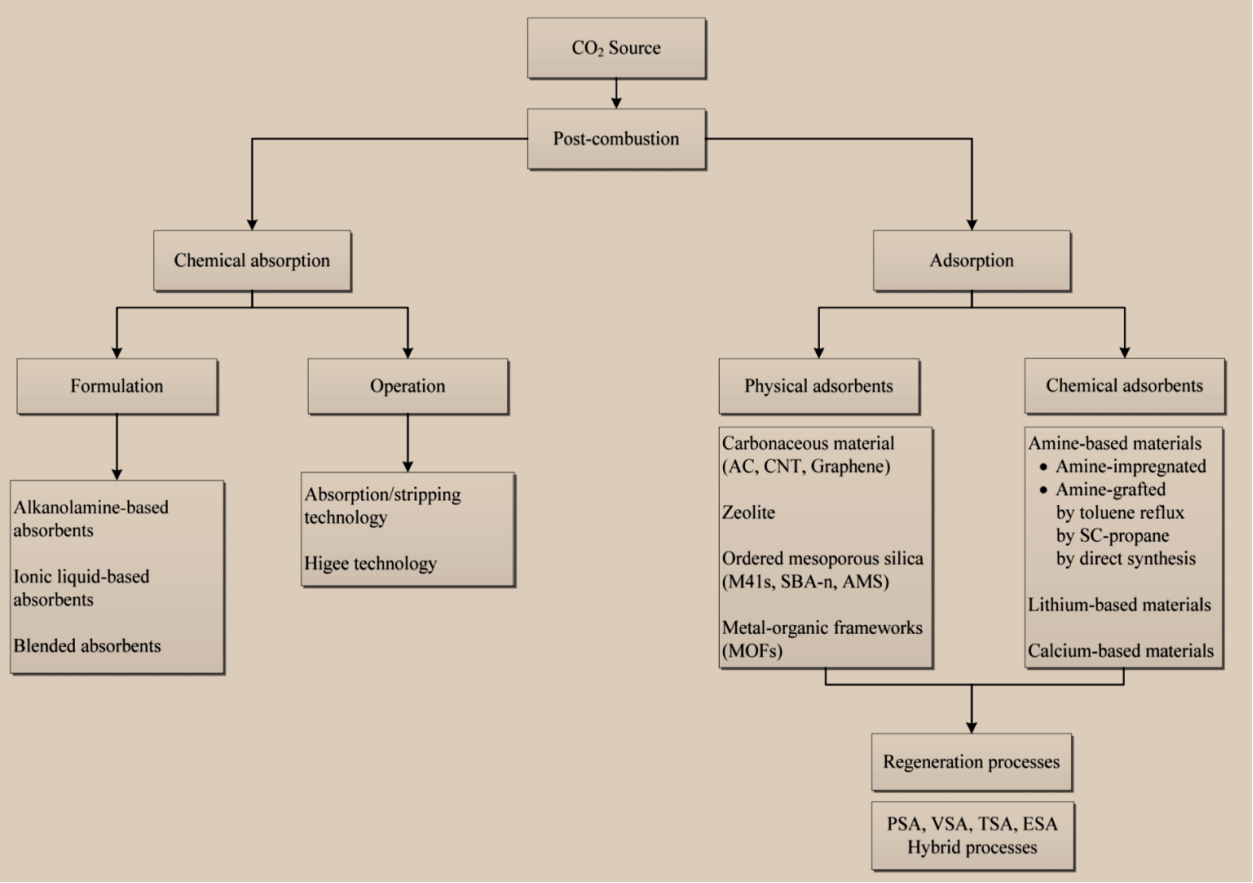

Figure 2.2.2 CO_2 capture by adsorption and absorption.
Collected from (C-H. Yu, et al., 2012).

According to (Ünveren et al, 2016) it is important to have a suitable adsorbent which consists of a porous support to which an amine can be attached to in a chemical adsorption of CO_2. Such absorbent is often called a solid amine sorbent. CO_2 can then be captured by adsorption on the surface of this specific sorbent.

2.3 Metal Organic Frameworks

2.3.1 MOF Structure

Metal organic framework “MOFs”, are made up of metal centres and organic linkers, as shown on the picture below (Zhang., 2020). There are innumerable variants, depending on different kinds of metal atoms and organic linker, and it can form both one-, two- or three-dimensional structures. According to (Berger., 2022), the metal ions form nodes that bind the arms of the linkers together to form a repeating, cage-like structure. Because of this hollow structure, the MOFs have an extraordinarily large internal surface area.

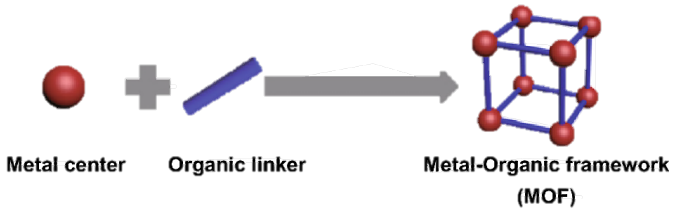

Figure 2.3.1 Structure of a general MOF. Collected from (Zhang., 2020).

The MOF is porous, crystalline organic-inorganic material. Due to the structure, porosity and the big internal surface, molecules could both be filtered, separated, and stored within the pores (Berger., 2022). Subsequently, MOFs are attractive candidates to meet the needs of energy storage technology (Baumann., 2019), and it has been reported a material that feature a surface area of more than 7800 square meters per gram.

Not more than 25 years ago, there was a noticeable absence of such structures where molecular building blocks were connected through strong bonds to form porous crystalline 2D- and 3D frameworks (Freund., et al, 2021). Several numbers of promising candidates have been discovered. Below one can see the development of these types of materials the recent years.

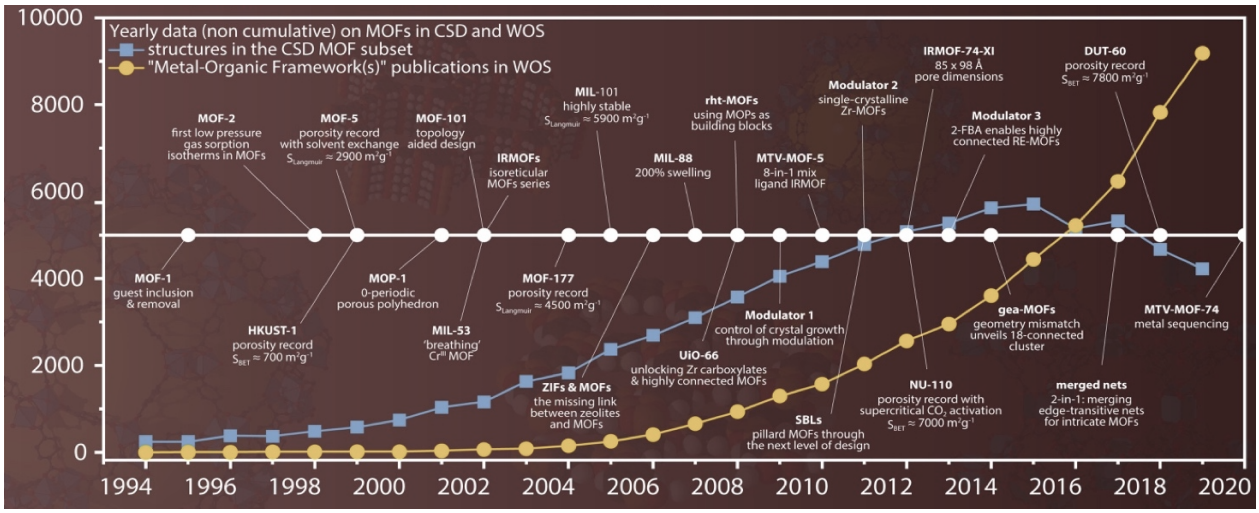

Figure 2.3.2. Timeline for the publication on some major MOFs. Collected from (Freund., et al, 2021)

The synthesis of MOFs includes the process of crystallization, where the nucleation and development of crystals occur. The MOFs structure are established by the nodes, metal-oxygen clusters, and the “bridges” formed by organic linkers.

The method for MOF synthesis is solvothermal (Marzouki., 2019), which is a chemical reaction that happens in a solvent, using a temperature higher than boiling point for this specific solvent. The solvent could be either water, ethanol, or other organic/inorganic liquid substance.

Reported by (Marzouki., 2019), the metal source and organic linkers are normally dissolved in a solvent and left with heat below 220°C. The reaction times varies from a couple of hours to several days.

Modulator is sometimes being added in the reaction mixture of MOFs, with the purpose to slow down the crystallization process, and to allow the MOFs to build up in a controlled way, which will make the structure better. Reported from (Jones., 2014), modulator normally consists of monocarboxylic acids, which competes with the organic linkers to bind to the metal centres.

2.3.3 Field of Application

MOFs has a unique structure and a wide range of applications, such as gas separation, gas storage, catalysis to drug delivery, and water treatment (Diab et al., 2021), which have been studied widely in the past years. The relationship between structure and field of application has a central role here. Due to the many structures, the properties and functions will be somewhat different.

In general, MOFs have shown good availability for membrane-based gas separation because of the very high pore volumes and surface areas. This part is depending on many factors, including purity, polarizability, and pore size. The differences in diffusion and sorption coefficient are crucial for gases to separate through the membrane (Qian et al, 2020). This method of separation is attractive for CO_2 capture because it does not require much energy. The MOF structure can be illustrated analogous to sponges, where “pockets” can capture and store chemicals like carbon dioxide for instant. These “pockets” can be micro-, meso- and macro pores. Free electrons either from linkers, clusters, or the modulators, can also react with CO_2 to capture it.

After capturing the chemical of need (CO_2), it can be pumped and stored safe underground in deep rock formations or even beneath the sea in suitable oil and gas reservoirs.

2.3.4 MIP-202

The MIP-202 (Materials of the Institute of porous materials from Paris), is a white powder with the general chemical formula $C_{24}H_{34}N_6O_{32}Zr_6$. This MOF consists of Aspartic acid as a linker and hexa-nuclear zirconium cluster as a metal centre. Aspartic acid is an amino acid, which has a lot of benefits, included that it is non-toxic, green, and cheap. Aspartic acid is available to purchase in D, L and DL form.

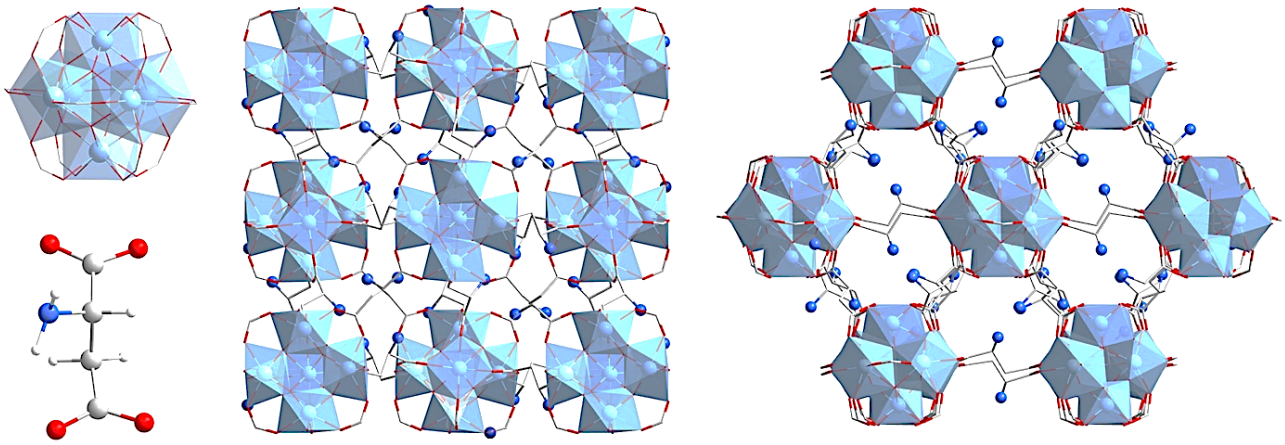

Figure 2.3.4.1 Structure MIP-202(Zr). Collected from (Wang et al., 2018)

As showed in the figure above, one can see the hexa-nuclear zirconium clusters as light blue, and the aspartic acid linkers showed to the bottom left, which is forming a 4-lattice structure. Six zirconium-oxo clusters are connected by 12 aspartic acid linkers giving the formula $Zr_6(\mu_3\text{-}O)_4(\mu_3\text{-}OH)_4(COO^-)_{12}$.

A fully protonated MIP-202(Zr), is reported to have a pore volume of 0.1 cm3 g−1 and a free pore diameter less than 0,4 nanometres (Wang et al., 2018), which could be classified as a microporous material.

The MIP-202 is also build from α-amino acid and has a steady and high proton conductivity (Wang et al., 2018). The material is chemically stable under various conditions, both for heat and for variations of the pH range, which makes this type a potential candidate for gas separation applications.

In this thesis, both L-, D-, and DL-Aspartic acid is used, which is an acidic amino acid that contains functional groups, more specific two carboxylic groups (-COOH) and one amine group (-NH2).

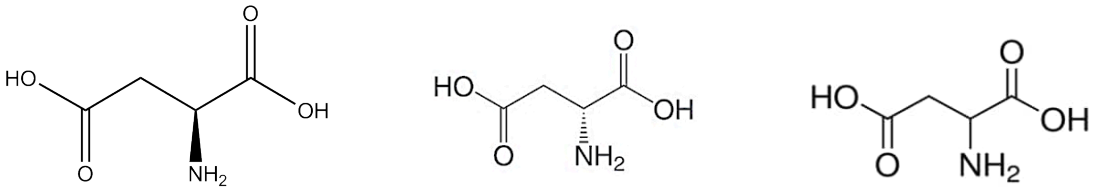

L-Aspartic Acid D-Aspartic Acid DL-Aspartic Acid

Figure 2.3.4.2 Differences in structure for Aspartic Acid.

There are not large dissimilarities between the isomers for aspartic acids. As shown in the figures above, they all have the same chemical formula, but the structure of L- and D-Aspartic acid are stereoisomers to each other, meaning that one enantiomer is the mirror image of the other enantiomer. Later in this thesis, it will be discussed if there are any essential differences between the isomers, presented from the analyzes.

The MIP 202 contains free amine functional groups attached to the linkers. This one is especially interesting, because it can interact with CO_2, and bind them together due to the valence electron on the amine (Shao and Stangeland, 2009). See figure below.

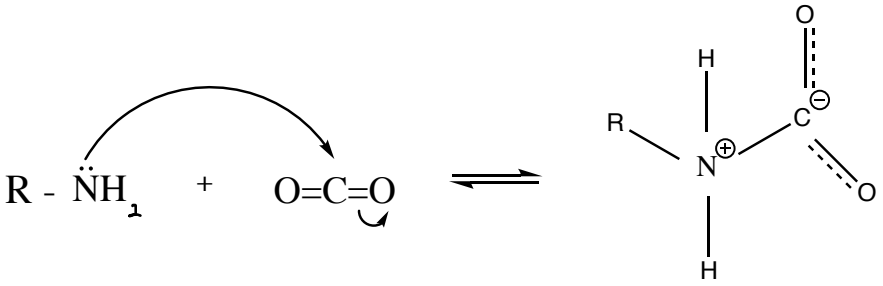

Figure 2.3.4.3 How amines and CO_2 can interact.

The reason for using aspartic acid, is because of the special structure and good properties it is giving. The MIP-202 contains both anions and amine group, which is two incompatible possible ways for capturing CO_2, and in this specific MOF it is probably the two main interactions for this mission.

As mentioned, the amine group originates from aspartic acid, and according to (Dutcher et al., 2015), amine-based materials is one of the notable technologies for CO_2 capture. Amines has a high affinity for acidic gas molecules like carbon dioxide, nitrogen and so on.

Amines are also known for their reversible reactions with CO_2, that makes it good for separation for this gas, including flue gas. That is perhaps the reason that MIP-202(Zr) is reported to be very selective and one of the MOFS with highest affinities for CO_2

uptake, indeed due to the amines. The material is reported to have a BET specific surface area on 350 m^2/g.

According to (Wang et al., 2018), the Zr^{4+} leads to a strong acidic solution, which infects the conformation of the amino group containing linkers. Because of this, it is necessary with high concentrations of the reactants to be able to give a solid product.

Zirconium is a transition metals which has valance electrons, and it is reported to be a non-toxic chemical to the environment and even organisms. (Wang et al., 2018) reports that MIP-202(Zr) shows very decent proton conductivity up to 0,011S cm^{-1} at 363 K and this makes this MOF one of the best noticeable so far. One of the reasons to use MIP-202 is also because of the good stability it has, considering how it reacts with many different solvents, like water, ethanol etc.

It is reported from (Chem. Sci., 2019), that MOFs containing high-valent metals, such as including Zr4+, Cr3+, Al3+, Fe3+ are forming great chemical stability. The MIP-202 contains Zr^{4+}, which are classified to be a hard acid. Based on the "Hard and Soft Acid and Base" Theory, where hard acids tend to bind to other hard bases and opposite, the Zr^{4+} in MIP-202 forms a strong interaction with the amines, which is a hard base. Because of the reaction between the basic metal and the acidic amines, a full protonation will most likely occur, which leads to zwitterionic ligand.

In agreement with (Wang et al., 2018), there are some challenges due to chloride, and it can connect to the MIP-202 in at least two different ways. The first one, is by reacting with NH_2, giving two extra chlorides. The problem with chlorine getting attached to the MOF, is not only because it could be polluted to the environment, but it could also "take up place" inside the MOF, instead of carbon dioxide. The other possible reason could be that some linkers are missing and replaced with chlorine, and in fact the main goal with these MOFs is to make a green and cruelty free compound, we would like to get rid of chlorine.

It is suggested from (Wang et al., 2018), that the amino groups in the MIP-202 are present in the form of $-NH_3^+-Cl^-$. If this is the case, it could play a critical role when it comes to the porosity, due to the pore size. That could be a possible reason for chlorine to "take up" space in the pores and lead to worse sorption uptake.

3. Thesis Objective

The main task was to create a MOF that showed good porosity and sorption of carbon dioxide. This led us to the article created by (Wang et al., 2018). They had reported a MOF called MIP-202, which is based on zirconium and aspartic acid. According to them, this MOF showed good stability under various conditions, as well as solutions of wide pH range and boiling water. They have also reported that this is the only amino acid-based MOF, that have a good hydrolytic and chemical stability. Various isomers of the amino acid were used, in fact L-isomer, D-isomer and a racemic mixture, and later in the thesis it will be discussed if there are any essential differences between them, as mentioned under future work in (Damås, 2022).

Furthermore, as suggested in (Skjærseth, 2021), analyses of the produced MIP-202 were taken to find out the chlorine content by using SEM-EDS. This turned out to be an issue, and various washing procedures and different synthesis were attempted. Tried to purify the products by using high temperatures and pressure in autoclaves. A new bulk using high through-put synthesis was also made, where both $Zr(SO_4)_2$ and $ZrOCl_2$ was attempted as metal source instead of ZrCl4, together with D,L-aspartic acid and either formic acid or acetic acid as modulator.

The active choices of parameters such as metal sources, linkers and solvents has shown to be central to make an optimal MOF. This led us to try out a new synthesis with high temperature, using autoclaves for 120 °C and 140 °C. This experiment was to see if it could help purify the materials.

Then found out that a previous student (Skjærseth, 2021), had reported that changes in reaction time could give remarkable difference. Therefore, made a new synthesis using 72 hours reaction time, and compared to the previous made 1 hour synthesis. To optimize the products, different washing methods was used. Below is an overview of the procedures that has been followed in this thesis, in particular order, to confirm if the products and adjustments made along the way, was useful or not. Then new alterations were tried out and followed same procedure over again.

1. Making synthesis
2. Washing part for optimalization
3. PXRD
4. SEM-EDS
5. TGA
6. Degassing
7. N_2 sorption → CO_2 sorption

4. Materials and Methods

4.1 Materials

Zirconium (IV) chloride, $ZrCl_4$ (99,5% Sigma Aldrich), D-Aspartic acid (99+%, Acros organics), L-Aspartic acid (99%, Merck), DL-Aspartic acid (98+%, Thermo scientific), Ethanol (absolute, Supelco), Acetone (≥99%, VWR), Zirconium (IV) sulfate, $(Zr(SO_4)*4H_2O$ (98%, Thermo scientific), Zirconium dichloride oxide octahydrate $(ZrOCl_2*8H_2O$ (98%, Thermo scientific), Acetic acid (≥99.8%, Merck), Formic acid (89-91%, Supelco).

4.2 Synthesis of MOFs and Preparations

To synthesis a MOF, there is a huge number of divergent methods, depending on what type to make. In this thesis it was made both MIP-202 and a new type of MOF using zirconium (IV) sulphate or zirconium (IV) oxychloride octahydrate as the metal source and formic acid or acetic acid as modulators. Some small differences along the way were tried out, to see if it could affect the results and analysis. This will be discussed later in this thesis.

4.2.1 Synthesis of MIP-202

The synthesis of MIP-202 was collected from (Wang et al., 2018). It was made three different samples, by using L-Aspartic acid, D-Asp, and a mixture of them both DL-Asp.

The synthesis was simply prepared following the procedure reported, and started by adding 2,7317g of L-Aspartic acid, 2,8003g D-Aspartic acid and 2,8005g of DL-Aspartic acid in three different 50ml round bottom flask and adding 5 ml water. Further 2,282g/2,3307/2,3318g in the same particularly order of $ZrCl_4$ was added to the three individual flasks in small portions, releasing heat, and making a specific sound. This sound, bubbles and heat that got released is probably coming from $ZrCl_4$ and H_2O reacting together to form HCl.

After, 5 more ml of water was added to the solutions to make sure to get the sides clean. The mixtures got clear and colorless. The compound got heated up to 120 degrees, under reflux for one hour with ambient pressure and continually stirring at 400 RPM. The solution got white, slightly grey within a few minutes, and then all white and cloudy when reached around 120 degrees. After the reaction time of 1 hour, the solution got cooled down to room temperature, and then washed and centrifugated 3 times with distilled water and then twice with ethanol. The mixture was air drying for 2-3 days, giving the amount of white solid product, MOF.

The theoretical weight for the samples using 1 hour reaction time was 2,39g, and the actual weight turned out 2,1717g for L-Asp, 2,7871g for D-Asp and 1,6519g for DL-Asp. Giving the percentage yield on the samples 90,87% for L-Aspartic acid, 116% for D-Aspartic acid and approximately 70% for DL-Aspartic acid.

For the products using 72 hours reaction time, the actual weight was 3,4756g L-Asp, 3,1209g D-Asp and 3,3789g DL-Asp. This gave the percentage yield 145% for L-Asp, 130% for D-Asp and 99,5% for DL-Asp. The reason for the yield to be more than 100% is probably due to that the product had not dried for enough time, causing the product to still be moist. Another reason could be that there are still some unreacted linkers, which can result from insufficient reaction time.

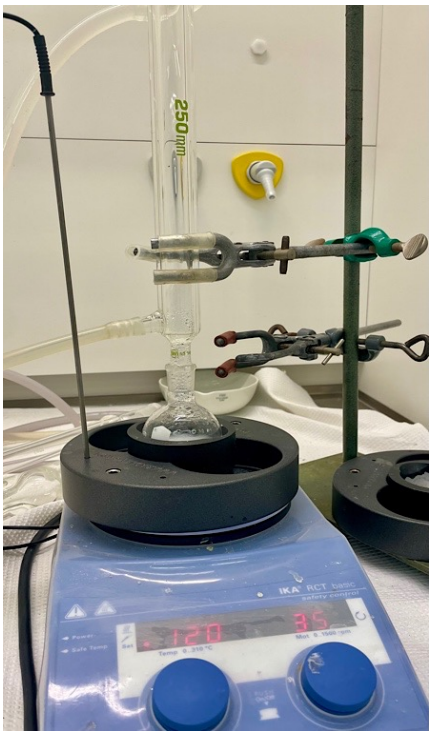

Figure 4.2.1. Synthesis set up for MIP-202, using a round bottom flask placed on a hot plate with continually stirring and a reflux condenser.

To optimize the materials, different methods has been used. Both changing the reaction time, wash the samples with different solvents and for different amount of time, filtration/centrifugation etc. Look at “4.2.4 Product Washing and Optimalization” below, to get an overview of exactly what has been done with the various samples.

4.2.2 MIP-202 Synthesis using Autoclaves

This synthesis was prepared in a similar way as the MIP-202 described above, but the differences was to do it in high temperatures. 2,8020g of DL-Asp was placed in one round bottom flask with 2,8083g $ZrCl_4$, and 2,3356g DL-Asp with 2,3372g $ZrCl_4$ in another round bottom flask. The reaction mixture was placed inside two separated Teflon liners, and then inserted the liners inside the autoclaves. The autoclaves were then placed into two different ovens, one set on 120°C and the other on 140°C for 24 hours. The autoclaves got cooled down to room temperature and collected the product by centrifugation and washed with water three times and ethanol twice. The product was a white, soft powder.

Figure 4.2.2. Autoclaves samples, using DL-Asp and 120°C/140°C.

4.2.3 Bulk synthesis using Zirconium (IV) sulfate/ Zirconium (IV) oxychloride octahydrate and Formic Acid/Acetic Acid

The bulk synthesis was prepared by using a high-throughput synthesis, giving 24 different samples. Metal salt ($ZrOCl_2$*$8H_2O$ or $Zr(SO_4)_2$ * $4H_2O$), was first dissolved in 609 ml water, and then added 25 mg of D,L-Aspartic Acid as the linker. Modulator, acetic acid or formic acid was then added in different amounts (0, 10, 20, 30, 40 and 50 equivalents). The solution was heated up to 97 degrees and stirred overnight.

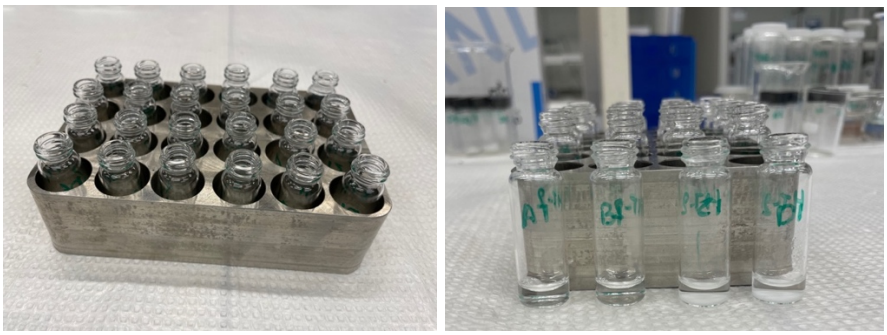

Figure 4.2.3. High-throughput synthesis, all these samples were placed on a hot plate, with continually stirring for 24h, using 97 degrees.

4.2.4 Product Washing and Optimalization

The synthesis and washing involves green solvents only, using water, ethanol, sodium acetone and/or >99% acetone to remove excess of unreacted free linker and unwanted chemicals, like chloride. The MIP-202 with both 1h reaction time and MIP-202 with 72h reaction time were washed differently many times, as showed below. The downside for these experiments, was that it could end up destroying the whole MOF structure, which truly happened to some of them.

Washing sample 1: Took 200 mg of the already made MIP-202 1h reaction time of both L-, D-, and DL-Asp and washed with 12ml 0,1M sodium acetate 3 times. The vials were centrifugated for 20 minutes each at 4000 RPM. Then washed the samples with 15 ml distilled water twice and once with 15 ml ethanol, and centrifugated for another 10 minutes each. The vials got shaken roughly between each washing. Then it airdried in the fume hood.

Washing sample 2: Took 0,2g DL-Asp from already made MIP-202 1h reacion time and washed with 20ml ethanol thrice in the centrifugation for 10 minutes each and 3000 RPM. Then the sample were left with 20ml ethanol on the bench for 24 hours. And after letting it airdry under the fume hood.

Washing sample 3: Took 500 mg sample of L-, D-, and DL-Asp from the already made MIP-202 72h reaction time and washed with 15ml ethanol placed on a stirring plate for 3 days. The ethanol got changed twice during the three days, after around 16 hours. Then the product was collected by filtration.

Washing sample 4: Took 500 mg sample of L-, D-, and DL-Asp from the MIP-202 1 hour reaction time and washed with 15ml ethanol placed on a stirring plate for 3 days. Changed the ethanol every 16 hours. The product was then collected by filtration.

4.3 Methods

Different methods and measurements were used to characterize and analyse the composition, stability, and crystallinity of the products, such as powder X-ray diffraction, thermogravimetric analysis, scanning electron microscope and energy dispersive X-ray spectroscopy. Nuclear magnetic resonance spectroscopy was also used for specific samples. Nitrogen and carbon dioxide sorption was also measured to identify if the MOFs were porous or not.

4.3.1 Powder X-ray Diffraction, PXRD

X-ray powder diffraction is used to analyze the products made, both after synthesis and after treatment. According to (Dutrow and Clark., 2022), PXRD, is an analytical technique mainly used to identify unknown crystalline material, by revealing information about its dimensions and geometry of the unit cells of the crystal structure. The material that will be analyzed, is first finely grinded and homogenized.

The instrument consists of three elements: an X-ray tube, a sample holder, and an X-ray detector. These X-rays are directed at the sample, and the diffracted beams are collected. All diffraction methods generate X-ray beams which are directed at the sample in the X-ray tube.

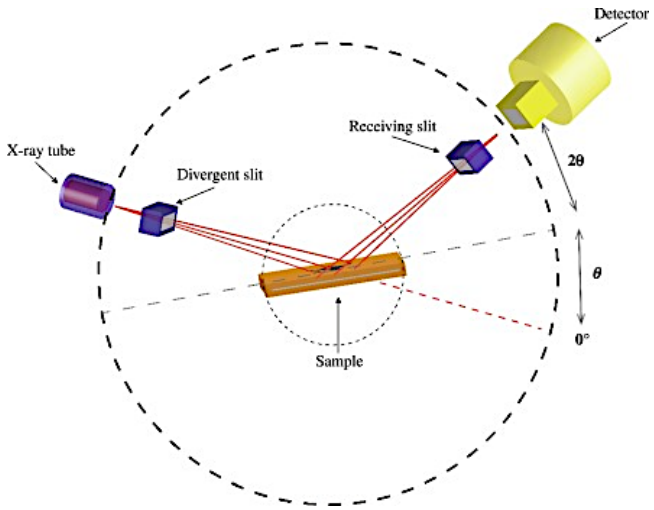

Figure 4.3.1 Powder X-ray Diffraction. Collected from (Falsafi et al., 2020)

The Bruker AXS D8 Advance/D8 Discover X-ray diffractometers are optimally designed for use in all X-ray diffraction applications in material research, powder diffraction and high-resolution diffraction. The benefit of using this machine is that it allows to quickly change between samples, environments, and optic setups *(*D8 Series, User Manual*,* 2014, p. 1).

Based on (D8 Series, User Manual, 2014, p. 18), X-rays are photons that are emitted when electrons strike a metal target and interact with the electrons orbiting the nuclei of the metal atoms. The electromagnetic waves in the λ-range 0.1-2 Å are emitted in all directions. In X-ray tubes electrons are emitted by heated cathode, accelerated, and strike an anode material.

Samples of different MOFs are using 2-70° theta, where 2 θ is the angle between transmitted beam and reflected beam. The analysis results could be compared to available structures from the same compounds using VESTA, with the purpose to identify if the structure wanted is present or not.

4.3.2 Nuclear Magnetic Resonance Spectroscopy, NMR

NMR are one of the most useful machines to analyze the molecular structure and the nuclear spin, and the relative intensity of radio wave adsorption is depending on the identity of the nucleus (Rayner-Canham and Overton, 2014, p. 246). By using strong static magnetic field, one can observe how the nuclear in the different compounds react. The procedure was conducted on the Ascend^{tm} 400 Sample Xpress, which allows automatic measurements of samples with Bruker.

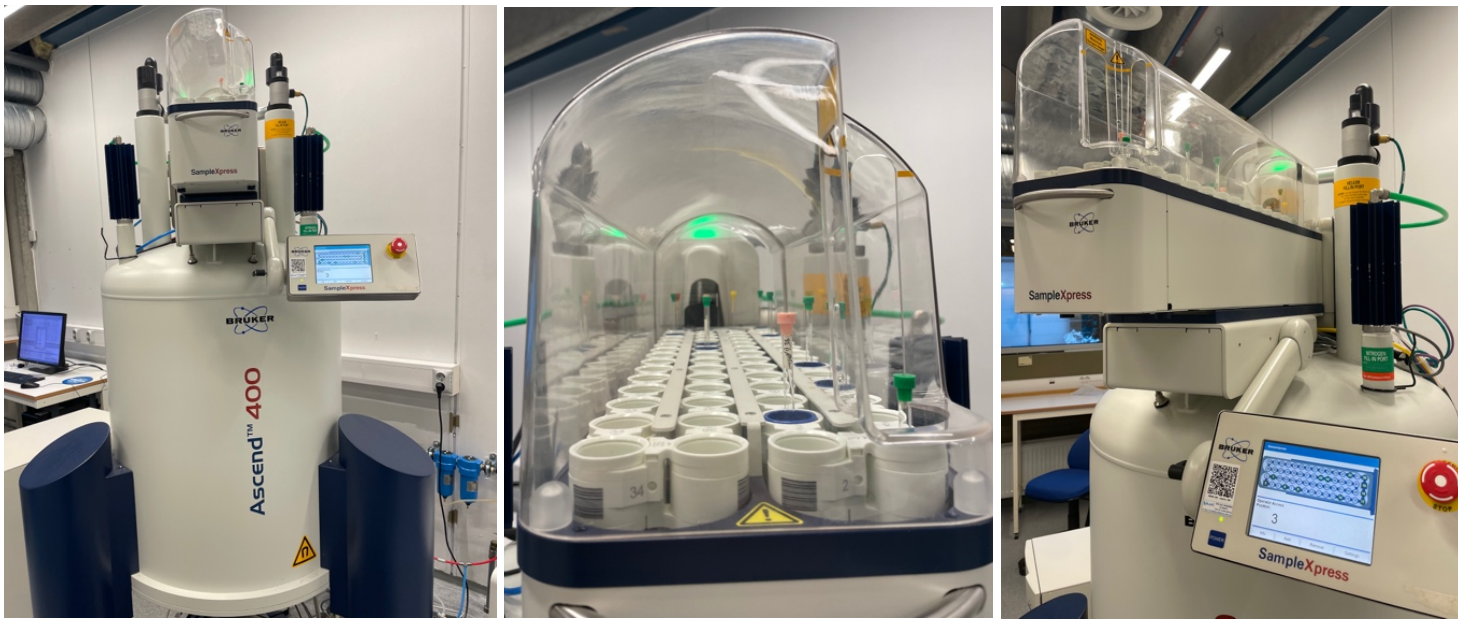

Figure 4.3.2 NMR Spectroscopy.

4.3.3 Thermogravimetric Analysis, TGA

Thermogravimetric analysis is a thermo-analytical technique that continually measures the weight changes of a sample at a given time, while heating or cooling it and looking at the gaseous biproducts that disappears. Around 15-20 mg of sample is placed in an alumina oxide crucible, and then the total weight of the product is measured. The analysis is turned on when the machine has reached 25 degrees. Furthermore, the temperature increases slowly and continuously from 25-900 degrees.

The released gas at certain temperatures, will change the total weight of the sample that is being analyzed. Both time and temperature measurements are essential to see when chemical changes take place, and to tell the stability of the products. Some of the benefits of the TGA machine includes very low minimum weight and wide temperature range.

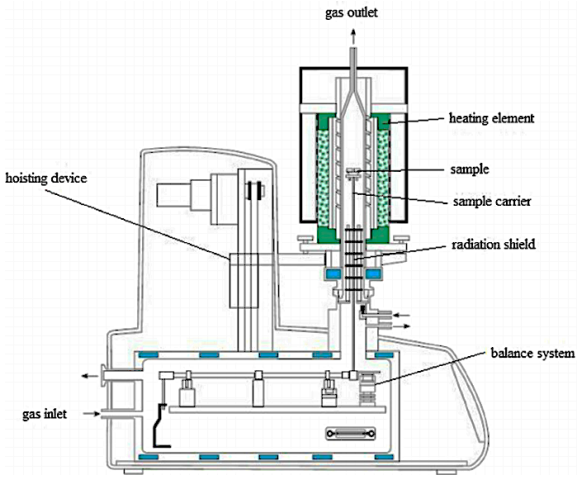

Figure 4.3.3.1 Thermogravimetric analysis. Collected from (Granados., 2014).

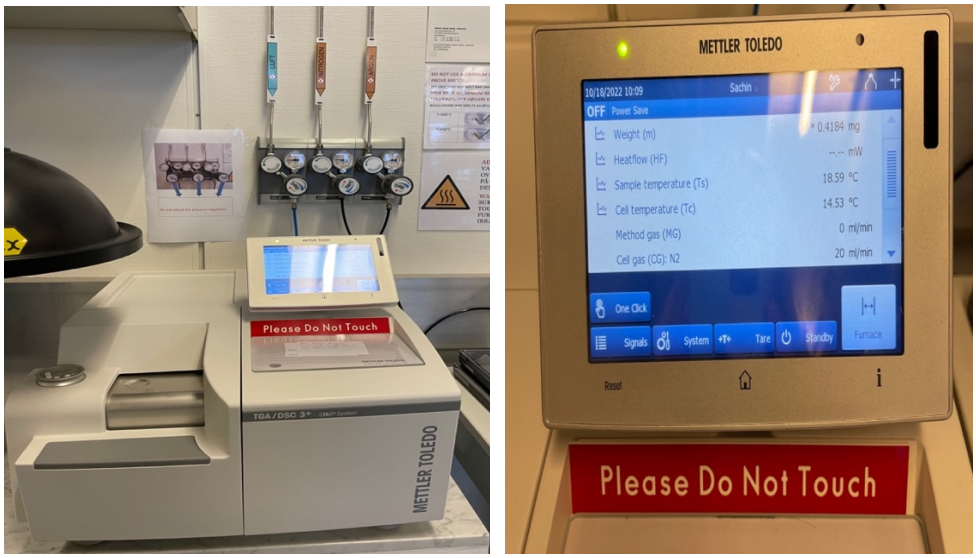

Figure 4.3.3.2 TGA, Mettler Toledo.

4.3.4 SEM-EDS

Scanning electron microscopes, SEM, are using electrons to strike the sample, which will make variation of surface images of the products analyzed (Yan., 2019). The images can give information about the size and how it is shaped. A bunch of electrons is produced at the top of the machine by an electron gun and follows a vertical path through the microscope and through the products. The electrons are held at place by a magnetic lens.

Some SEM machines are also available to do EDS measurements. The EDS detector is used to identifying and characterize the compositions of a compound in small samples (Goodge, 2017). EDS are made up of a sensitive x-ray detector, liquid nitrogen for cooling down and a software to analyze the energy for the different compounds (Goodge, 2017). The detector also consists of a crystal that absorbs energy into X-rays by ionization. The individual X-rays are different from each other in terms of proportional parts to different elements (Goodge, 2017), which therefore will determine the specific elements. The cons with EDS, is that there are some chemicals it will not indicate, for example hydrogen and lithium.

4.3.4 Degassing

The degas system consists of a vacuum pump and a heating element with controllable temperature. Degassing is a method to get rid of dissolved gases, and the samples were activated at 60 °C for mainly 22 hours (one sample was tried degassed over the weekend). The purpose by this is to reduce the atmospheric pressure and to ensure that the material, in this case the MOF, does not contain natural gases that can take up place for other gases that are going to be measured, such as nitrogen and carbon dioxide. Figure 4.3.6.1 below, shows a good image of how gases are stored within the cages of the MOF structure.

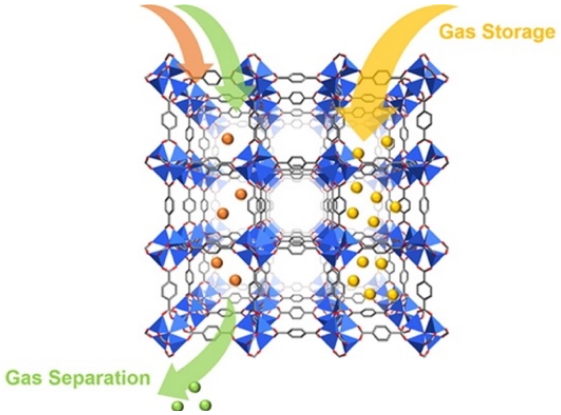

Figure 4.3.4. Gas storage in MOFs. Collected from (Li et al., 2018)

4.3.5 Sorption

The nitrogen and carbon dioxide sorption are a method for analyzing the porosity and surface area. For N_2 sorption this is measured by the amount of nitrogen that is being absorbed into the surface of the samples. Nitrogen is common to use, due to its high purity and strong interaction with many other solid adsorbents.

The micropores will be filled up first at low relative pressure, and by using liquid nitrogen obtaining temperature at 77K and the higher gas pressure will fill up meso- and macropores as well by time. It will first be formed a monolayer, before making multilayers as showed in picture below.

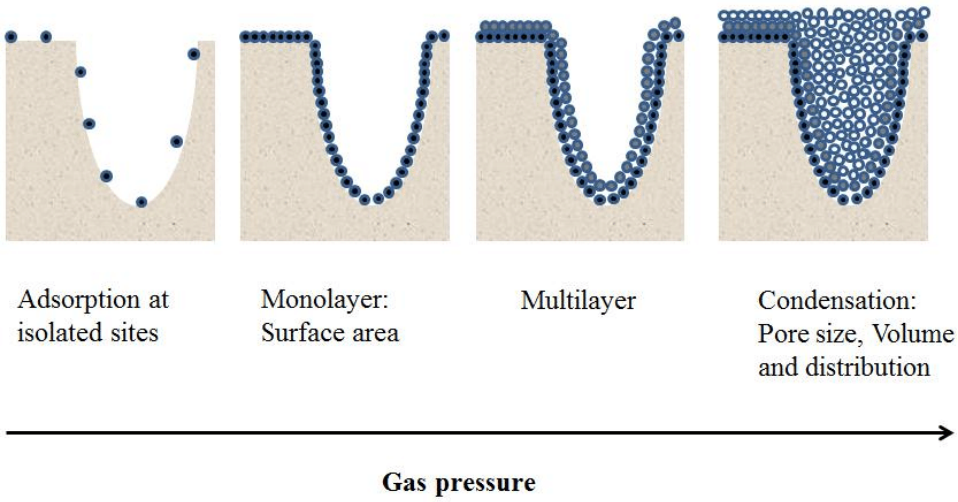

Figure 4.3.5.1 Sorption of gases, monolayer vs multilayers. Collected from (Sun., 2014),

The nitrogen sorption shows if the material examined is porous or not, which is crucial for further measuring of CO_2 uptake. If the products are not porous, further analysis of CO_2 uptake is not necessary. The same instrument is being used to measure the CO_2 sorption.

Temperature is an important parameter when analyzing the sorption kinetics (Hulscher and Cornelissen., 1996), and it is kept constant or under isothermal conditions, during the analysis. When measuring carbon dioxide sorption, ice cubes and room temperature distilled water is used to obtain 273K (0 °C). When for nitrogen sorption, measurements using much lower temperature at 77K, has been the standard tool for analysis for materials with a pore range between 0,5-50nm (Zelenka, 2016). To reach 77K, liquid nitrogen is filled up in the container. Pressure is however increased.

Figure 4.3.5.2 Micromeritics, VacPrep 061. Sample Degas System

Figure 4.3.5.3. Micromeritics Tristar 2. Surface Area and Porosity

To calculate the surface area and pore size for the synthesized samples, the BET theory developed by Stephen Brunauer, Paul Emmett and Edward Teller has been used (Raja and Barron., 2022). This theory extends the Langmuir theory from monolayer adsorption to multilayer adsorption, and it is specific used for microporous materials.

$$\frac{1}{V[(P0/P)-1]} = \frac{1}{VmC} + \frac{C-1}{VmC} * \left(\frac{P}{Po}\right) \quad \text{Equation 1}$$

Where V is the weight of nitrogen absorbed at the given relative pressure (P/Po). Vm is the monolayer capacity, which is the volume of gas absorbed at standard temperature and pressure, and C is the BET constant, related to the heat of absorption (Raja and Barron., 2022).

To calculate the monolayer absorbents, Vm, and the BET constant, numeric values for slope and intercept is being used:

Slope = $\frac{C-1}{VmC}$, and Equation 2

Intercept = $\frac{1}{VmC}$, leading to: Equation 3

$$Vm = \frac{1}{slope+intercept} \quad \text{Equation 4}$$

$$C = 1 + \frac{slope}{intercept} \quad \text{Equation 5}$$

Once Vm, the monolayer absorbed gas and the BET constant is determined, the total and specific surface area can be found by following equations, below.

$$St = \frac{Vm*N*S}{V} \qquad \text{Equation 6}$$

Where St is the total surface area. Vm is the monolayer of absorbed gas, and S is the cross-sectional area of the adsorbate, V is molar volume of adsorbed gas and N is Avogadro's number ($6{,}02*10^{23}$ mol^{-1}). The specific surface area can be determined by the equation below.

$$S_{BET} = \frac{St}{a} \ (m^2/g) \qquad \text{Equation 7}$$

There are different types of isotherms, as shown in the picture below.

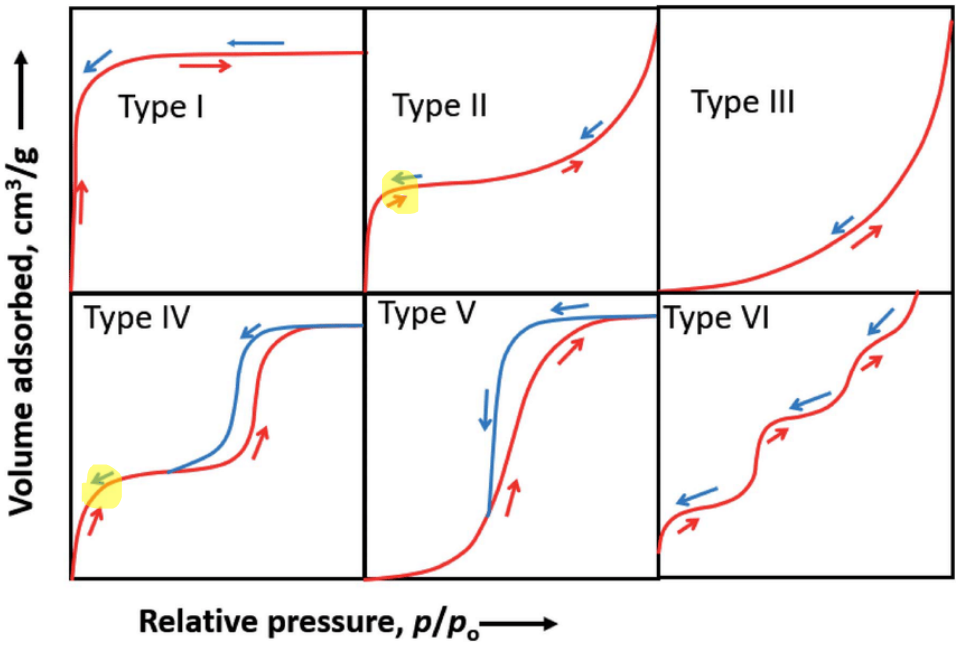

Figure 4.3.5.4. Different types of physisorption isotherms. Collected from (Kumar et al., 2019).

This figure shows both the adsorption and desorption. The top line indicates desorption and bottom line the adsorption. In isotherm two and four, it is marked out a specific place, which specify to the monolayer adsorption capacity (Lundstedt, 2019). Type I is microporous, Type II is non-porous or microporous, Type III is non-porous or microporous with weak interaction, Type IV is mesoporous, Type V is mesoporous with weak interactions and Type VI is layer by layer adsorption.

5. Results and Discussion

All the synthesis done in this thesis, is showed below in table 5.0. It includes the synthesis procedure and type of MOF that has been made, involving the metal source, linker, solvent and possibly use of modulators. In addition to reaction time, temperature during the synthesis and description of the product. The yield was also calculated for some samples. Washing procedures are also described more in detail under "4.2.4 Product Washing and Optimalization".

Experiment number	Sample	Metal	Linker	Solvent	Modulator	Reaction time	Reaction temperature	Product description	Theoretical weight	Actual weight	Actual yield	Synthesis	Washing procedures / comments
1	MIP-202	$ZrCl_4$	L-Aspartic acid	H_2O	-	1h	120°C	White powder	2,39g	2,1717g	90,87 %	Reflux	Washed with water and ethanol + centrifugation
2			D-Aspartic acid							2,7871g	116 %		
3			D/L-Aspartic acid							1,6519g	70 %		
4			L-Aspartic acid						-				Washed with ethanol 24h (after normal washing routine: 3xwater, 2xethanol)
5			D-Aspartic acid										
6			D/L-Aspartic acid										
7			L-Aspartic acid										Washed with 12ml 0,1M sodium acetone x3 in centrifugation.
8			D-Aspartic acid										
9			D/L-Aspartic acid										
10	Bulk-sample	$ZrOCl_2 * 8H_2O$	D/L-Aspartic acid	H_2O	Acetic acid, 0ml	Overnight	97°C	Gel	-			High-throughput synthesis	-
11					Acetic acid, 10ml			Gel					
12					Acetic acid, 20ml			Gel					
13					Acetic acid, 30ml			Gel					
14					Acetic acid, 40ml			Powder					
15					Acetic acid, 50ml			Powder					
16	Bulk-sample	$ZrOCl_2 * 8H_2O$	D/L-Aspartic acid	H_2O	Formic acid, 0ml	Overnight	97°C	Gel	-			High-throughput synthesis	
17					Formic acid, 10ml			Gel					
18					Formic acid, 20ml			Gel					
19					Formic acid, 30ml			Gel					
20					Formic acid, 40ml			Powder					
21					Formic acid, 50ml			Powder					
22	Bulk-sample	$Zr(SO_4)_2 * 4H_2O$	D/L-Aspartic acid	H_2O	Acetic acid, 0ml	Overnight	97°C	Powder	-			High-throughput synthesis	-
23					Acetic acid, 10ml								
24					Acetic acid, 20ml								
25					Acetic acid, 30ml								
26					Acetic acid, 40ml								
27					Acetic acid, 50ml								
28	Bulk-sample	$Zr(SO_4)_2 * 4H_2O$	D/L-Aspartic acid	H_2O	Formic acid, 0ml	Overnight	97°C	Powder	-			High-throughput synthesis	-
29					Formic acid, 10ml								
30					Formic acid, 20ml								
31					Formic acid, 30ml								
32					Formic acid, 40ml								
33					Formic acid, 50ml								
34	MIP-202	$ZrCl_4$	D/L-Aspartic acid	H_2O	-	24h	120°C	White soft powder	-			Autoclaves	
35							140°C						
36	MIP-202	ZrCl4	L-Aspartic acid	H_2O	-	72h	120°C	White powder	2,39g	3,4756g	145 %	Reflux	Followed same procedure as Petters sample #13. 72 hours activation, washed with distilled water and collected sample by filtration.
37			D-Aspartic acid							3,1209g	130 %		
38			D/L-Aspartic acid							3,3789g	99,50 %		
39	MIP-202	ZrCl4	L-Aspartic acid	H_2O		72h	120°C	White powder	-			Reflux	Washed with 15ml ethanol placed on stirring plate. Changed the ethanol twice, after approximately 16h. Then collected product by filtration.
40			D-Aspartic acid										
41			D/L-Aspartic acid										

Table 5.0. An overview of all the synthesis

5.1 Chlorine-Free Route

5.1.1 High Put-Through Synthesis

One of the first experiments, was to try produce a chlorine-free MOF. $ZrOCl_2$ and $Zr(SO_4)_2$, and different amounts of modulators, acetic acid or formic acid, was then tried.

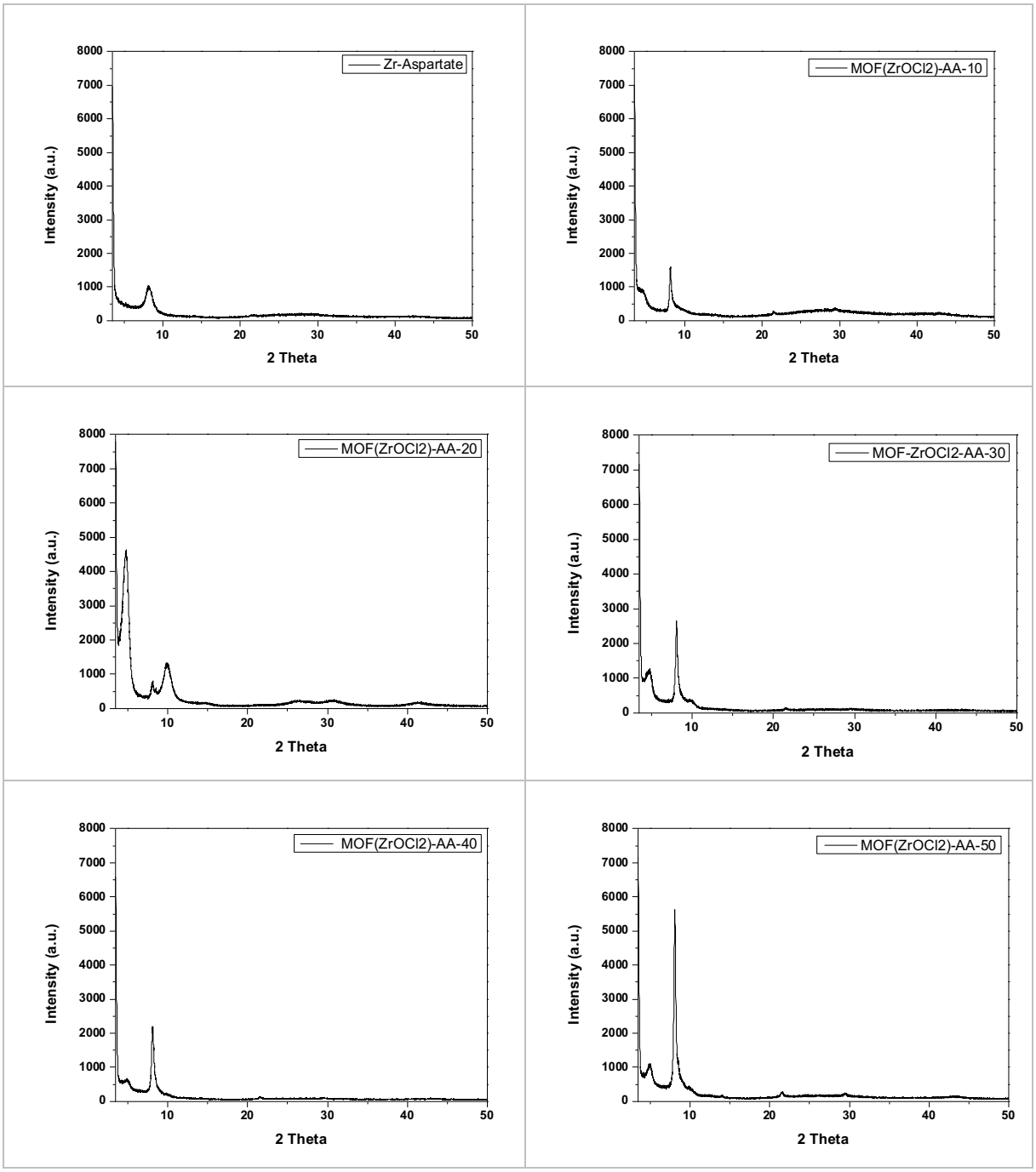

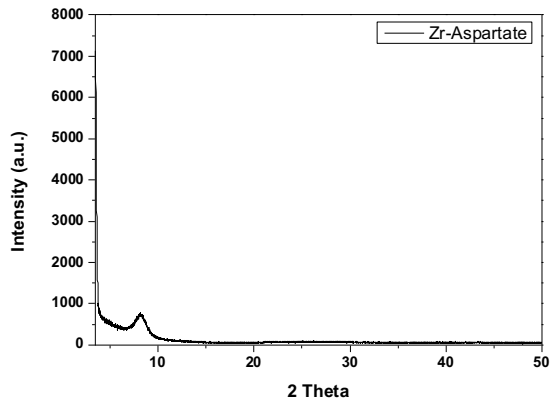
Zr-Aspartate
Intensity (a.u.)
2 Theta

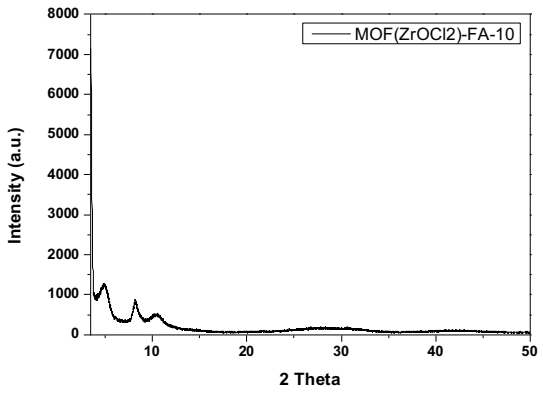
MOF(ZrOCl2)-FA-10
Intensity (a.u.)
2 Theta

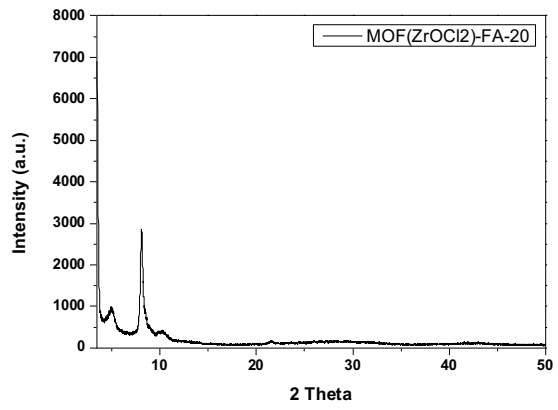
MOF(ZrOCl2)-FA-20
Intensity (a.u.)
2 Theta

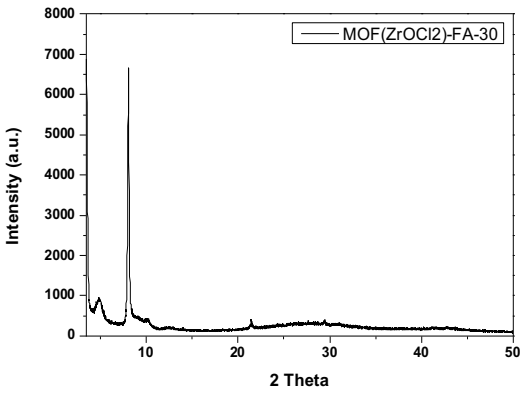
MOF(ZrOCl2)-FA-30
Intensity (a.u.)
2 Theta

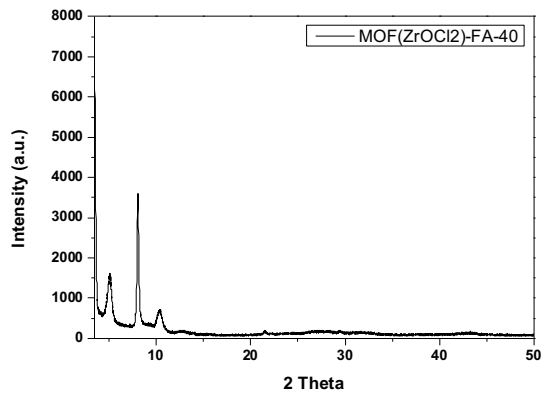
MOF(ZrOCl2)-FA-40
Intensity (a.u.)
2 Theta

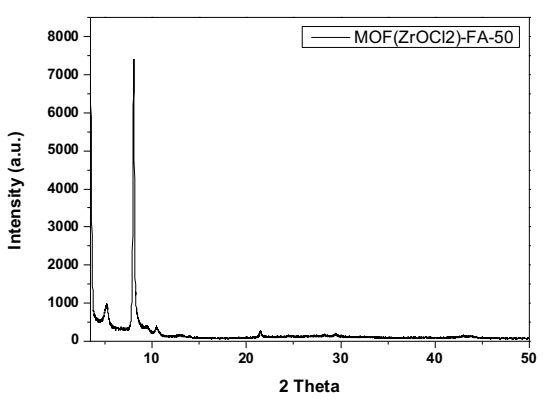
MOF(ZrOCl2)-FA-50
Intensity (a.u.)
2 Theta

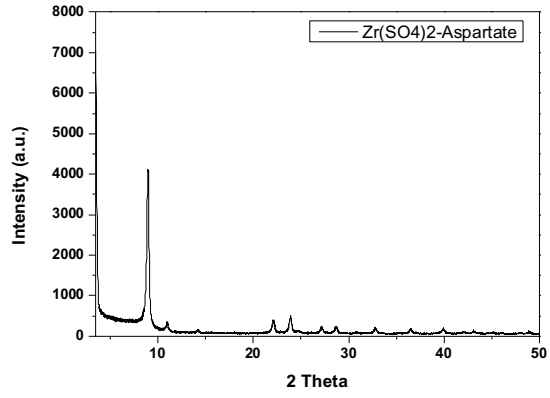
Zr(SO4)2-Aspartate
Intensity (a.u.)
2 Theta

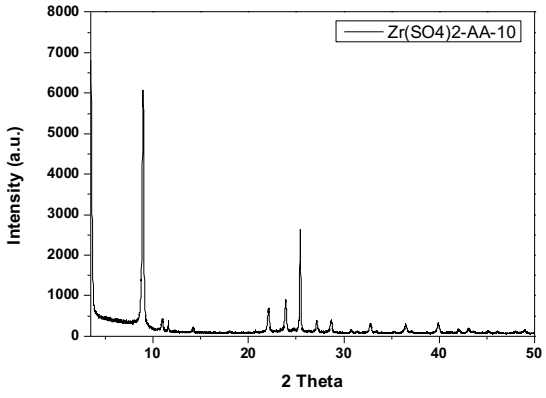
Zr(SO4)2-AA-10
Intensity (a.u.)
2 Theta

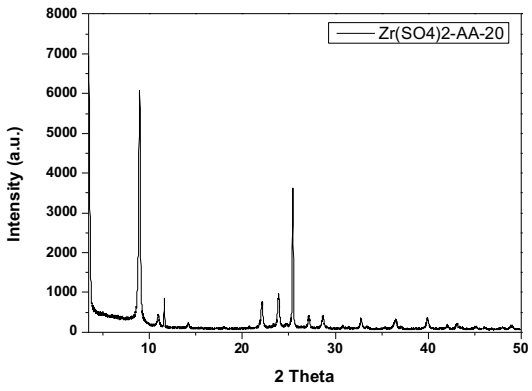
Zr(SO4)2-AA-20
Intensity (a.u.)
2 Theta

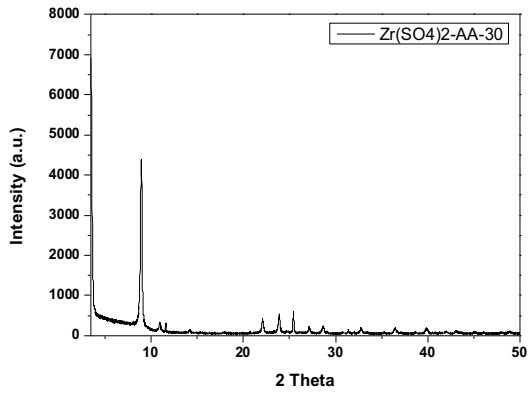
Zr(SO4)2-AA-30
Intensity (a.u.)
2 Theta

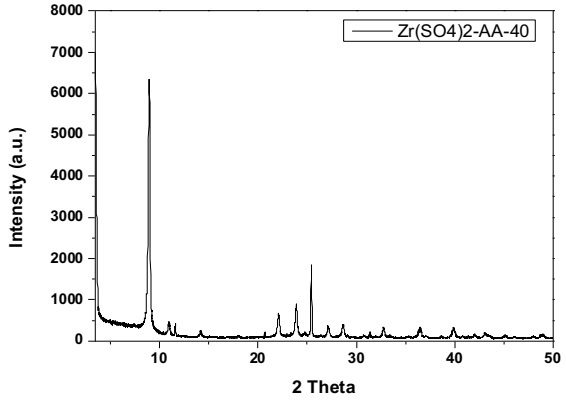
Zr(SO4)2-AA-40
Intensity (a.u.)
2 Theta

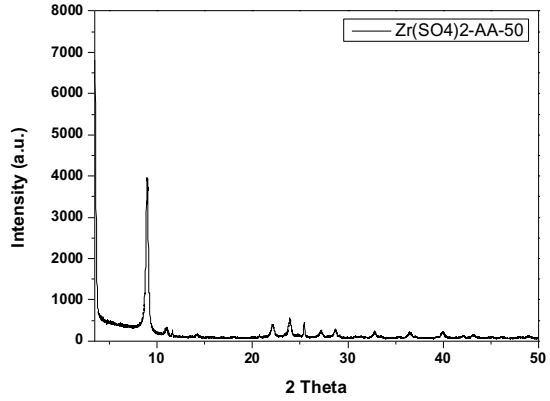
Zr(SO4)2-AA-50
Intensity (a.u.)
2 Theta

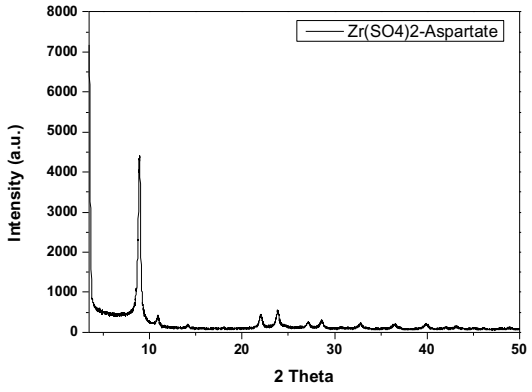
Zr(SO4)2-Aspartate
Intensity (a.u.)
2 Theta

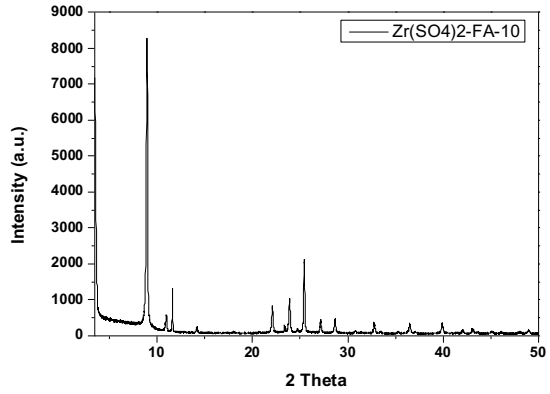
Zr(SO4)2-FA-10
Intensity (a.u.)
2 Theta

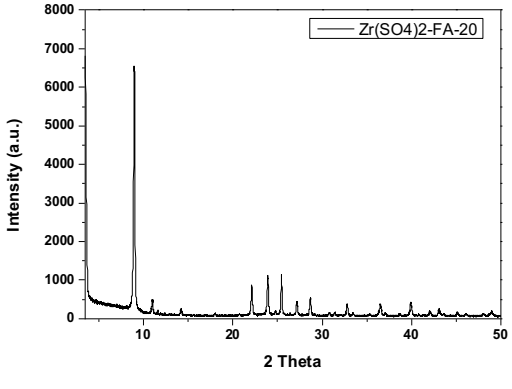
Zr(SO4)2-FA-20
Intensity (a.u.)
2 Theta

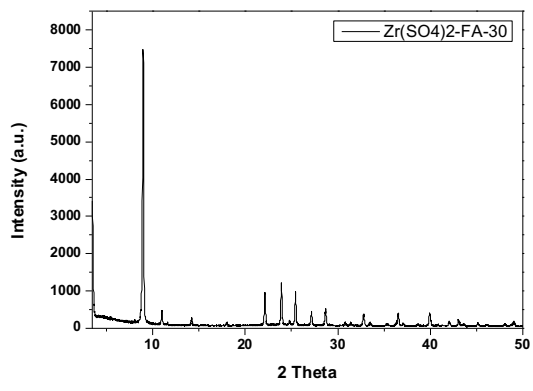
Zr(SO4)2-FA-30
Intensity (a.u.)
2 Theta

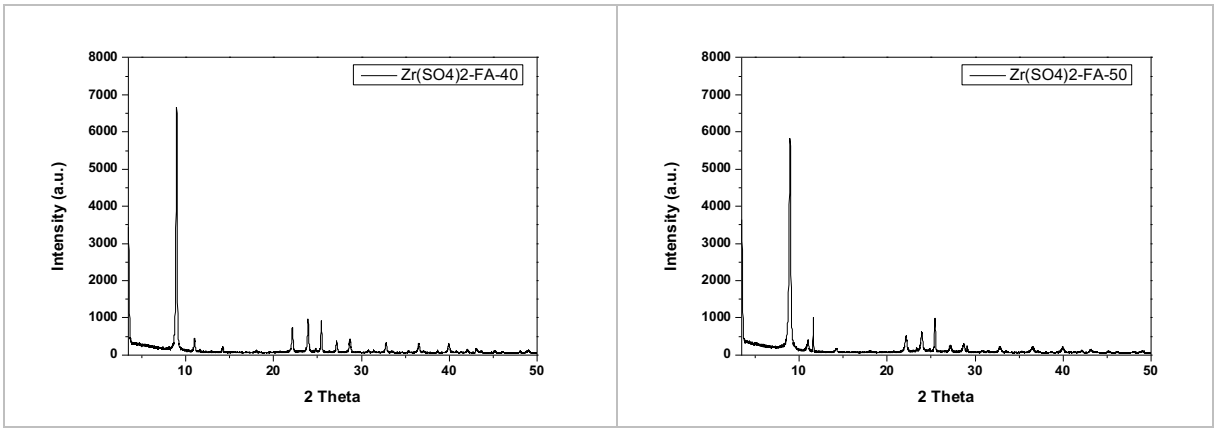

Figure 5.1.1 PXRD of 24 High-Throughput syntheses.

The materials made had slightly different compositions. And as one can see in figure 5.1.1 from the PXRD results, some of the products did form a MOF-structure. Some of them also made the characteristic powder, while others were more like gel, as showed in figure 5.1.2. The first two rows show $ZrOCl_2 \bullet 8H_2O$, and acetic acid/formic acid. And the two rows in the bottom is $Zr(SO_4)_2 \bullet 4H_2O$, followed by the same order with acetic acid first and then formic acid. It looks like as if there is a connection between this, where those that became gel-like did show the worst PXRD results, and those in powder form showed somewhat better MOF structure, even though they were not faultless.

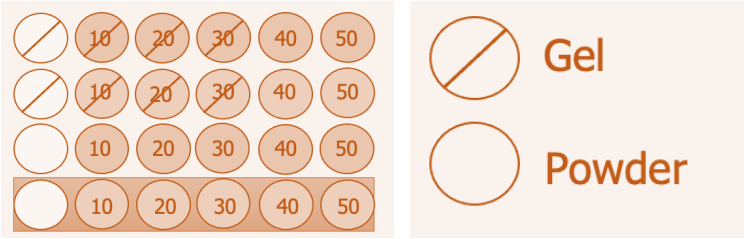

Figure 5.1.2. High through-put synthesis outcome powder vs. gel.

The best results from this synthesis were from using $Zr(SO_4)_2 \bullet 4H_2O$ as the metal source, DL-Asp as linker and both 0 equivalent and 30 equivalent formic acid. These two were analyzed further, but unfortunately a chlorine free product was not succeeded, which was detected from the SEM analysis.

5.1.2 MIP-202 Washed with Sodium Acetate

To make a chlorine-free MOF, different washing procedures was also tried. As known, chlorine is very reactive due to the octet rule, and to solve this problem the idea was to wash the solution with a chemical that chlorine could react with, for example sodium acetate. Chlorine has 7 electrons in the outer shell and could gain an electron from sodium which has one valence electron, forming a strong iconic bond.

The downside of this experiment was to potentially destroy the entire MOF, which indeed happened this time. As showed from the PXRD results the characteristic crystalline structure collapsed.

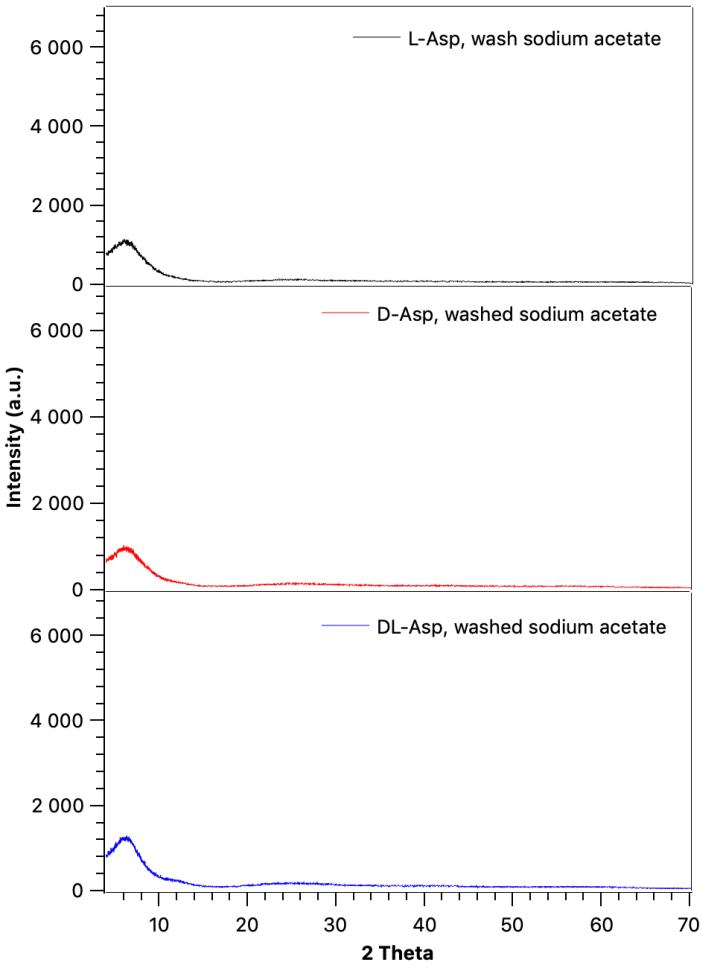

Figure 5.1.2 PXRD after washing MIP-202 with Sodium Acetone.

5.1.3 High Temperature Synthesis

Two different MIP-202 was made as reported, by using DL-Aspartic acid and high temperatures and pressure in autoclaves.

Both the autoclave synthesis using 120 °C and 140 °C made good MOF structures showed from PXRD below. However, the idea was to see if it could help purify the products, but unfortunately chlorine was still present, which was conducted from SEM-analysis, see below.

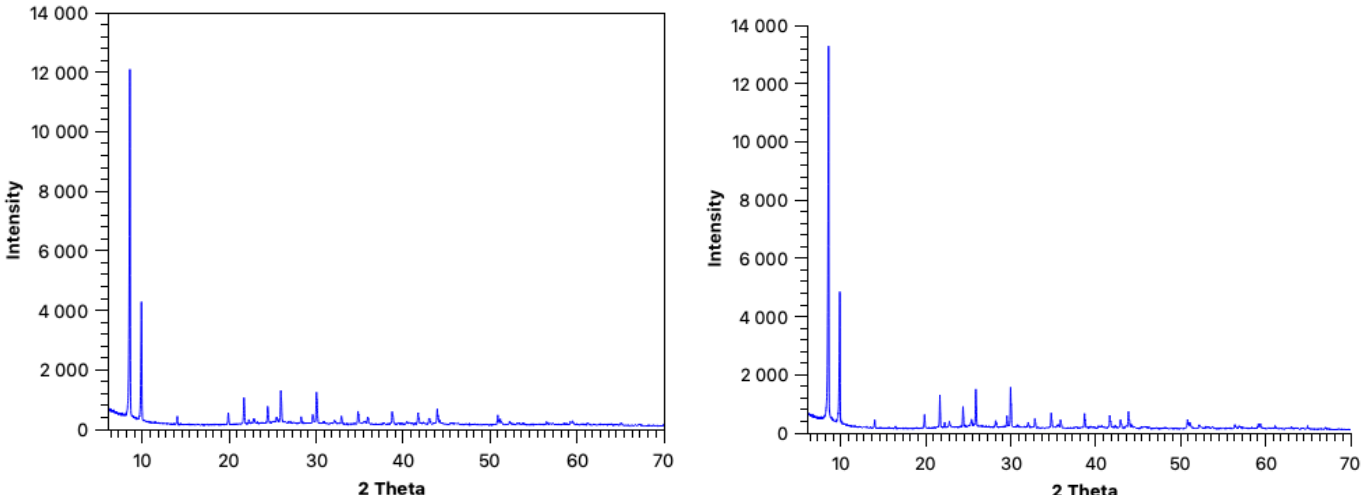

a) 120 °C b) 140 °C

Figure 5.1.3 PXRD for autoclave samples.

SEM-analysis:

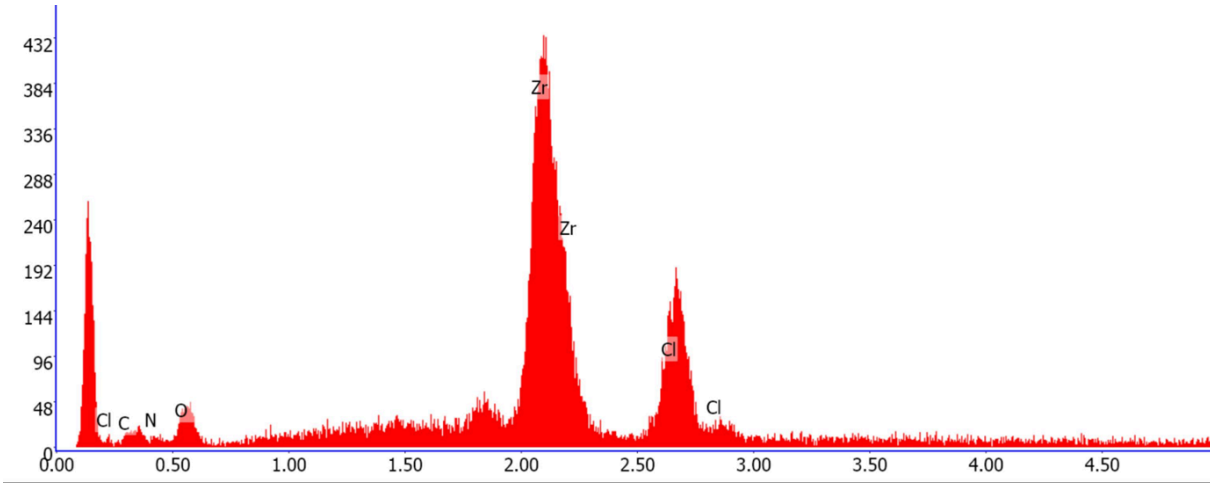

a) 120 °C

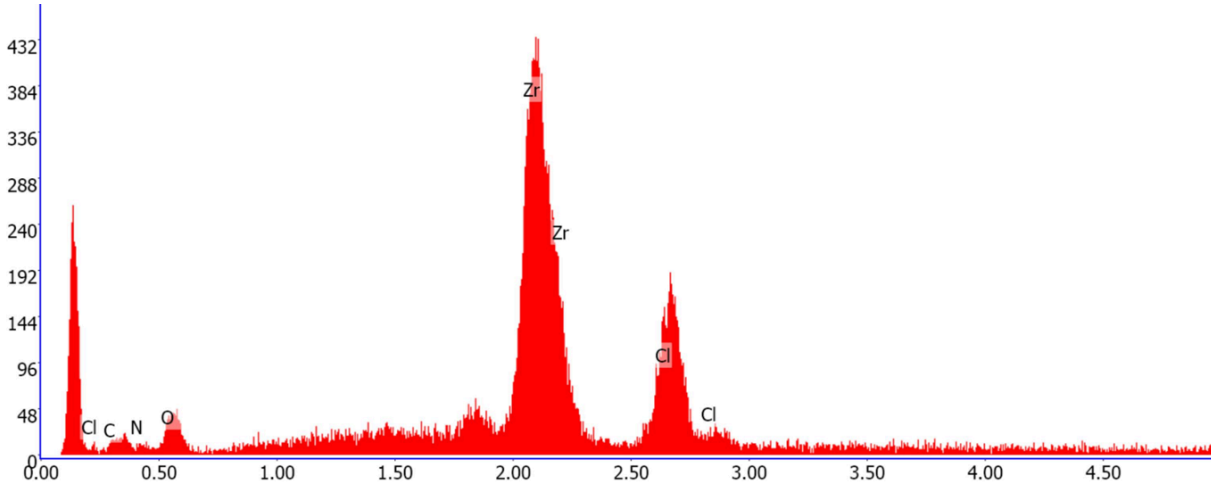

a) 140 °C

Figure 5.1.4. SEM-analysis for autoclave samples

The chlorine is still present inside the MOFs, which most likely derives from $ZrCl_4$, that is being used as the metal source in the synthesis. However, by comparing the chloride content from 120 °C and 140 °C, it seems like increasing the temperature could give slightly less content, even though the results are not as desired. The 120 degrees sample contains between 18-36 weight percentage of Cl, while the samples from 140 degrees contains between 15-24 weight percentage of chlorine, based on the different spots analysed.

Based on these results from both washing with sodium acetate and high temperature synthesis, it seems like MIP-202(Zr) needs the chlorine to stay stable. The products were analyzed further to see if there was any uptake of nitrogen, but the results were not satisfying.

Because of the results from both sodium acetate washing, high through-put synthesis and high temperature failed, the focus on $ZrCl_4$ based MOF continued.

5.2 MIP-202 1 Hour Reaction Time

5.2.1 PXRD

The three products from the as-reported MIP-202 synthesis, was analyzed with PXRD and plotted with a 2 Theta angle (x-axis) and the intensity a.u. (y-axis).

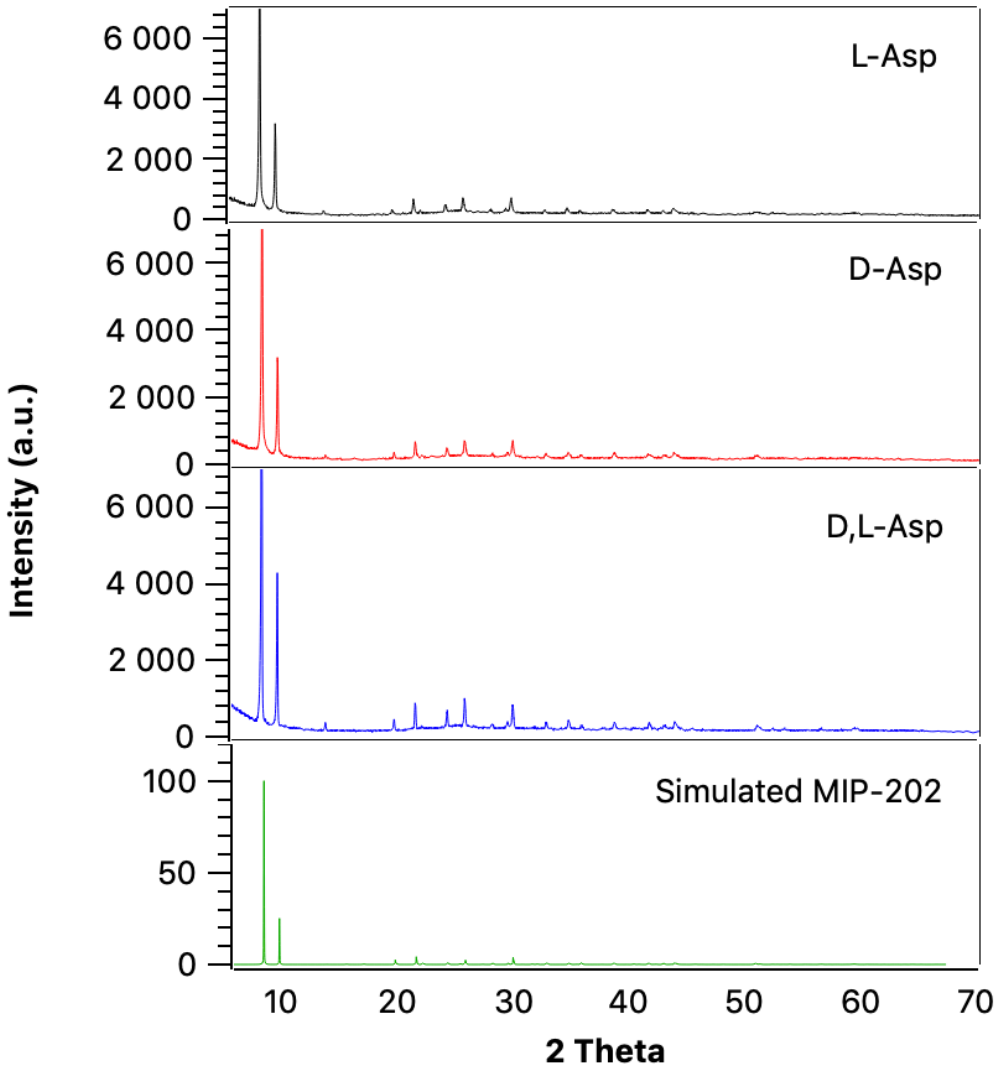

Figure 5.2.1 PXRD of MIP-202, 1h reaction time

Likened to the simulator, all the products illustrate sharp and clear peaks, which indicates the crystalline structure of a MIP-202. The simulated MIP-202 has been conducted from (Cambridge Crystallographic Data Centre, CCDC, 2018), under deposition number 1842337.

5.2.2 TGA

TGA-analysis was carried out on the reported MIP-202, to study decomposition and thermal stability of the materials. The TGA analysis conducts the continuously weight loss in percentage, while the temperature increases from 25-900 degrees, as seen on the graph below.

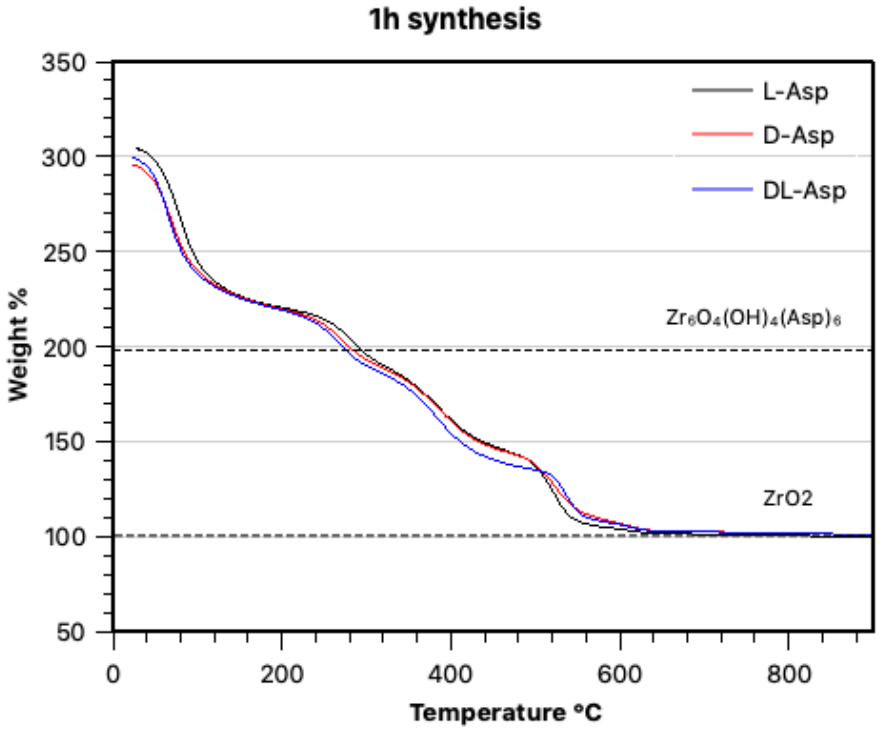

Figure 5.2.2.1 TGA of MIP-202, 1h reaction time, no treatment

The last weight measured from the analysis at 900 degrees, is calculated to be 100%. On the y-axis, the theoretical line at 100 shows the final product of 6 ZrO_2, while the theoretical line at 198,3, is the theoretical weight of $Zr_6O_6(OH)_4(Asp)_6$, which is calculated to be 198,3 % heavier than ZrO_2. This if found by following the equation below, by dividing the molecular weight for MIP-202 (1465.89 g/mol), on the end-product which is 6 ZrO_2 and multiply with 100%.

$$\frac{Zr6(O)4(OH)4(Asp)6}{6\ ZrO2} = \frac{1465{,}9\ g/mol}{739{,}3\ g/mol} * 100\% = 198{,}3\%$$

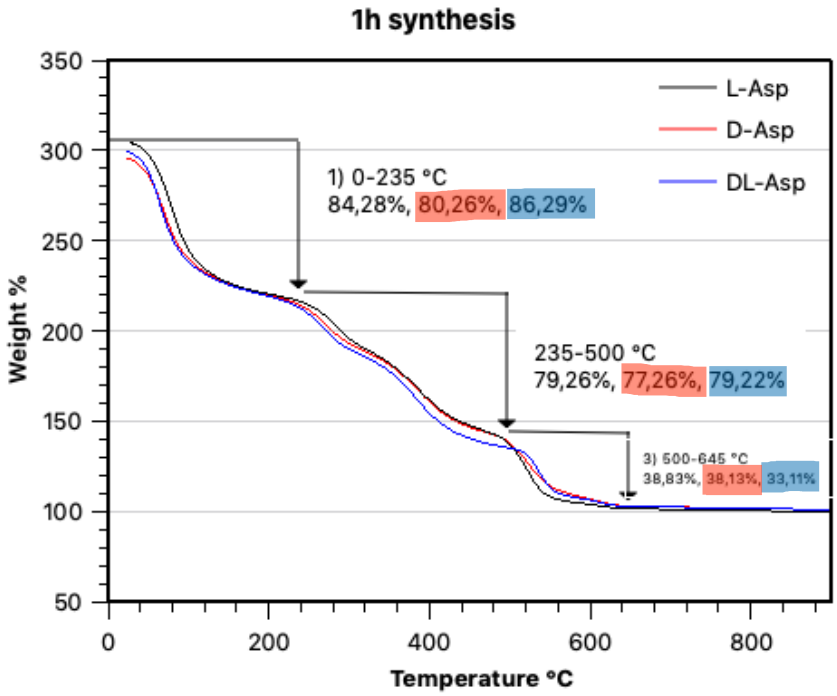

Figure 5.2.2.2 TGA Chart 1h synthesis

This chart shows the mass loss due to the increased temperature, which can signify decomposition of the materials. The first weight loss before 200 degrees, is most likely because of liquid evaporation. After this step, the weight loss could be due to unreacted linkers or the structural decomposition of the framework as mentioned. However, it is not possible to determine exactly temperature for the decompositions because of the many steps.

As seen, the mass loss is almost the same for each sample, which can indicate that there are not big differences between the isomers when it comes to the thermal stability. According to (Lv et al., 2019) the MIP-202 structure is stable up to 398K, which seems to be the case for these products as well, as the first weight loss-step is from 25- to approximately 125 degrees.

5.2.3 SEM-EDS for MIP-202, 1h reaction time

SEM-EDS is conducted to analyze the morphology of the different compositions of MIP-202, and by applying SEM-EDS it is possible to confirm what kind of molecules the product analyzed consists of.

a) 1 hour reaction time, no treatment

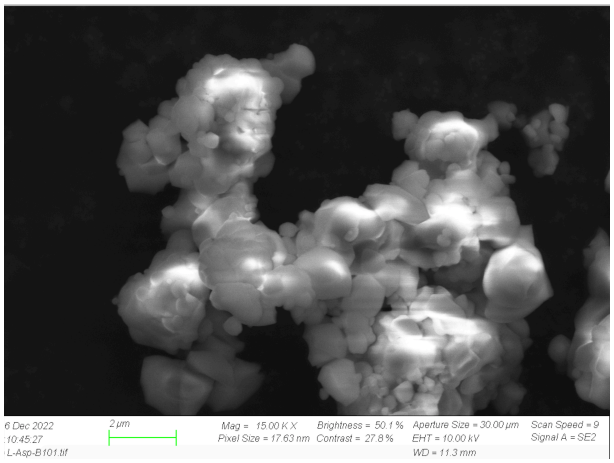

a)

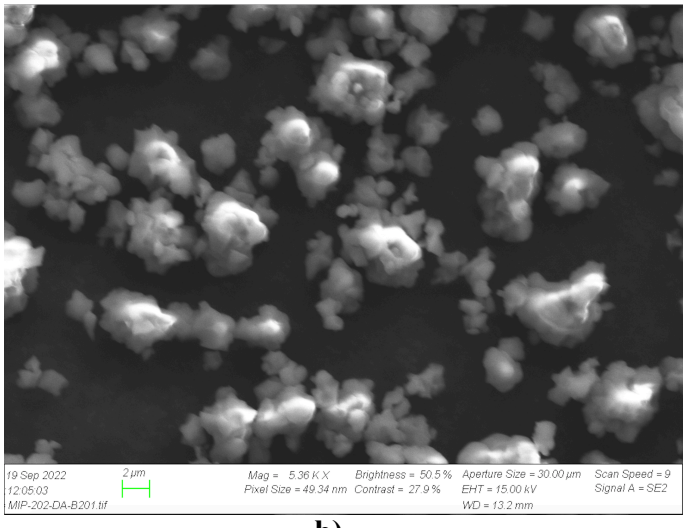

b)

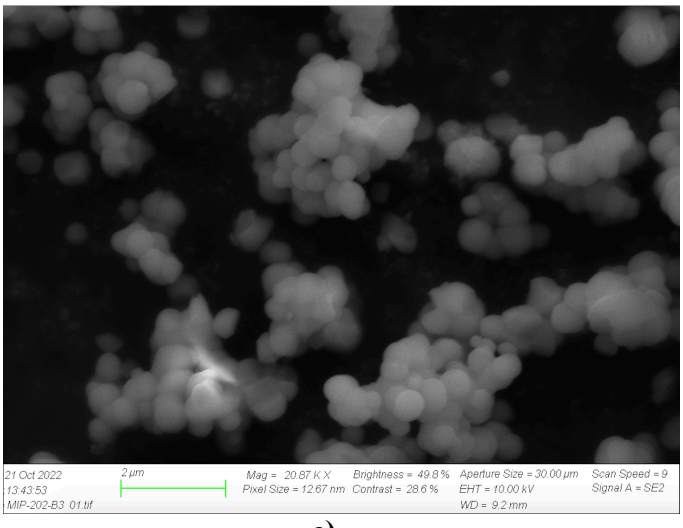

c)

Figure 5.2.3.1 SEM micrographs of MIP-202, 1h reaction time.
a) L-Asp, b) D-Asp and c) DL-Asp.

b) 1 hour reaction time, washed with EtOH for 3 days

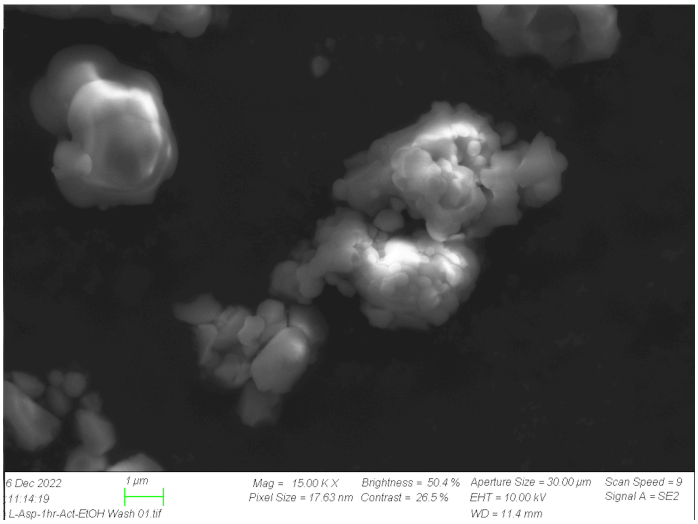

a)

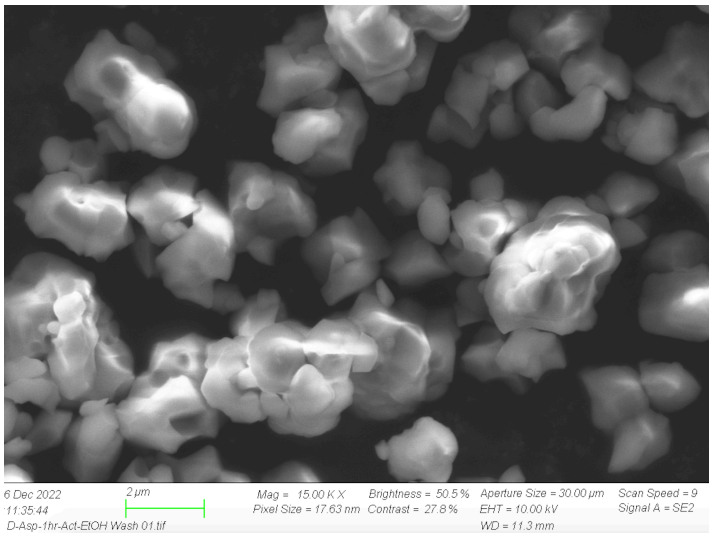

b)

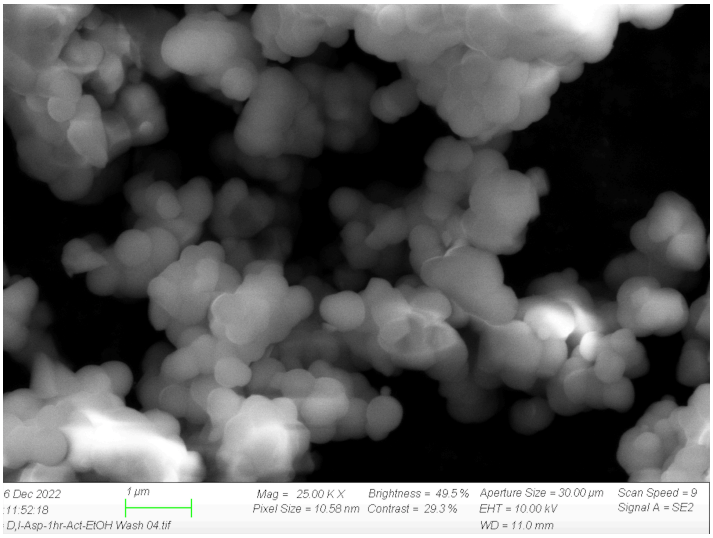

c)

Figure 5.2.3.2 SEM micrographs of MIP-202, 1h reaction time, washed with ethanol for 3 days.
a) L-Asp, b) D-Asp and c) DL-Asp.

These pictures shows that the material has a repetitive particle size, between 1-2 micrometer. As mentioned earlier, it has been reported from (Wang et al., 2018), that there are some challenges due to chloride trapped inside MIP-202. The results from our analysis, shows that the washing part was not sufficient to remove this chemical using 1 hour synthesis.

5.2.4. Nitrogen sorption

a)

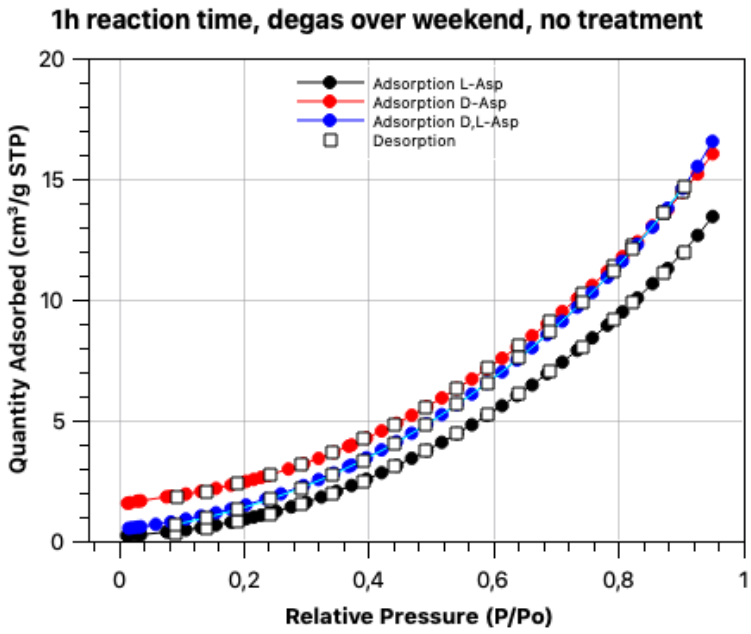

Figure 5.2.4.1 N2 sorption of MIP-202, 1h reaction time, degas over the weekend, no treatment

b)

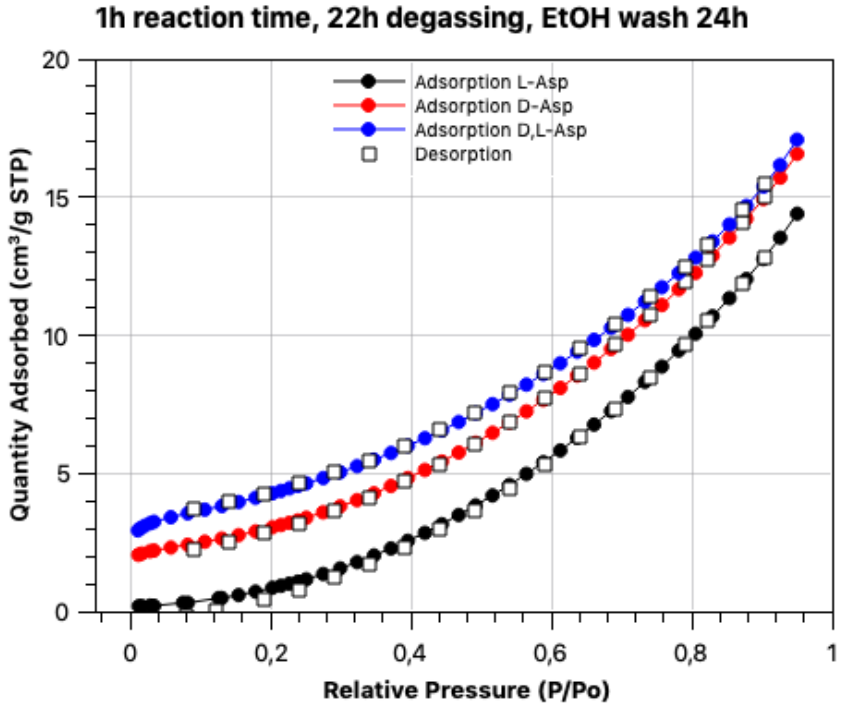

Figure 5.2.4.2 N2 sorption of MIP-202, 1h reaction time, 22h degassing, EtOH wash 24h

c)

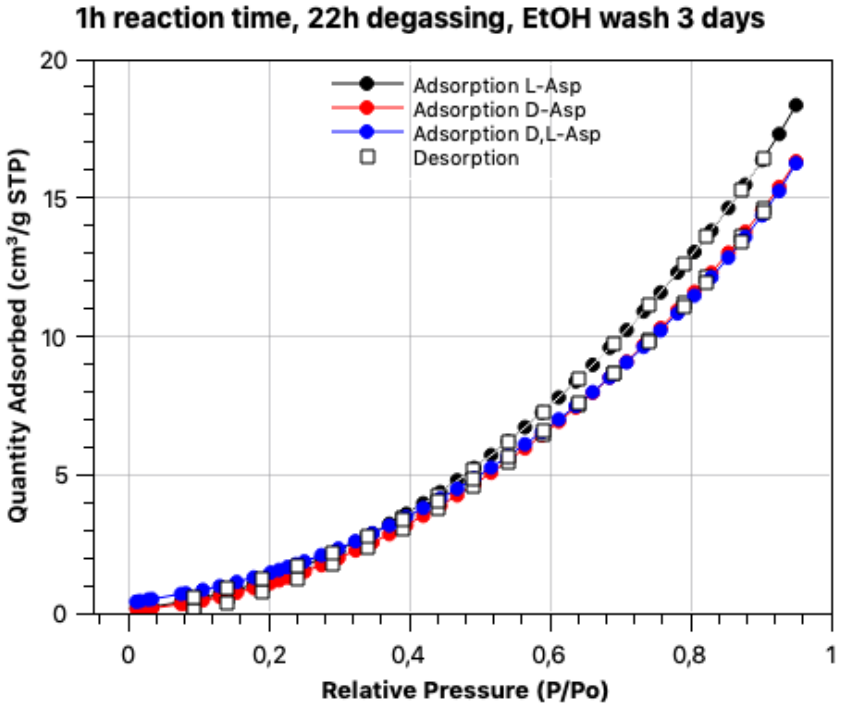

Figure 5.2.4.3 N2 sorption of MIP-202, 1h reaction time, 22h degassing, EtOH wash 3 days

The nitrogen adsorption and desorption isotherms were conducted at 77K after degassing at 60 degrees, with the purpose to determine the porosity and BET surface area for the materials.

All these analysis for nitrogen sorption using 1 hour synthesis, shows a type III isotherm, and expresses very low or no surface area and uptake, and can be ascertained nonporous. Comparing the results, the product degassed for 22 hours and washed with ethanol for 24 hours shows the best results, which had a BET surface area on 16 m^2/g. However, must mention that this also is very low and comparing it with the specific surface area that has been reported on MIP-202 to be 350 m^2/g, this is not outstanding.

The 1-hour synthesis has been washed with ethanol for both 24h and 72h but this did not affect the results as wanted. This reinforces the theory that the washing part is not the parameter that is crucial, but rather the reaction time, which will be shown later.

5.2.5 PXRD after N_2 sorption

a) Degas over the weekend – no treatment

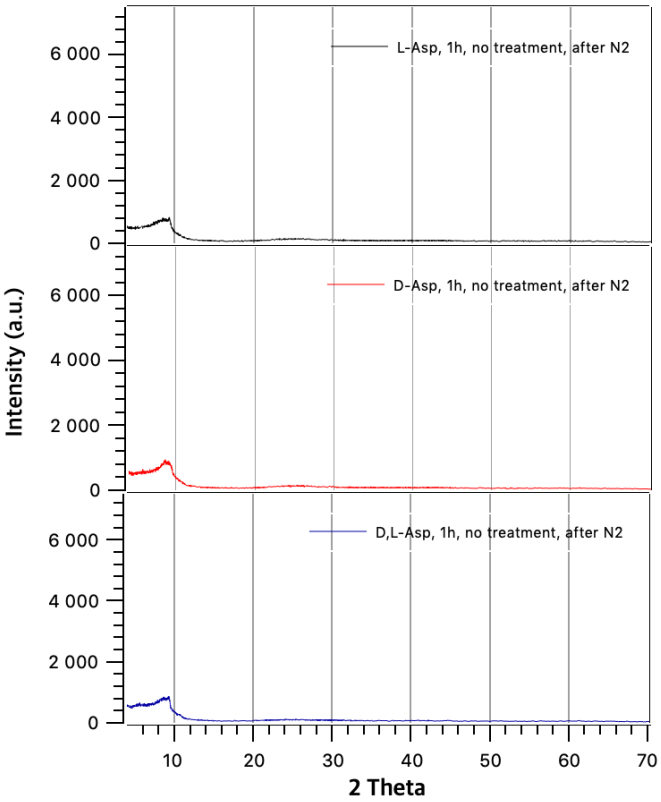

Figure 5.2.5.1 PXRD of MIP-202 (1h reaction time) after measured N2 uptake, using 60 degrees over the weekend

b) 22 hours degassing – EtOH wash 24h

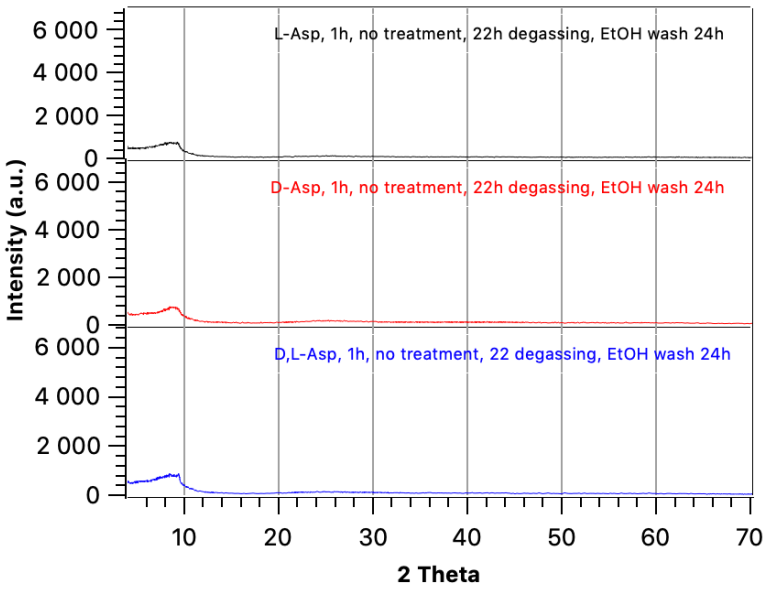

Figure 5.2.5.2 PXRD of MIP-202 (1h reaction time) after measured N2 uptake, using 60 degrees for 22h

c) 60 degrees – 22h degassing– EtOH wash for 3 days

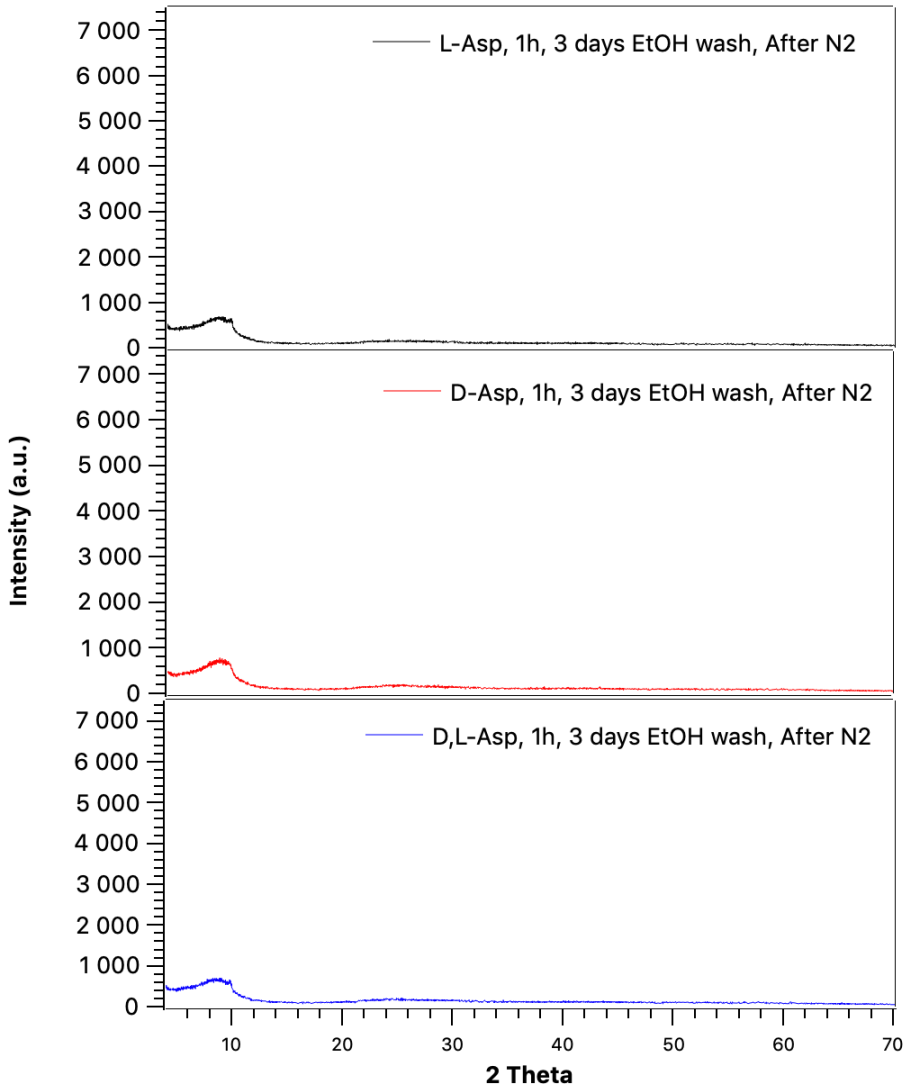

Figure 5.2.5.3 PXRD of MIP-202 (1h reaction time) after measured N2 uptake, using 60 degrees for 22h, EtOH wash 3 days

All the samples from 1 hour reaction time, after washing treatment and nitrogen sorption were collected to later analyze the structure again in PXRD. The idea behind this, was to see if the crystalline structure was still present after the different treatments. Compared to the previous faultless PXRD results, the peaks are considerably reduced. Showed in the figures above, the crystalline MOF structures was all collapsed, regardless of whether it was used degassing for 22 hours or over the weekend. Washing with ethanol for both 24- or 72 hours did not make any differences either. This specifies that the products could not stand the treatments and the material is not porous.

5.3 MIP-202 72 Hour Reaction Time

5.3.1 PXRD

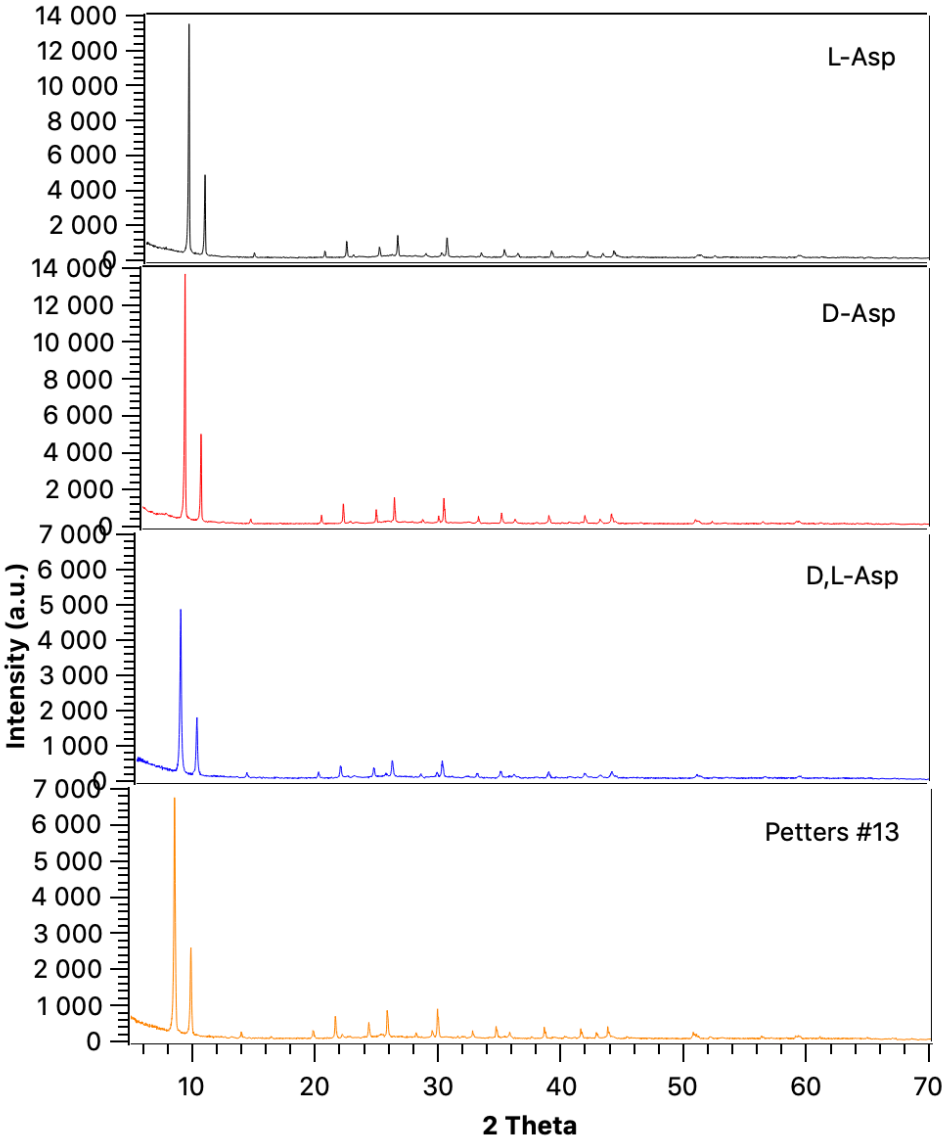

Figure 5.3.1. PXRD of MIP-202, 72h reaction time, no treatment

The MIP-202 using 72h reaction time also shows good PXRD results.
The previous student, Petter, used DL-Asp and reaction time for 72 hours. These PXRD results confirms how good stability this product has. Indeed, this MOF`s crystalline structure is still present, after two years, which also shows the robustness of the product.

5.3.2 TGA

a) As prepared, no treatment:

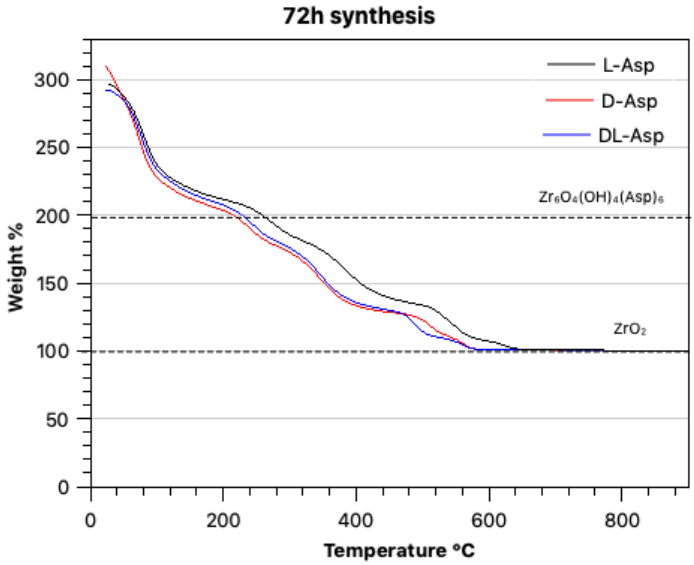

Figure 5.3.2.1 TGA of MIP-202, 72h reaction time with no treatment.

These results from 72 h synthesis are very similar to the previous TGA analysis using 1h synthesis. There are many degradation steps indicating the weight loss while increasing the temperature. It is difficult to determine an accurate temperature where the decomposition happens for these samples as well, but it will most likely be after 215 °C. Another possible way to find out the accurate decomposition temperature, is to do PXRD with different temperatures and see exact where the MOF structure collapses.

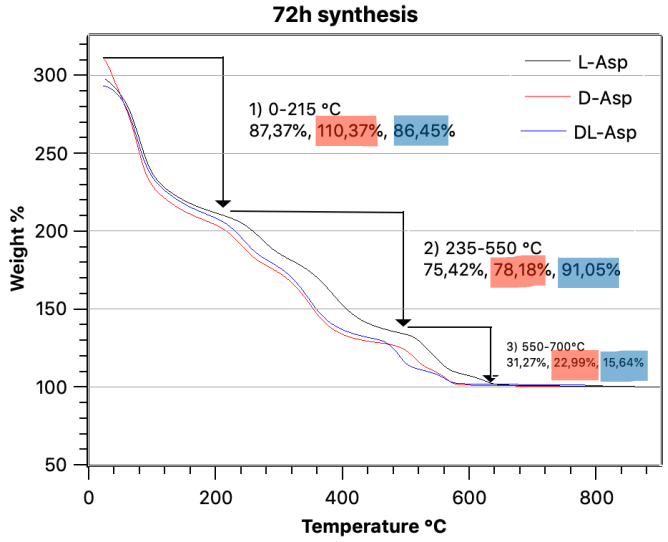

Figure 5.3.2.2 TGA Cart for 72h synthesis

The first weight loss step is from 25 °C to 215 °C, which is a bit lower than for the previous sample were the first weight loss step is from 25 °C to 235 °C. The last mass drop for all the sample is right above 600°C. Noticeable they are all very similar, and there are no significant differences.

5.3.3 SEM-EDS for MIP-202, 72h reaction time

a) 72 hours reaction time, washed with EtOH for 3 days

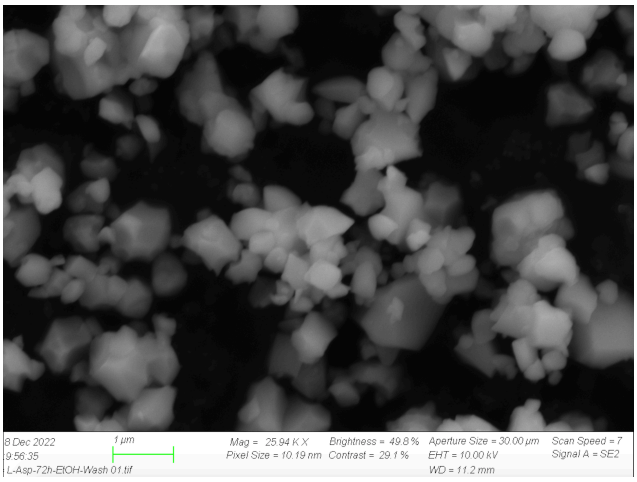

a)

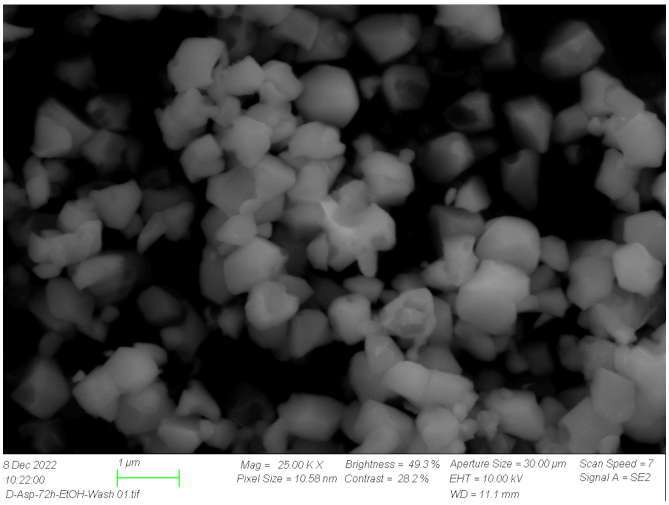

b)

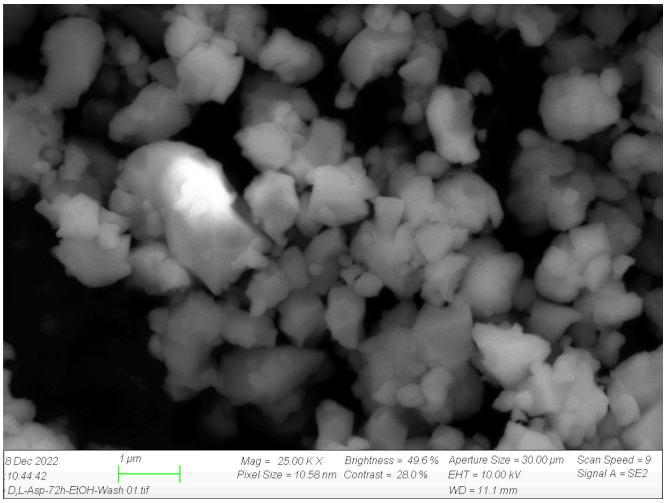

c)

Figure 5.3.3.1 SEM micrographs of MIP-202, 72h reaction time, washed with ethanol for 3 days. a) L-Asp, b) D-Asp and c) DL-Asp.

The SEM-EDS analysis evidence that chlorine is still trapped inside the MOFs porosity for both 1h- and 72h synthesis, as expected, since it is already reported from (Wang et al., 2018), that the MIP-202(Zr) contains chlorine. However, the MIP-202 shows great “ball” shape with the particle size ranging from 1-2 micrometer.

Several procedures have been tried to get rid of this chemical, such as washing procedures and high temperatures synthesis without any luck, as discussed previous. Other methods must then be tried, which is suggested under “future work”.

5.3.4 Nitrogen sorption

a)

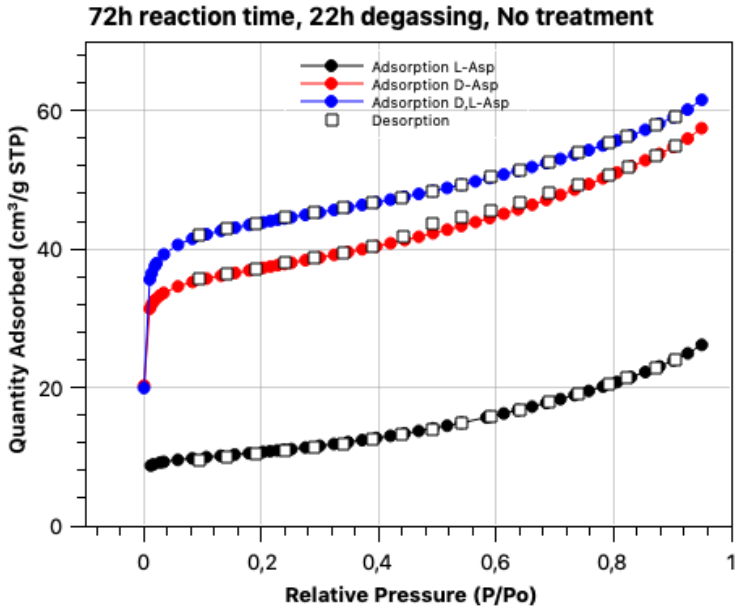

Figure 5.3.4.1. Nitrogen sorption isotherms of MIP-202, 72h reaction time with no treatment.

b)

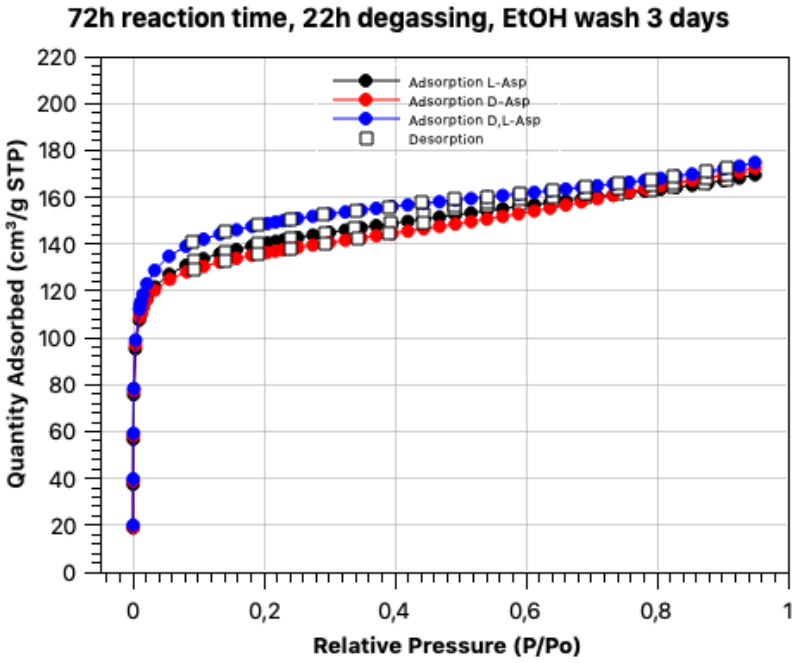

Figure 5.3.4.2. Nitrogen sorption isotherms of MIP-202, 72h reaction time with ethanol wash for 3 days.

The results for nitrogen sorption of the 72h reaction time using 60 degrees and 22 hours degassing, just washed with distilled water, and collected with filtration (figure 5.3.4.1), was still low, and did not show as good results as the previous student has reported (see below). However, there was some nitrogen uptake, and even though it was not as much as wanted, it still was better than the previous results from 1 hour synthesis.

As one can see the nitrogen uptake is significantly better for the samples that has been washed with ethanol for three days (figure 5.3.4.2). Especially DL-Aspartic acid shows very good nitrogen uptake.

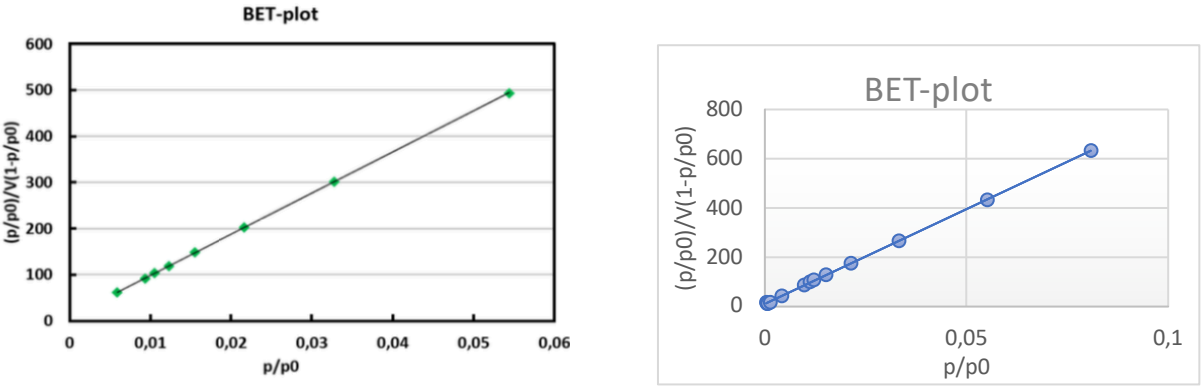

a) Petters sample #13 (Skjærseth, 2021) **b)** 72h synthesis, EtOH wash 3 days, DL-Asp

Figure 5.3.4.3 BET-plot

(Skjærseth, 2021) has reported that his sample using 72h synthesis and D-Asp had a surface area on 488 $m^2 g^{-1}$ and pore volume 0,263 $cm^3 g^{-1}$. Compared to the DL-Asp 72 hours synthesis with no treatment, gave a surface area on 164 $m^2 g^{-1}$ and pore volume 0,024 $cm^3 g^{-1}$.

However, the best results were for the product washed with ethanol, following the same degas procedure, which showed significant improvement giving a surface area 565 $m^2 g^{-1}$ and pore volume 0,268 $cm^3 g^{-1}$. The rest of BET-plot and adsorption isotherm plots for each sample, can be found under “Appendix”.

The pore size for all the samples is expressed in table 5.4 below, and for all the samples it is over 2nm, and could therefore be considered as meso porous material. In accordance with (Yuan et al., 2017), the pore size of most MOFs is limited to micro pores and have a pore diameter below 2nm, which is suitable for uptake and separation of small molecules. Because of that, an increase in pore diameter is highly required. However, many of the samples do not take up any nitrogen, and one of the reasons for this, could possibly be due to chlorine stuck inside the pores.

5.3.5 Nitrogen sorption overview for 1h - and 72h synthesis

A fully protonated MIP-202(Zr), is reported to have a pore volume of 0.1 cm3 g−1 and a free pore diameter less than 4 Å (Wang et al., 2018), which could be classified as a microporous material. Below is a table that shows the results for the different treated and non-treated samples made in this thesis. This data is collected from using the "BET Consistency Criteria Blank Spreadsheet".

Description	MIP-202, isomer	Surface Area (m^2/g)	Pore Volume (cm^3/g)	Pore size (nm)
1 hour synthesis. 60 degrees – 22h degas – no treatment	L-Asp	0 [m2 g-1]	0,021 [cm3 g-1]	5,6173 nm
	D-Asp	0 [m2 g-1]	0,024 [cm3 g-1]	5,5697 nm
	DL-Asp	16 [m2 g-1]	0,025 [cm3 g-1]	5,6018 nm
1 hour synthesis. 60 degrees – degas over the weekend – no treatment	L-Asp	0 [m2 g-1]	0,020 [cm3 g-1]	5,6344 nm
	D-Asp	0 [m2 g-1]	0,024 [cm3 g-1]	5,6046 nm
	DL-Asp	0 [m2 g-1]	0,024 [cm3 g-1]	5,6234 nm
1h synthesis. 60 degrees – 22h degas – EtOH wash for 3 days	L-Asp	14 [m2 g-1]	0,027 [cm3 g-1]	5,5035 nm
	D-Asp	12 [m2 g-1]	0,024 [cm3 g-1]	5,4820 nm
	DL-Asp	12 [m2 g-1]	0,024 [cm3 g-1]	5,5053 nm
72h synthesis 60 degrees – 22h degas – no treatment	L-Asp	40 *[m2 g-1]*	0,102 *[cm3 g-1]*	5,5145 nm
	D-Asp	143 [m2 g-1]	0,087 [cm3 g-1]	4,7907 nm
	DL-Asp	164 *[m2 g-1]*	0,093 *[cm3 g-1]*	4,3587 nm
72h synthesis 60 degrees – 22h degas – EtOH wash 3 days	L-Asp	530 [m2 g-1]	0,260 [cm3 g-1]	3,1260 nm
	D-Asp	523 [m2 g-1]	0,264 [cm3 g-1]	3,5110 nm
	DL-Asp	565 [m2 g-1]	0,268 [cm3 g-1]	3,0056 nm

Table 5.3.5 N2 sorption overview for all samples

5.3.6 PXRD after N_2 sorption

a) No treatment

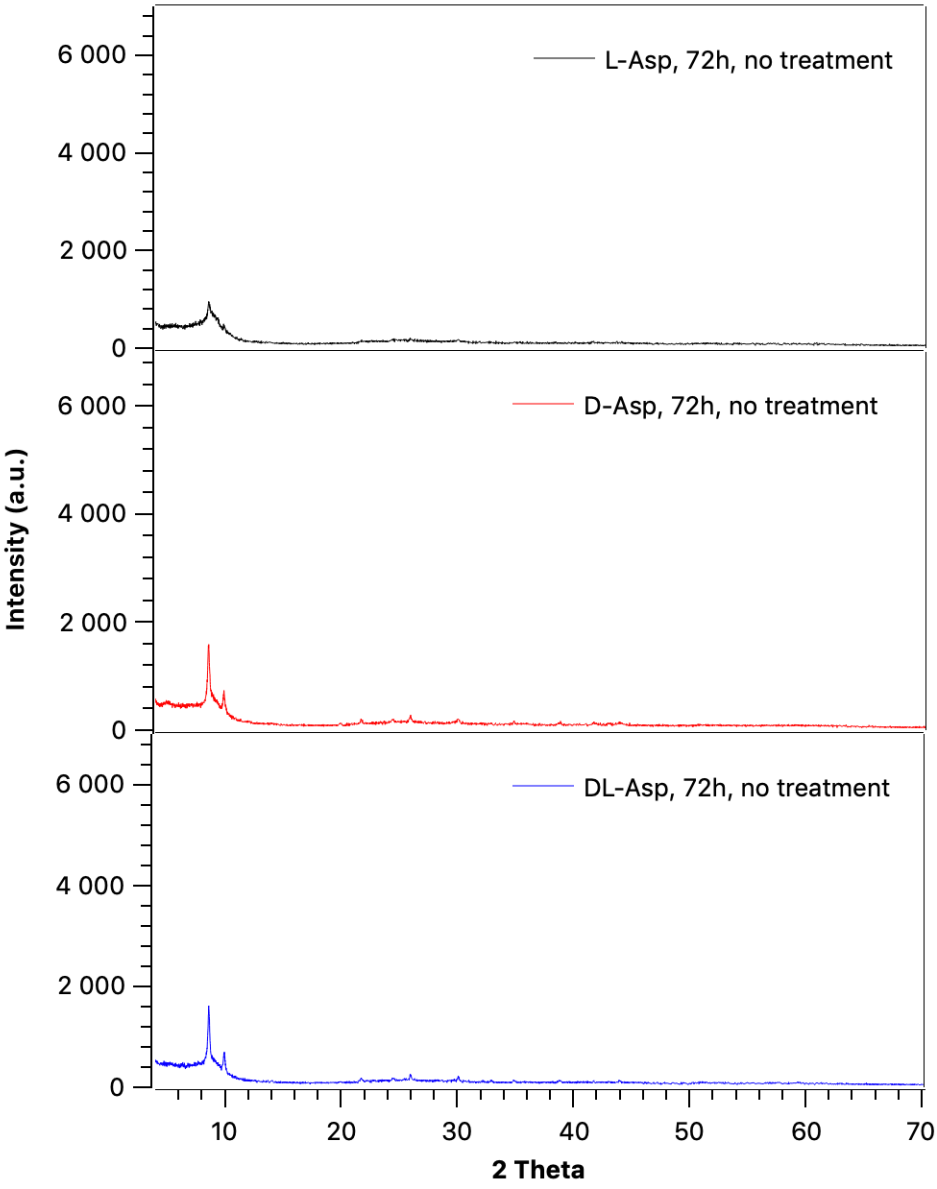

Figure 5.3.6.1 PXRD of MIP-202, 72h reaction time with no treatment.

b) EtOH wash

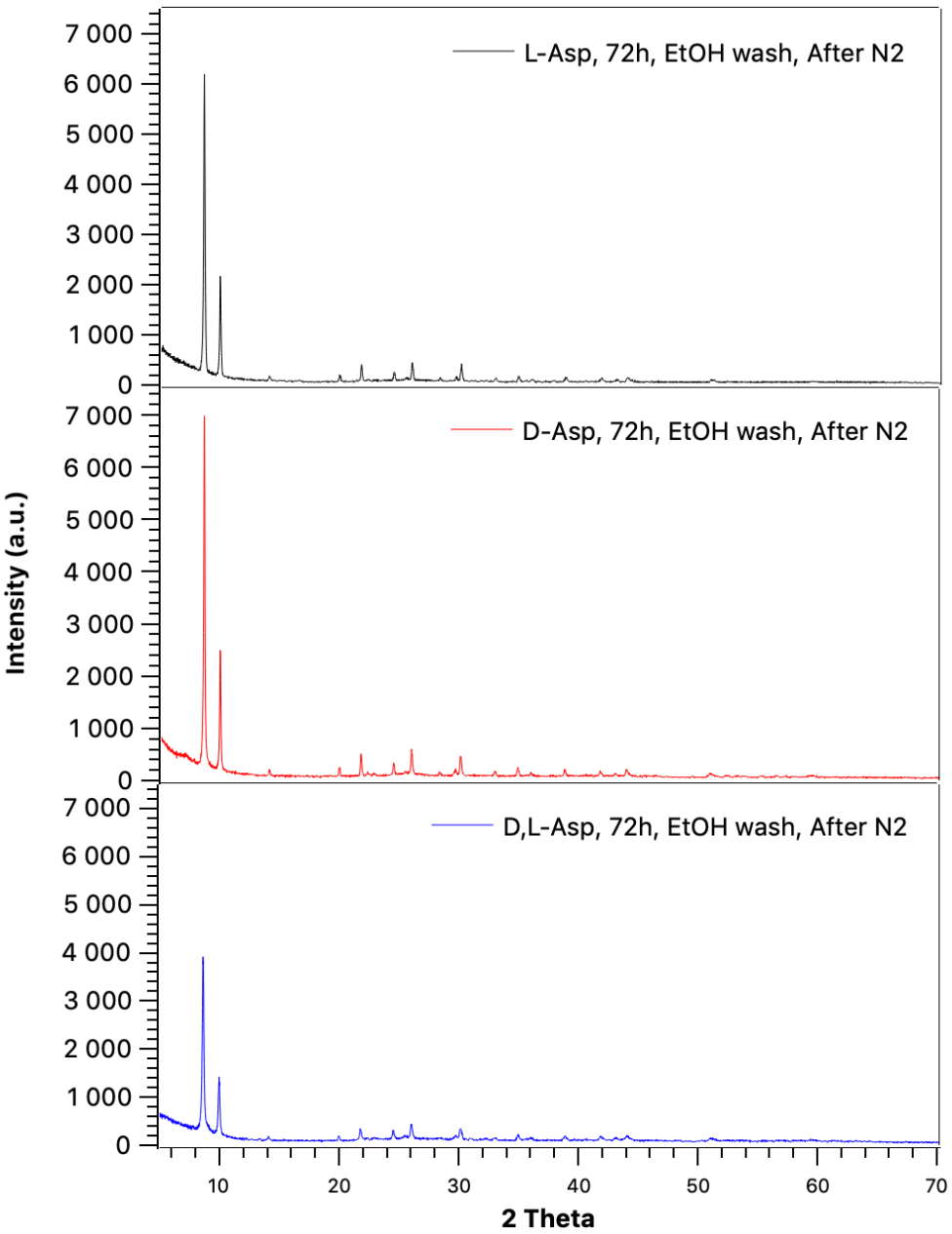

Figure 5.3.6.2 PXRD of MIP-202, 72h reaction time wash with EtOH for 3 days

From PXRD for untreated samples, one can see that the crystalline structure got destroyed, giving an unstable and non-porous MOF, just like the previous ones. Though, the PXRD results from the 72h synthesis products with ethanol wash, shows that the MOF structure is still present, after degassing and nitrogen treatment. This strengthens the theory that ethanol wash is crucial to keep a stable structure in addition to using 72h synthesis.

5.3.7 CO_2 uptake

Because of the many poor nitrogen sorption analysis, the CO_2/N_2 sorption is only done for the samples that showed good uptake and indeed is porous, in fact the samples with 72 hours reaction time, washed with ethanol for three days. These samples were first activated in vacuum at 60 degrees for 22 hours. The CO_2 and N_2 is conducted by using 273K.

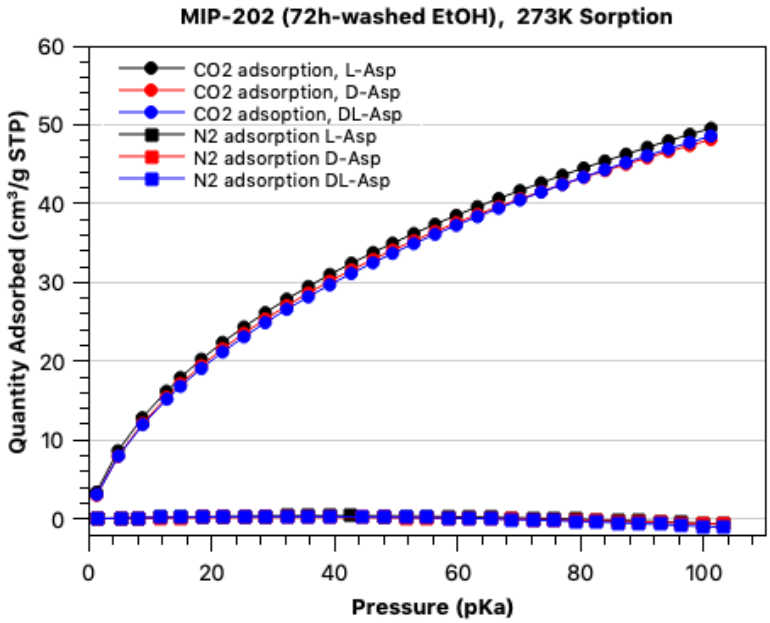

Figure 5.3.7.1. CO2/N2-adsorption of MIP-202 72h, washed with EtOH, at 273K

As shown in figure 5.3.7.1, the products are showing much better CO2 sorption, than nitrogen, where the nitrogen adsorption isotherms is equal to zero or less. This is as expected because higher temperatures lead to decrease of adsorption for nitrogen.

However, the result using DL-Asp, showed better surface area for the CO_2 sorption 273K with BET surface area of 1,9381 m^2/g, compared to N_2 sorption 77K with surface area of -0,0190 m^2/g. This can indicate that the material is more selective for carbon dioxide, which is good since that is the primary aim wanted to capture.

The sample analysed above shows better CO_2 uptake than reported in (Skjærseth, 2021), where the MIP-202 is synthesized with D-aspartic acid giving an uptake for 1,38 mmol/g, compared to this analysis showing an uptake of around 2,2 mmol/g at 100 pKa.

6. Conclusion and Future Work

6.1 Conclusion

The MIP-202 synthesized as reported, did not show similar results, and had poor porosity which was strange since it was the opposite results of what has been reported by (Wang et al., 2018). The conclusion of this is unclear, but it could possibly be due to a difference in the reaction time.

It may appear that the choice of isomers from aspartic acid could have an impact on the porosity of the material, and from the nitrogen plots for all the products made, it seems like that DL-Asp has a slightly better sorption for all the analysis. However, for CO_2 sorption the L-isomer had a marginally better uptake.

According to the results from both washing with sodium acetate and trying to remove excess chlorine by doing high temperature and pressure synthesis using autoclaves, it seems like MIP-202 is dependent on chlorine to stay stable. As we could see from the PXRD, the crystalline structure got destroyed after washing, which supports this conclusion.

PXRD from the synthesis using both 1 hour- and 72 hours reaction time, showed good results. However, only the 72h synthesis washed with ethanol for three days survived the degas- and sorption treatment as showed in PXRD after N_2 sorption. The rest of the samples collapsed. This supports the statement that 1 hour is not enough for MIP-202 to react the optimal structure to be porous and robust.

It was not clear if it was the reaction time or different washing procedures that was the clue to make a good MOF. However, from comparing all these nitrogen sorption results, using different reaction time, and washing procedures, we can confirm what (Skjærseth, 2022) found in his master thesis, and that 72 hours reaction time is crucial to get a material with porosity. It also seems like that washing the porous material with ethanol for 3 days, is essential to persist the degas treatment. This sample made the best carbon dioxide sorption so far, with a total specific surface area for 1,9381 m^2/g, using DL-Asp.

The PXRD on the previous student`s sample (Skjærseth, 2021), shows that the MOF structure is still present. This is great evidence since it tells how good the stability this MOF has, and how robust the product is, relying on the fact that this sample is two years old.

6.2 Future Work

For future work, further analyzation to attempt clarifying how to get rid of chlorine from MIP-202(Zr) could be pleasant. (Wang et al., 2018) also reports that extensive washing of the MIP-202 using boiling ethanol or methanol over a longer period, could be efficient to remove the free chlorine trapped inside the pores of the MOF, giving the ratio 1:1 for both chlorine, zirconium, and nitrogen.

During the high through-put synthesis, the results from PXRD was not as wanted. The problem could be due to using the ration 1:1. It is truly reported from (Wang et al., 2018) the importance of running the synthesis with excess of linker, using the ratio linker:metal equal 2:4.

It could also be worthy to make a new synthesis using 24 hours as the reaction time, and follow the exact same washing procedure, using ethanol for 3 days, as the gap between 1 hour and 72 hours is quite big.

For future work, it is also very essential to look at the isotherms for adsorption of both nitrogen and CO_2, to be able to calculate the selectivity from IAST and enthalpy of adsorption. The University of Stavanger got this instrument later than expected and because of that, the time was running out.

7. References

Artioli, Y., (2008). *Adsorption*. Available from: https://www.sciencedirect.com/science/article/pii/B9780080454054002524 (Information collected on 5.12.22)

Baumann, A., Burns, D., Lui, B., Thoi, V. (2019), *Metal-organic framework functionalization and design strategies for advanced electrochemical energy storage devices.* Available from: https://www.nature.com/articles/s42004-019-0184-6 (Information collected on 10.10.22)

Berger, M., (2022), *What is a MOF (metal organic framework)?* Available from: https://www.nanowerk.com/mof-metal-organic-framework.php

Bernstein, L., et al, (2007). *Climate change 2007.* Available from: https://www.ipcc.ch/site/assets/uploads/2018/02/ar4_syr_full_report.pdf (Information collected on 10.10.22)

Brewer, P., Chen, B., Haugan, P., Iwama, T., Johnston, P., Kheshgi, H., Li, Q., Ohsumi, T., Pörtner, H., Sabine, C., Shirayama, Y., Thomson, J. (2018.) *Ocean storage.* Available from: https://www.ipcc.ch/site/assets/uploads/2018/03/srccs_chapter6-1.pdf. (Information collected on 5.10.22)

Chem. Sci., 2019, 10, 10209. Available from: https://pubs.rsc.org/en/content/articlepdf/2019/sc/c9sc03916c (Information collected on 12.10.22)

Colpan, C., and M. Ercelik. (2014), *Surface and Material Characterization Techniques.* Available from: https://www.sciencedirect.com/topics/engineering/energy-dispersive-x-ray-spectroscopy (Information collected in 12.10.22)

D8 Series, User Manual. (2014). Karlsruhe: Germany.

Damås, J. (2022). *Carbon capture: Characterization of CO2 adsorption by Metal-organic frameworks and Zeolite.*

Demir, H., Aksu, G., Gulbalkan, H,. Keskin, S. (2022), *MOF Membranes for CO2 Capture: Past, Present and Future.* Available from: https://www.sciencedirect.com/science/article/pii/S2772656821000269 (Information collected on 11.10.22)

Diab, K. E., Salama, E., Hassan, H. S., El-Moneim, A. A., & Elkady, M. F. (2021*). Bio-Zirconium Metal- Organic Framework Regenerable Bio-Beads for the Effective Removal of Organophosphates from Polluted Water*. Available from: https://doi.org/10.3390/polym13223869

Ding, M., Cai, X., Jiang, H-L. (2019), *Improving MOF stability: approaches and applications*. Available from: https://pubs.rsc.org/en/content/articlepdf/2019/sc/c9sc03916c (information collected on 2.12.22)

Dutcher, B., Fan, M., Russel, A., (2015). Amine-Based CO2 Capture Technology Development from the Beginning of 2013. Available from: https://pubs.acs.org/doi/full/10.1021/am507465f*

Dutrow, B., and C. Clark. (2022), *X-ray Powder Diffraction (XRD).* Available from: https://serc.carleton.edu/research_education/geochemsheets/techniques/XRD.html (Information collected on 12.10.22)

Falsafi, S., Rostamabadi, H., Jafari, S. (2020), *Chapter Nine - X-ray diffraction (XRD) of nanoencapsulated food ingredients.* Available from: https://www.sciencedirect.com/science/article/pii/B9780128156674000092 (Information collected on 12.10.22)

Freund, R. et al. (2021), *25 Years of Reticular Chemistry.* Available from: https://onlinelibrary.wiley.com/doi/10.1002/anie.202101644 (Information collected on 13.12.22)

Garcia-Herrera, L., and Price, H., (2020), *Thermogravimetric analysis (TGA)*. Available from: https://chem.libretexts.org/Courses/Franklin_and_Marshall_College/Introduction_to_Materials_Characterization__CHM_412_Collaborative_Text/Thermal_Analysis/Thermogravimetric_analysis_(TGA) (Information collected on 12.10.22)

Global CCS Institute (2018). *CAPTURING CO_2.* Available from: https://www.globalccsinstitute.com/wp-content/uploads/2018/12/Global-CCS-Institute-Fact-Sheet_Capturing-CO2.pdf (Information collected on 18.10.22)

Goodge, J. (2017). *Energy-Dispersive X-Ray Spectroscopy (EDS).* Available from: https://serc.carleton.edu/research_education/geochemsheets/eds.html (Information collected on 12.10.22)

Granados, D.A.. (2014). *Thermogravimetry / Thermogravimetric analysis (TGA).* Available from: https://www.researchgate.net/figure/TGA-scheme-used-in-the-experimental-torrefaction-process-of-biomass-250_fig2_263049766 (Information collected on 12.10.22)

Helmenstine, (2022). *Adsorption vs Absorption – Differences and examples.* Available from: https://sciencenotes.org/adsorption-vs-absorption-differences-and-examples/ (Information collected on 10.11.22)

Hulscher, T., and Cornelissen, G. (1996), *Effect of temperature on sorption equilibrium and sorption kinetics of organic micropollutants - a review.* Available from: https://www.sciencedirect.com/science/article/abs/pii/0045653595003452 (Information collected on 2.12.22)

Jones, G., (2014), *Modulating the MOF.* Available from: https://blogs.rsc.org/ce/2014/09/17/modulating-the-mof/?doing_wp_cron=1670064120.4459071159362792968750 (Information collected on 5.12.22)

Kumar, V., Ramisetty. K., Hef, C., Beloshapkin, S. (2019). Available from: https://www.researchgate.net/figure/Different-types-of-adsorption-isotherms-as-classified-by-IUPAC-25_fig6_331250869 (Information collected on 11.12.22)
Li, H.., Wang, K., Sun, Y., Lollar. C., Li, J., Zhou, H-C.. (2018), *Recent advances in gas storage and separation using metal–organic frameworks.* Available from:

https://www.sciencedirect.com/science/article/pii/S1369702117302407 (Information collected on 11.11.22)

Lundstedt, C. (2019). Available from: https://static.horiba.com/fileadmin/Horiba/Products/Scientific/Particle_Characterization/Webinars/Slides/BET_Theory_Explained.pdf (Information collected on 11.12.22)

Lv, D., Chen, J., Yang, K., Wu, H., Chen, Y., Duan, C., Wu, Y., Xiao, J., Xi, H., Li, H., Xia. H. (2019). Chemical Engineering Journal. *Ultrahigh CO2/CH4 and CO2/N2 adsorption selectivities on a cost-effectively L-aspartic acid based metal-organic framework.*

Manousi, N., Giannakoudakis, D., Rosenberg, E., Zachariadis, G. (2019), *Extraction of Metal Ions with Metal–Organic Frameworks.* Available from: https://www.ncbi.nlm.nih.gov/pmc/articles/PMC6943743/ (Information collected on 14.11.22)
Marzouki, R (2019) *Synthesis Methods and Crystallization*. Available from: https://www.intechopen.com/chapters/71021 (Information collected on 08.11.22)

Qian, Q., Asinger, P., Lee, M., Han, G., Rodrigues, K., Lin, S., Benedetti, F., Wu, A., Chi, W., Smith Z. (2020). *MOF-Based Membranes for Gas Separations.* Available from: https://pubs.acs.org/doi/10.1021/acs.chemrev.0c00119 (Information collected 12.10.22)

Raja, P., and Barron, A. (2022). BET Surface Area Analysis of Nanoparticles. Available from: https://chem.libretexts.org/Bookshelves/Analytical_Chemistry/Physical_Methods_in_Chemistry_and_Nano_Science_(Barron)/02%3A_Physical_and_Thermal_Analysis/2.03%3A_BET_Surface_Area_Analysis_of_Nanoparticles (Information collected on 07.12.22)

Rayner-Canham, G., and Overton, T., (2014) *Descriptive Inorganic Chemistry.* United States of America: W.H. Freeman and Company. (Information collected on 08.11.22)

Ruud, M., (2019). *Hvordan virker fangst og lagring av CO2?* Available from: https://www.tu.no/artikler/hvordan-virker-fangst-og-lagring-av-co2/454353

Shao, R., and Stangeland, A. (2009), *Amines Used in CO2 Capture*. Available from: https://bellona.org/assets/sites/3/2015/06/fil_Bellona_report_September__2009_-_Amines_used_in_CO2_capture-11.pdf (Information collected 28.11.22)

Skjærseth, P. (2021). *Synthesis optimization and characterization of MOFs for carbon capture.*

Solano, V., and Vega-Baudrit, J. (2015). *Micro, Meso and Macro Porous Materials on Medicine.* Available from: https://www.researchgate.net/publication/282660600_Micro_Meso_and_Macro_Porous_Materials_on_Medicine (Information collected to 14.11.22)

Solano., and Vega-Baudrit., (2015), Journal of Biomaterials and Nanobiotechnology (2015). *Micro, Meso and Macro Porous Materials on Medicine.* Available from: https://www.researchgate.net/publication/282660600_Micro_Meso_and_Macro_Porous_Materials_o Medicine (Information collected to 14.11.22)

Speybroeck, V., and Mauri, G. (2022), *Metal-organic frameworks.* Available from: https://www.nature.com/subjects/metal-organic-frameworks (Information collected on 6.10.22)

Stanger, R., Wall, T., Spörl, R., Paneru, M., Grathwohl, S., Weidmann, M., Scheffknecht, G., McDonald, D., Myöhänen, K., Ritvanen, J., Rahiala, S., Hyppänen, T., Mletzko, J., Kather, A., Santos, S. (2015). *Oxyfuel combustion for CO2 capture in power plants. International Journal of Greenhouse Gas Control.* Available from: https://doi.org/10.1016/j.ijggc.2015.06.010 (Information collected on 2.10.22)

Sun, J., (2014), *4 Adsorption and pore filling.* Available from: https://www.researchgate.net/figure/Adsorption-and-pore-filling-96_fig4_314081363 (Information collected on 8.12.22)

Ünveren, E., Monkul, B., et al, 2016. *Solid amine sorbents for CO2 capture by chemical adsorption.* Available from: https://www.sciencedirect.com/science/article/pii/S2405656116301249

Wang, S., Wahiduzzaman, M., Davis, L., Tissot, A., Shepard, W., Marrot, J., Martineau-Corcos, C., Hamdane, D., Maurin, G., Devautour-Vinot, S., & Serre, C. (2018). *A robust zirconium amino acid metal- organic framework for proton conduction.* Nature Communications. Available from: https://doi.org/10.1038/s41467-018-07414-4. (Information collected 29.09.22)

Yan, Y., (2019). Available from: https://www.sciencedirect.com/science/article/pii/B9780081026663000079 (Information collected on 24.09.22)

Yu, C.-H., Huang, C.-H., & Tan, C.-S. (2012). *A Review of CO 2 Capture by Absorption and Adsorption. Aerosol and Air Quality Research.* Available from: https://aaqr.org/articles/aaqr-12-05-ir-0132.pdf (Information collected on 10.11.22)

Yuan, S., Zou, L., Qin, J-S., Li, J., Huang, L., Feng, L., Wang, X., Bosch, M., Alsalme, A., Cagin, T., Zhou, H-C. (2017). *Construction of hierarchically porous metal–organic frameworks through linker labilization.* Available from: https://www.nature.com/articles/ncomms15356 (Information collected on 14.12.22)

Zelenka, T., (2016). Adsorption and desorption of nitrogen at 77 K on micro- and meso- porous materials: Study of transport kinetics. Available from: https://www.sciencedirect.com/science/article/abs/pii/S138718111630035X (Information collected on 7.12.22)

Zeman, F. (2008). *Overview of CCS for Industrial Processes.* Available from: https://www.researchgate.net/figure/Overview-of-CCS-for-Industrial-Processes_fig3_238586206 (Information collected on 2.11.22)

Zhang, J., Li, Z., Qi, X-L., Wang, D-Y. (2020), *Recent Progress on Metal–Organic Framework and Its Derivatives as Novel Fire Retardants to Polymeric Materials*. Available from: https://link.springer.com/article/10.1007/s40820-020-00497-z (Information collected on 20.09.22)

8. Appendix A

Below one can see the figures for nitrogen sorption and surface area for each of the samples, using the "BET Consistency Criteria Blank Spreadsheet".

a) 1h synthesis - 60 degrees – degas over the weekend – no treatment

L-Aspartic acid:

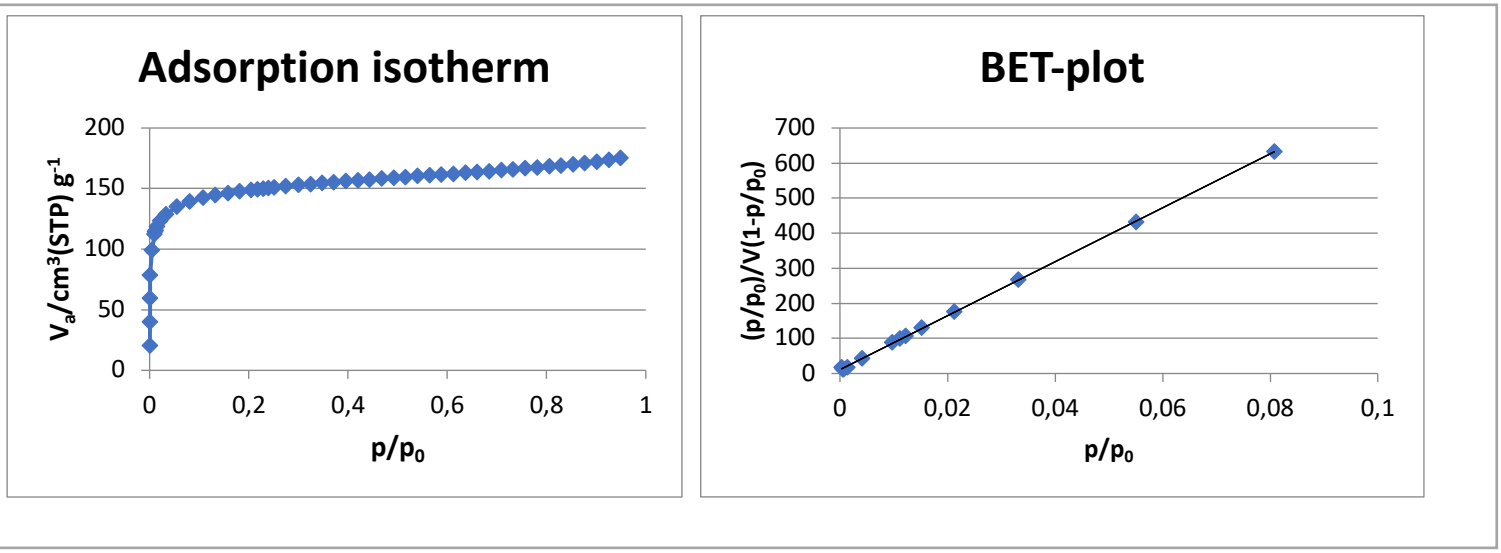

BET: 10 *[m2 g-1]*, p/p0 = 0,02 *[cm3 g-1]*

D-Aspartic acid:

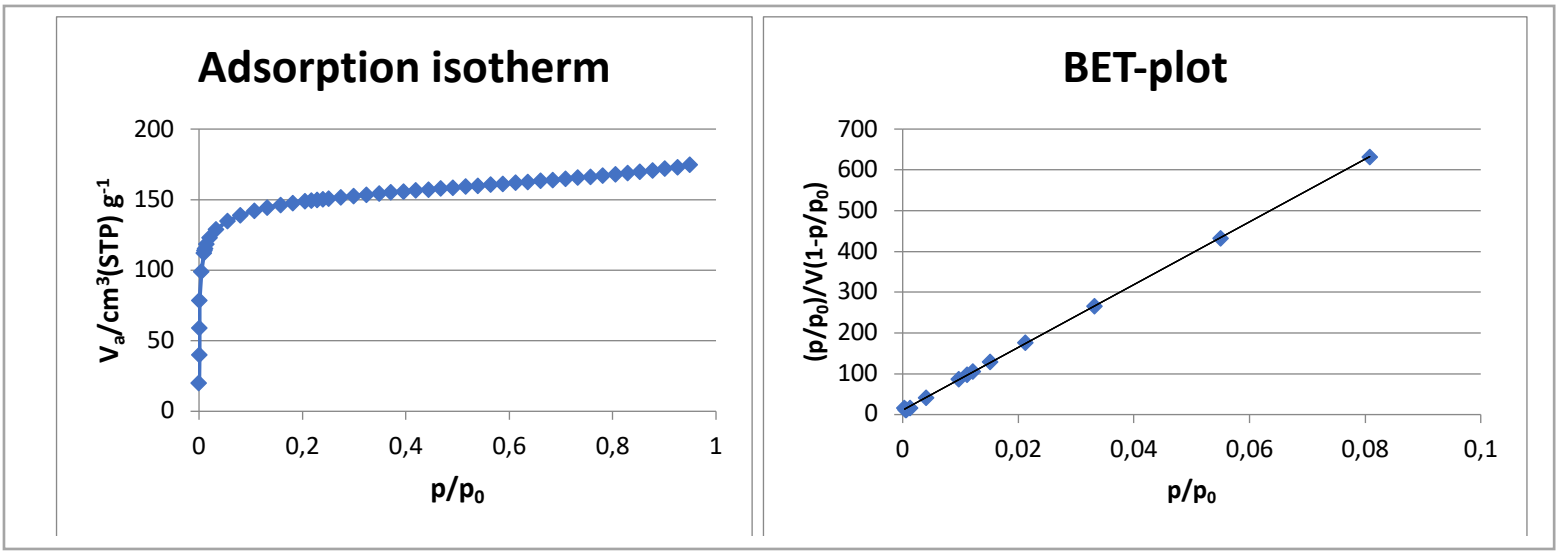

BET: 13 *[m2 g-1]*, p/p0 = 0,024 *[cm3 g-1]*

D,L-Asp:

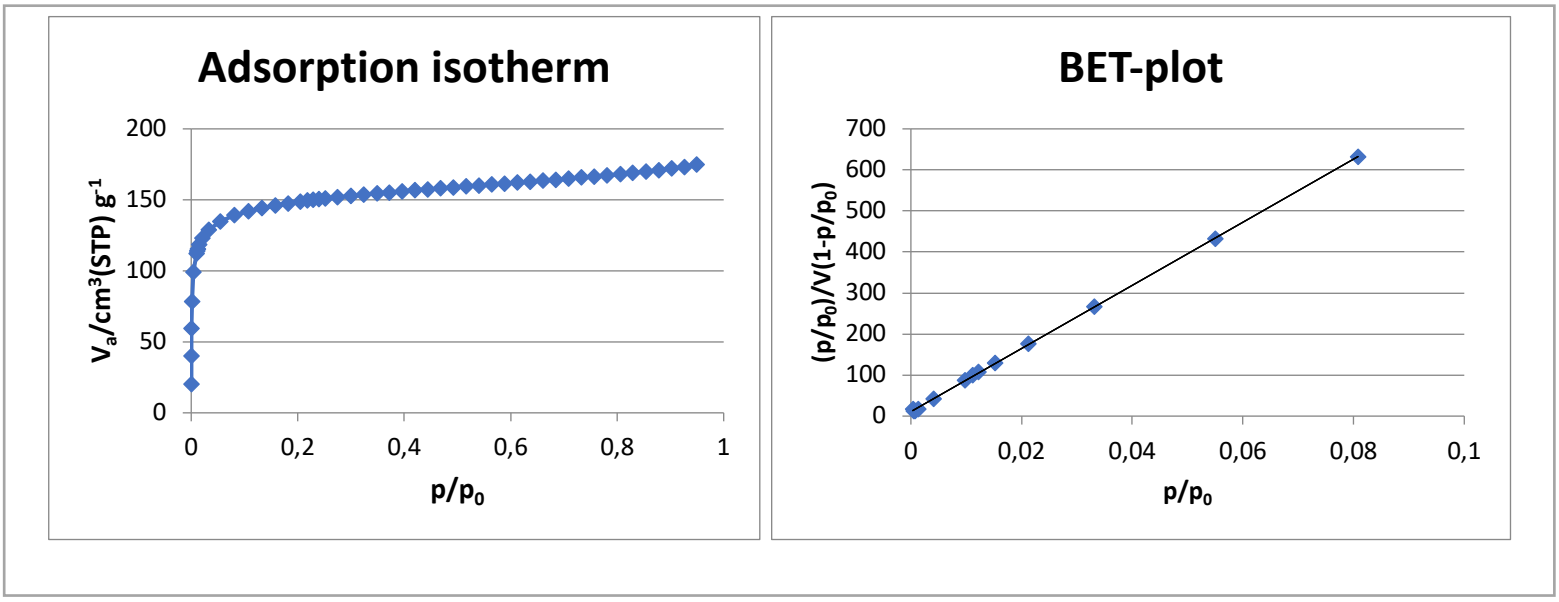

BET: 12 *[m2 g-1]*, p/p0 = 0,024 *[cm3 g-1]*

b) 1h synthesis - 60 degrees – 22h degassing – washed 24h in ethanol

L-Aspartic acid:

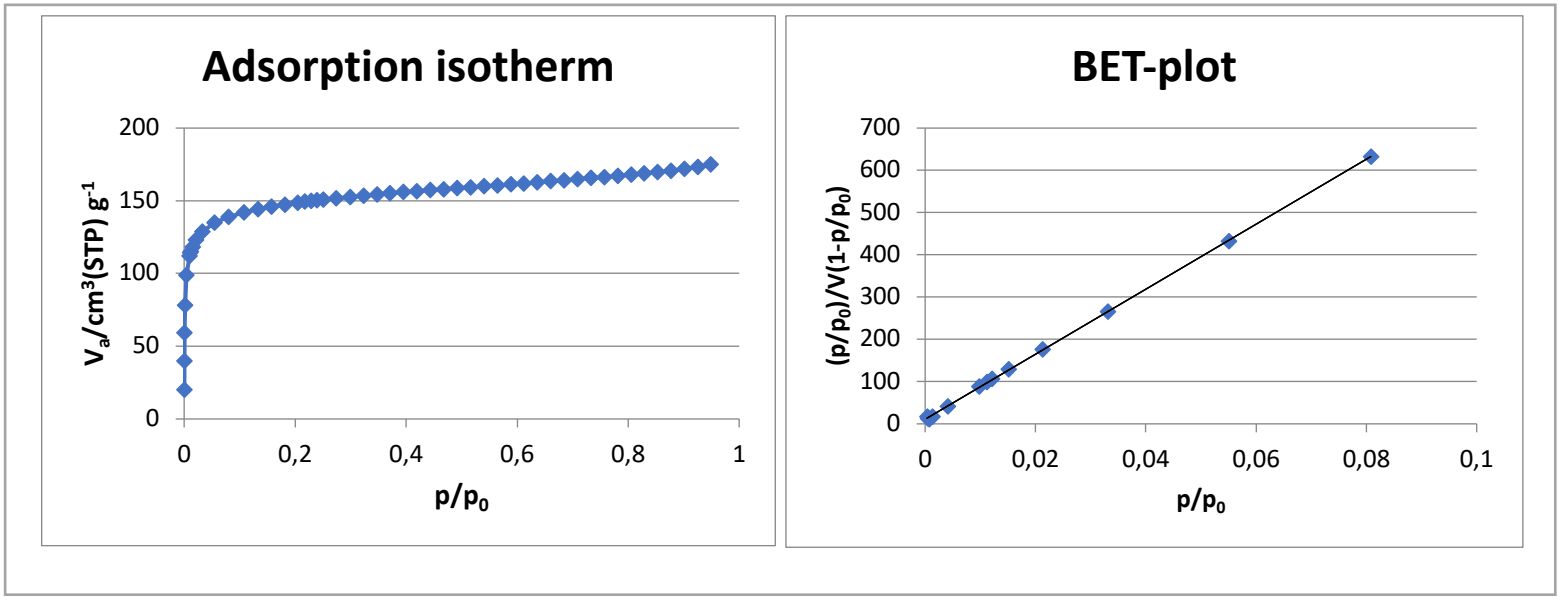

BET: 10 *[m2 g-1]*, p/p0 = 0,021 *[cm3 g-1]*

D-Aspartic acid:

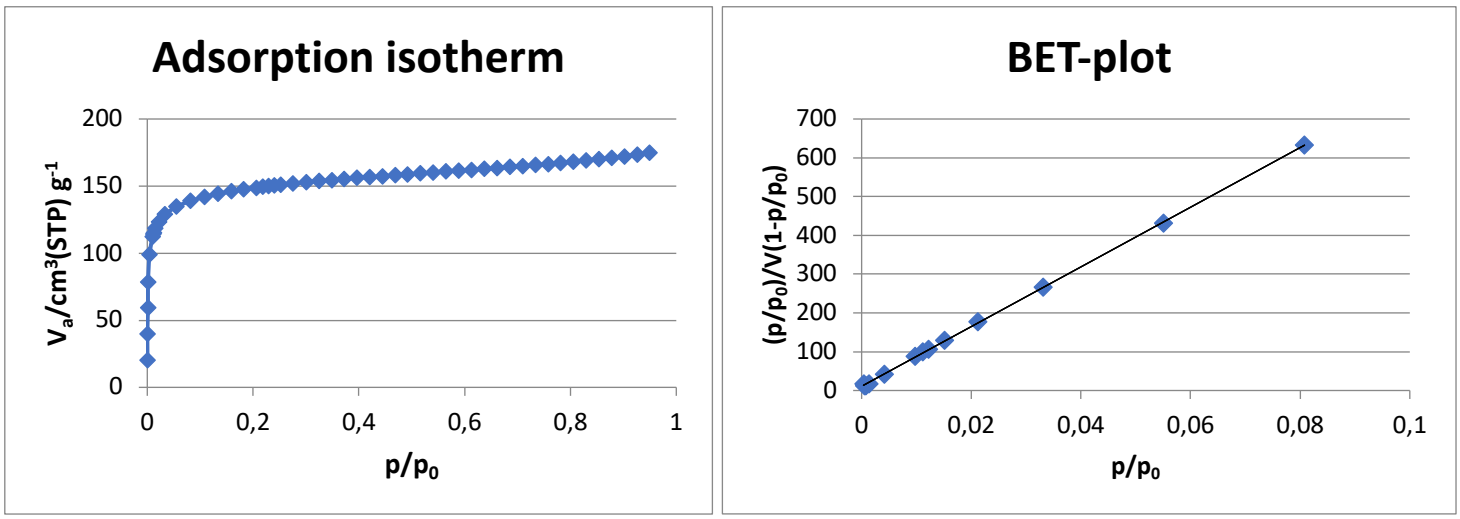

BET: 14 *[m2 g-1]*, p/p0 = 0,024 *[cm3 g-1]*

D,L-Aspartic acid:

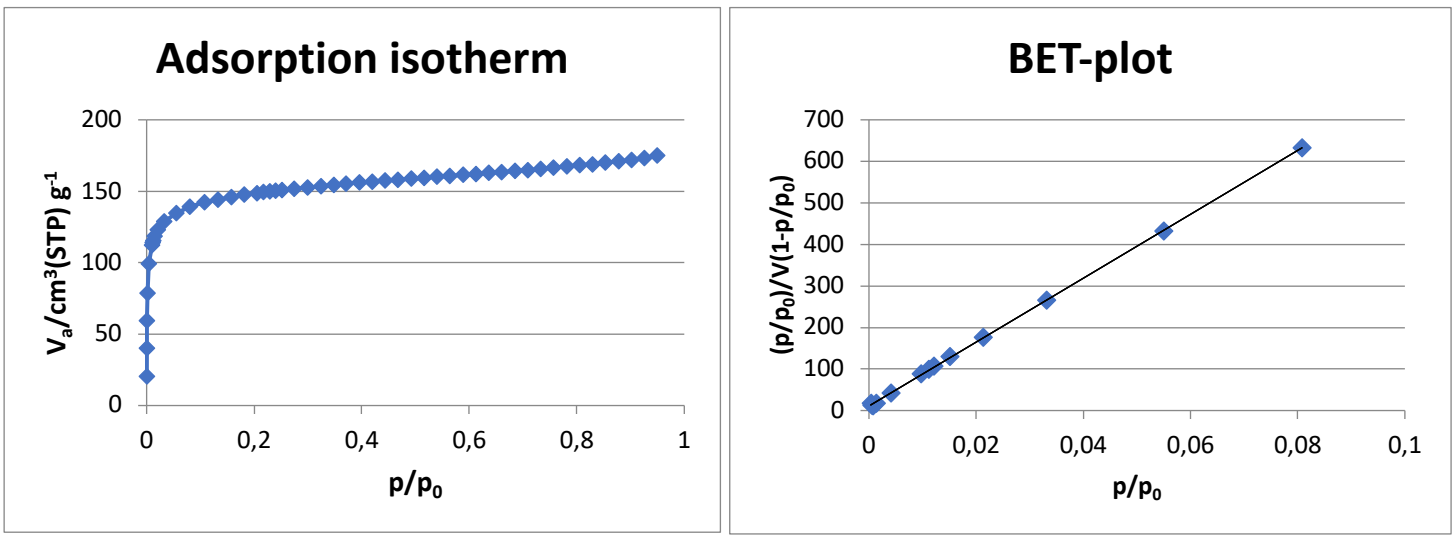

BET: 16 *[m2 g-1]*, p/p0 = 0,025 *[cm3 g-1]*

c) 1h synthesis - 60 degrees – 22h degassing– EtOH wash 3 days

L-Aspartic acid:

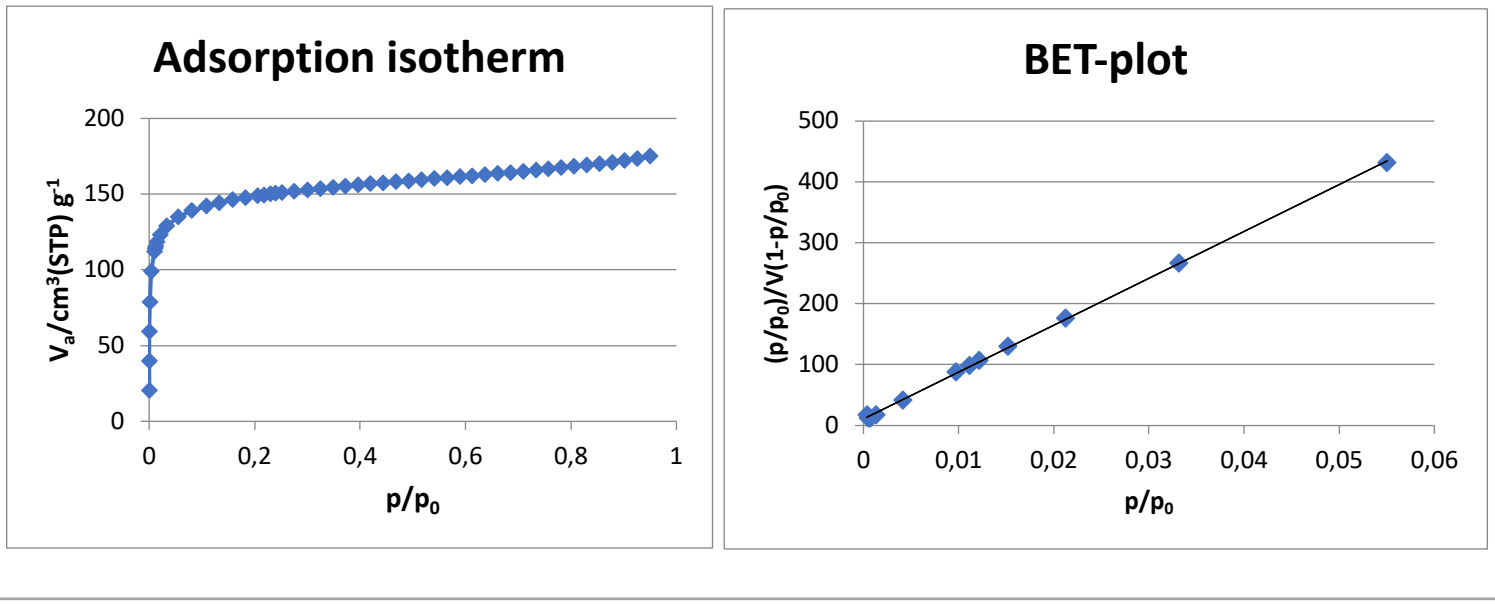

BET: 14 *[m2 g-1]*, p/p0 = 0,027 *[cm3 g-1]*

D-Aspartic acid:

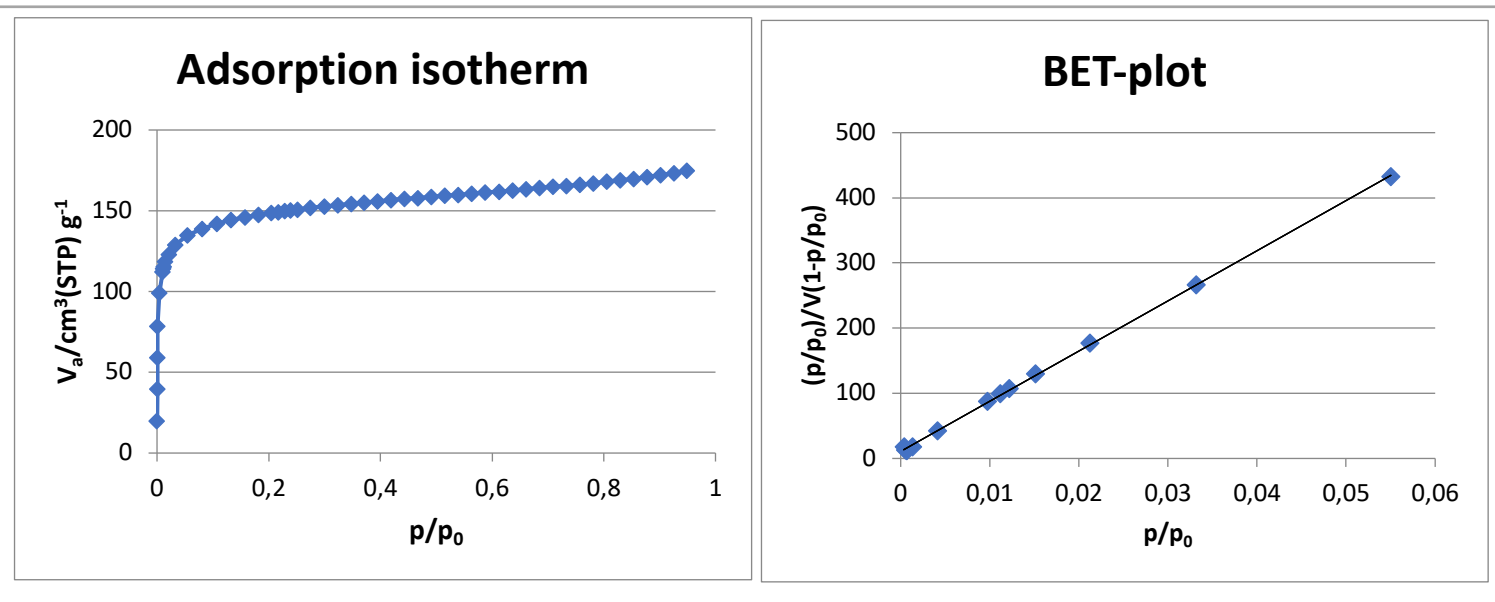

BET: 12 *[m2 g-1]*, p/p0 = 0,024 *[cm3 g-1]*

D,L-Aspartic acid:

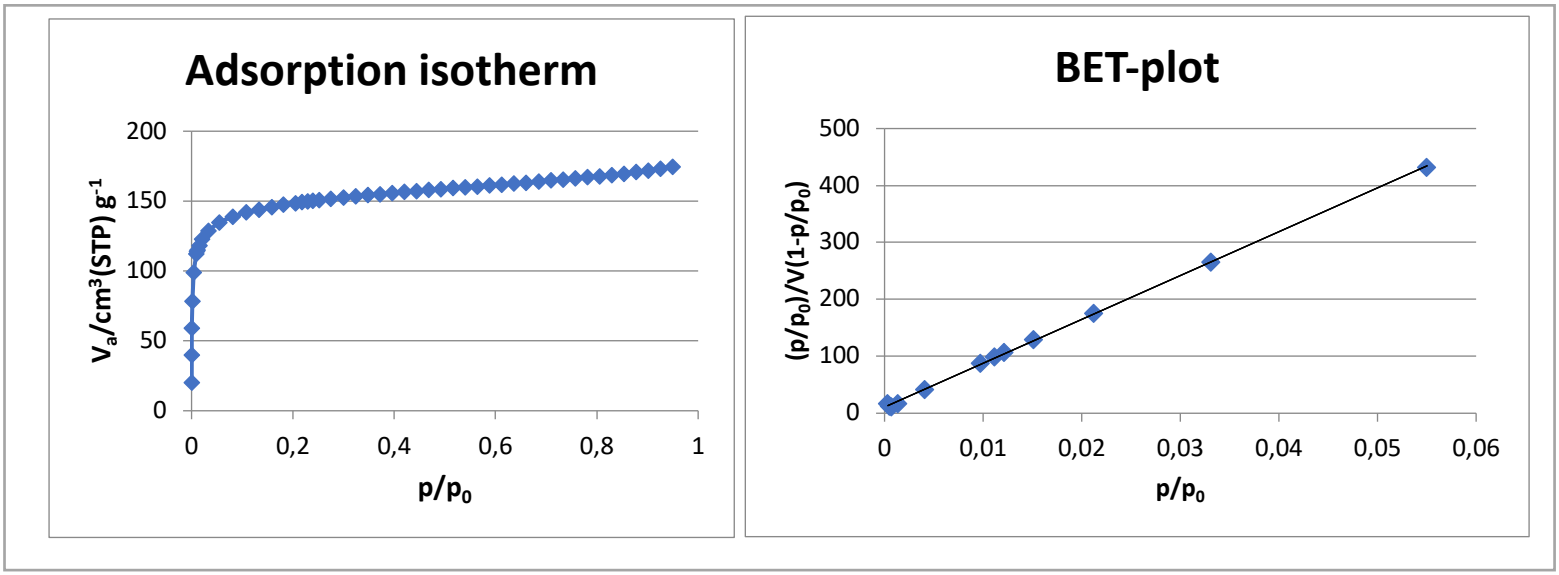

BET: 12 *[m2 g-1]*, p/p0 = 0,024 *[cm3 g-1]*

d) 72h synthesis - 60 degrees – 22h degassing– no treatment

L-Aspartic acid:

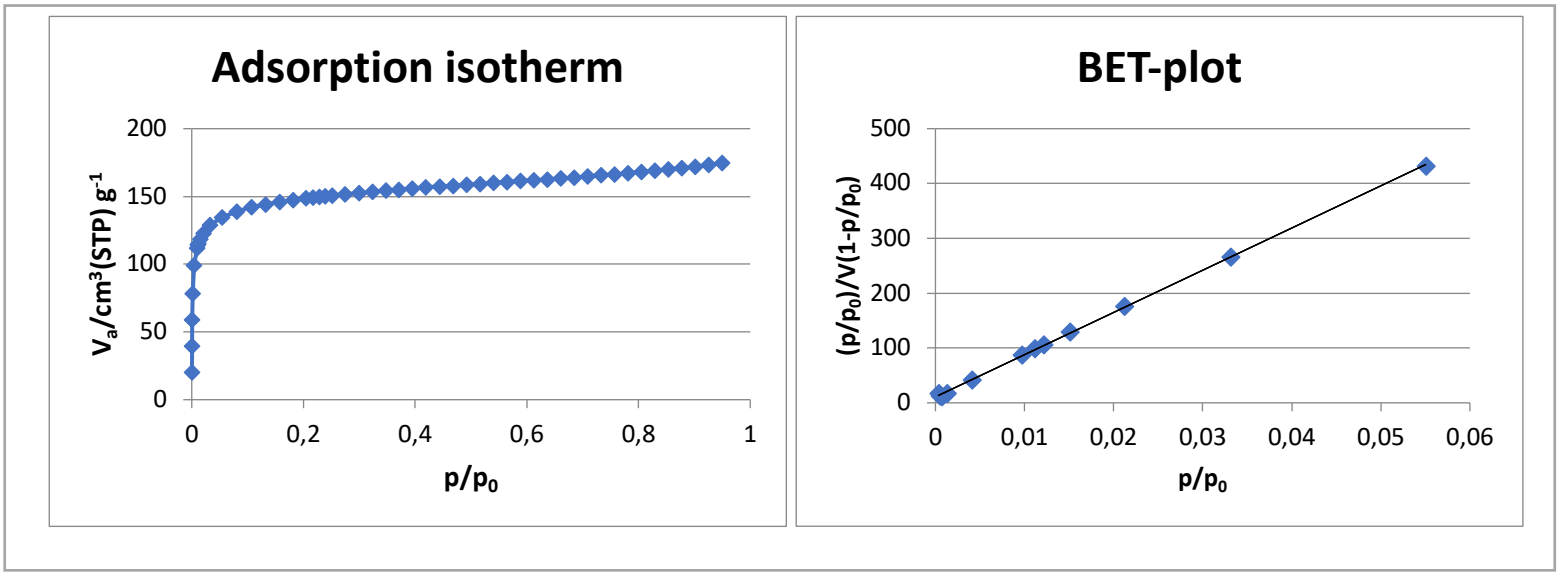

BET: 40 *[m2 g-1]*, p/p0 = 0,039 *[cm3 g-1]*

D-Aspartic acid:

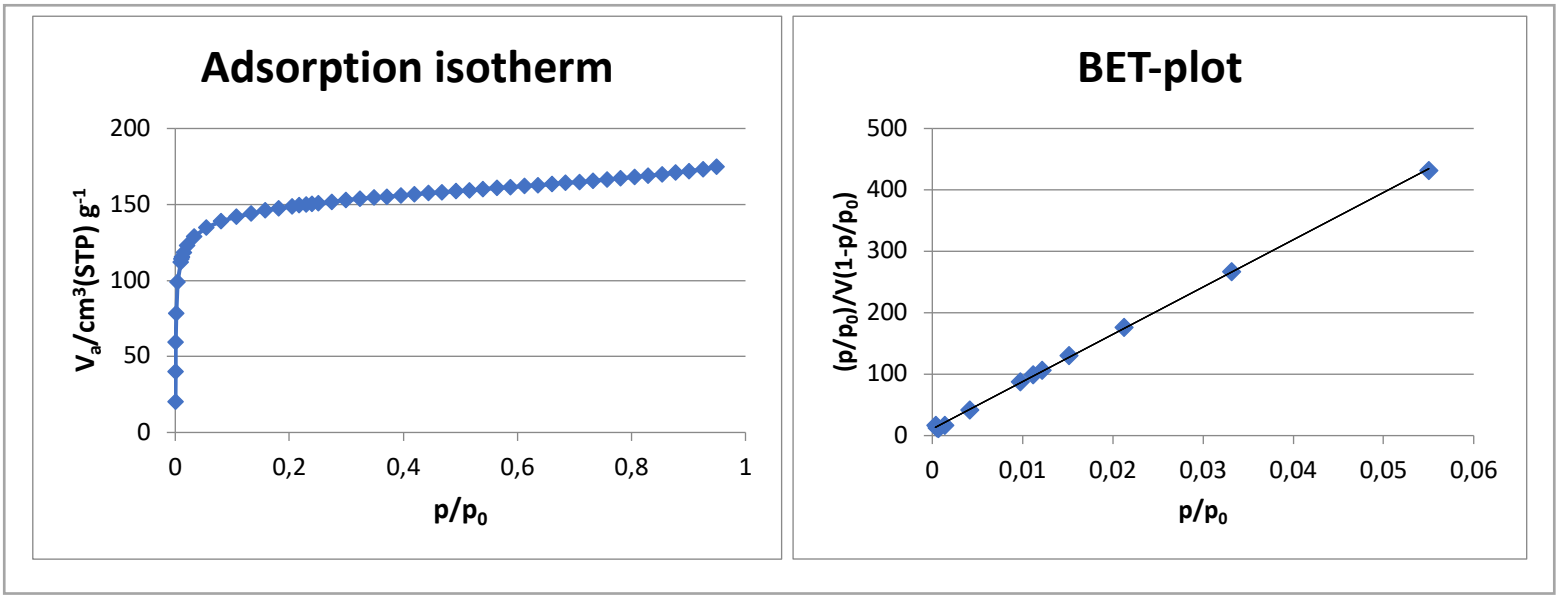

BET: 143 *[m2 g-1]*, p/p0 = 0,087 *[cm3 g-1]*

D,L-Aspartic acid:

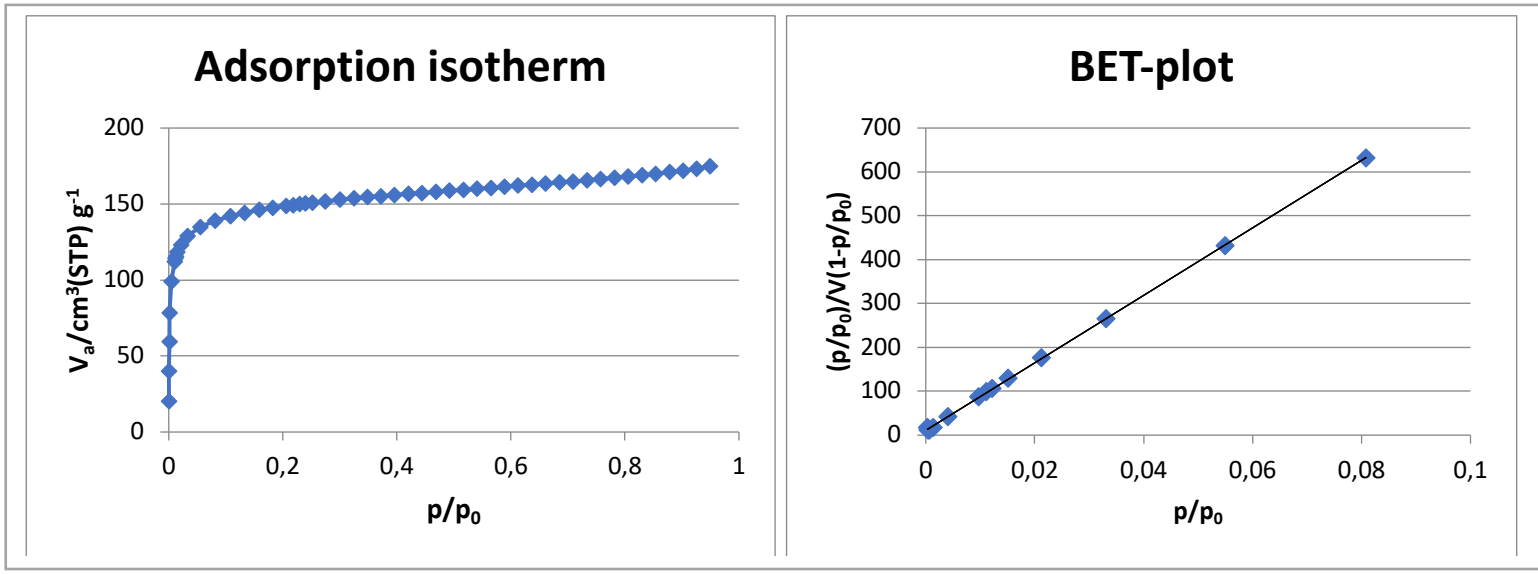

BET: 168 *[m2 g-1]*, p/p0 = 0,093 *[cm3 g-1]*

e) **72h synthesis - 60 degrees – 22h degassing – EtOH wash 3 days**

L-Aspartic acid:

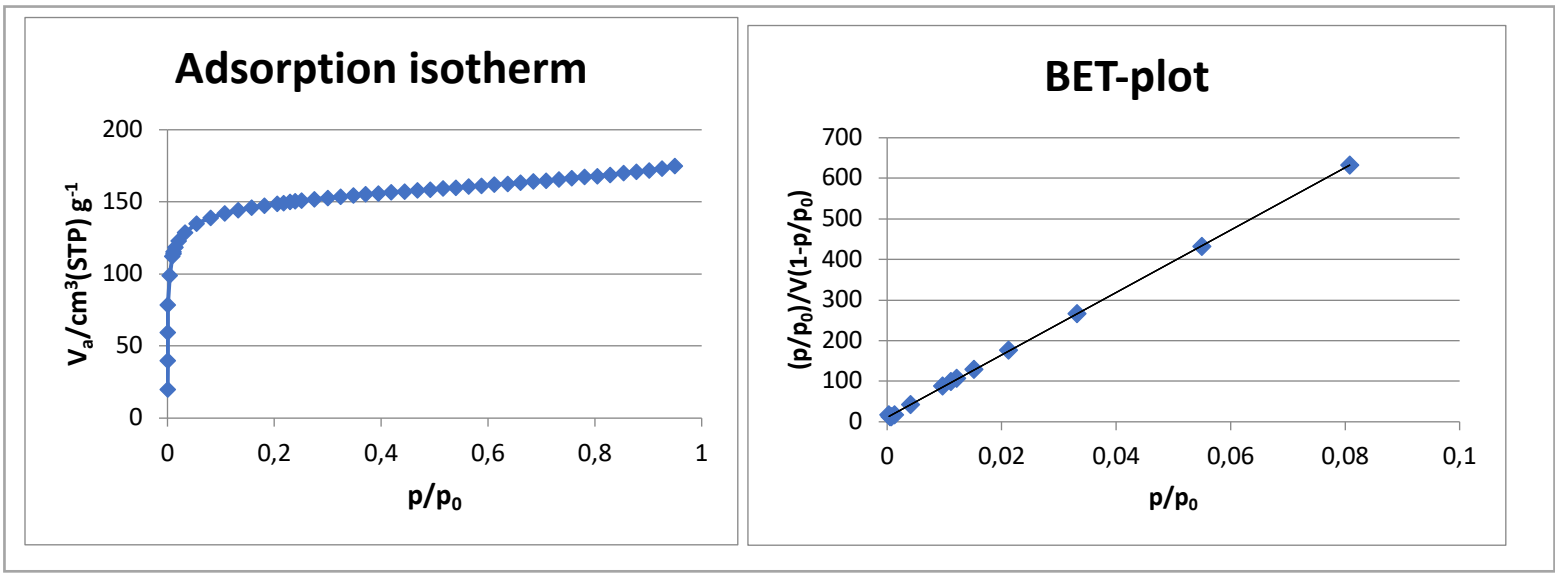

BET: 530 *[m2 g-1]*, p/p0 = 0,260 *[cm3 g-1]*

D-Aspartic acid:

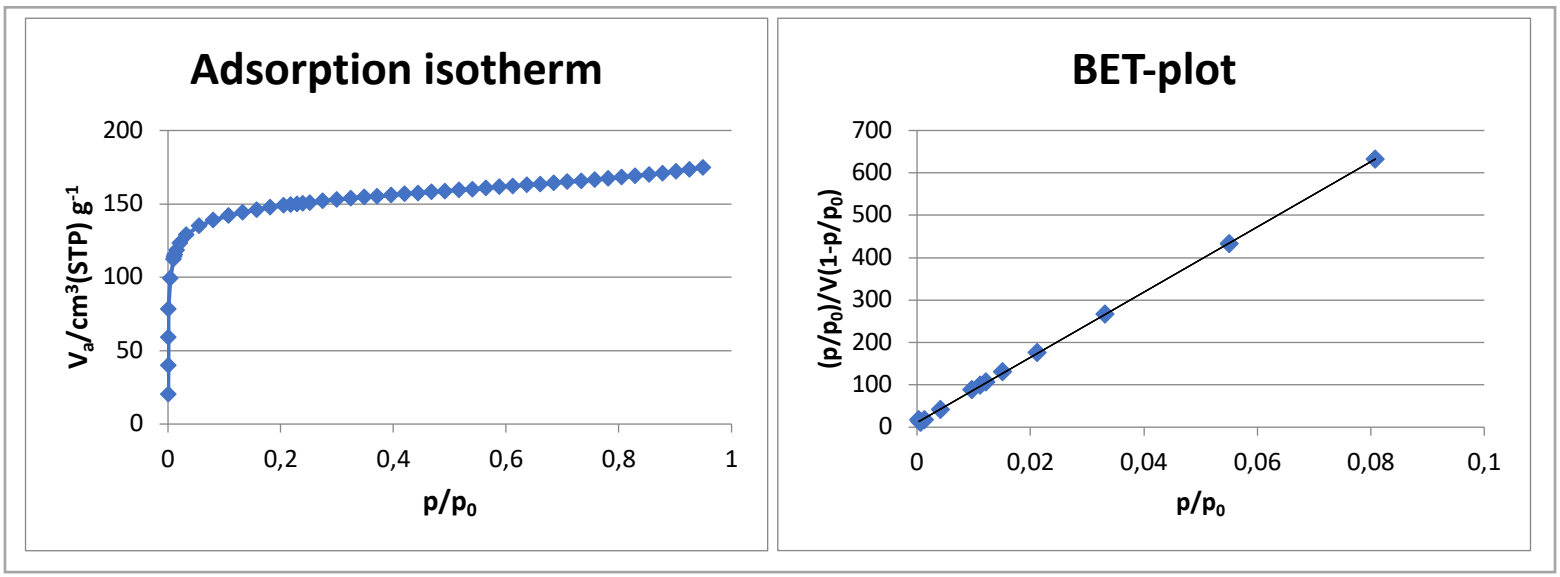

BET: 523 *[m2 g-1]*, p/p0 = 0,264 *[cm3 g-1]*

D,L-Aspartic acid:

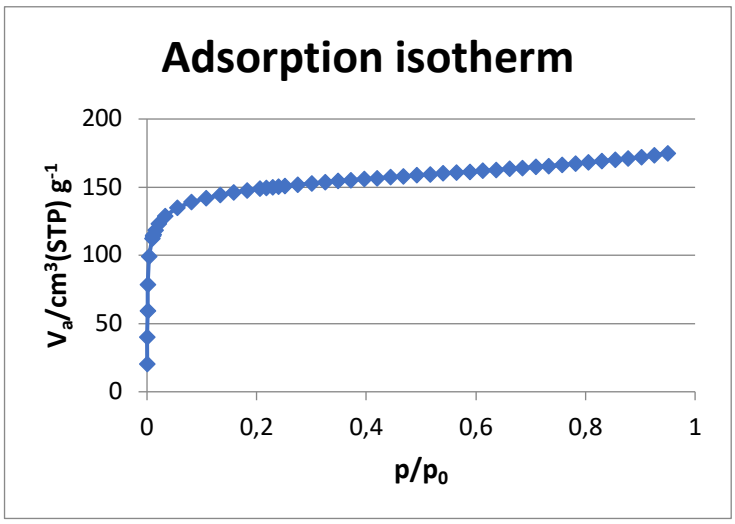

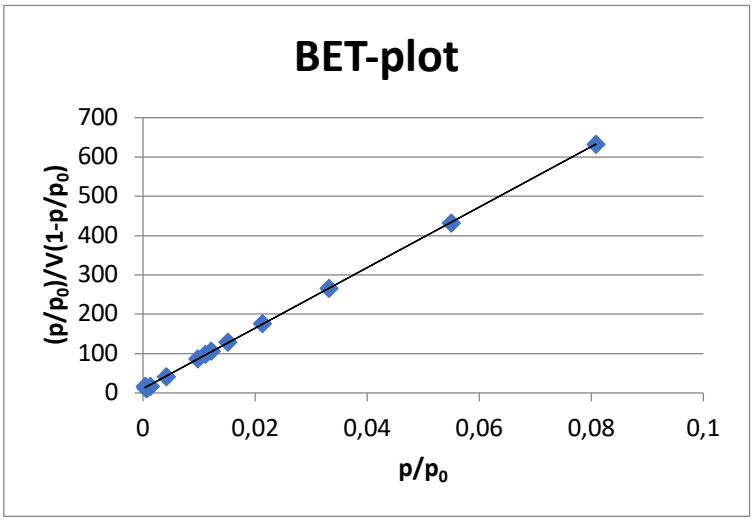

BET: 565 *[m2 g-1]*, p/p0 = 0,268 *[cm3 g-1]*